CELL-BASED MECHANISMS MEDIATING PRION LOSS AND STABILITY

by

Fen Pei

A Dissertation Submitted to the Faculty of the

DEPARTMENT OF MOLECULAR AND CELLULAR BIOLOGY

In Partial Fulfillment of the Requirements

For the Degree of

DOCTOR OF PHILOSOPHY

In the Graduate College

THE UNIVERSITY OF ARIZONA

2017

THE UNIVERSITY OF ARIZONA
GRADUATE COLLEGE

As members of the Dissertation Committee, we certify that we have read the dissertation prepared by Fen Pei, titled Cell-based Mechanisms Mediating Prion Loss and Stability and recommend that it be accepted as fulfilling the dissertation requirement for the Degree of Doctor of Philosophy.

09-29-17

Dr. Tricia Serio Date

09-29-17

Dr. Joyce Schroeder Date

09-29-17

Dr. Tim Bolger Date

09-29-17

Dr. Indraneel Ghosh Date

Final approval and acceptance of this dissertation is contingent upon the candidate's submission of the final copies of the dissertation to the Graduate College.

I hereby certify that I have read this dissertation prepared under my direction and recommend that it be accepted as fulfilling the dissertation requirement.

09-29-17

Dissertation Director: Dr. Tricia Serio Date

STATEMENT BY AUTHOR

This dissertation has been submitted in partial fulfillment of the requirements for an advanced degree at the University of Arizona and is deposited in the University Library to be made available to borrowers under rules of the Library.

Brief quotations from this dissertation are allowable without special permission, provided that an accurate acknowledgement of the source is made. Requests for permission for extended quotation from or reproduction of this manuscript in whole or in part may be granted by the head of the major department or the Dean of the Graduate College when in his or her judgment the proposed use of the material is in the interests of scholarship. In all other instances, however, permission must be obtained from the author.

SIGNED: Fen Pei

ACKNOWLEDGEMENTS

First, I would like to thank my thesis advisor, Dr. Tricia Serio, for her help and guidance during my graduate studies. She sets a great example as an independent scientist for me. And she always encourages me to think critically, share my ideas without fear and develop more confidence in my abilities. I really appreciate all of her support and help.

I would also like to thank my committee members, Dr. Hanna (Johnny) Fares, Dr. Joyce Schroeder, Dr. Indraneel Ghosh and Dr. Tim Bolger for all of the helpful discussions and suggestions. I appreciate that they are always willing to help me throughout my graduate studies.

Furthermore, I would like to thank Dr. Jeff Laney for his advice and scientific suggestions, which greatly helps my project progression and also offers me insights from a different perspective.

My time and also research in the laboratory has gained a lot of help from all the members of the Serio and Laney labs: Dr. Christine Langlois, Dr. Courtney Klaips, Dr. Jennifer Norton, Dr. Wesley Naeimi, Xuezhen Ge, Teal Bretchel and Diane Jurcin. Not only have these members share their ideas and thoughts with me, but they also provided great friendships.

Finally, I would like to thank my family, Guangbo Liu, Gene Liu, Dechun Wang, Shengcai Pei, Fengqing Yang and Daozhen Liu for the full support and encouragements.

TABLE OF CONTENTS

LIST OF TABLES

Chapter 2:

Chapter 3:

Chapter 4:

LIST OF FIGURES

Chapter 2:

Chapter 3:

Abstract

The prion protein underlies several previously inexplicable phenomena, including transmissible neurodegenerative disease in mammals and the non-Mendelian inheritance of unique traits in fungi. These proteins can adopt multiple stable conformations, and each of these forms can self-replicate by assembling into ordered aggregates, which template the conversion of the newly synthesized protein into the prion form as these monomers join the aggregates. These complexes must then be fragmented to generate additional templates and to promote the spread of the aggregates both within and between individuals. Despite its efficient and autocatalytic pathways of protein misfolding, changes in prion self-replication cycles can inhibit prion persistence and thus the transmission of prion-associated phenotypes. In our studies, we first explored this inhibition process using a yeast prion [*PSI*$^{+}$], the prion form of a translation termination factor Sup35, and a dominant-negative mutant of this protein. Prion variants with distinct conformations were differentially sensitive to prion inhibition, despite the fact that each of the variants were impacted by the mutant in the same way - a reduction in kinetic stability and an increased sensitivity to fragmentation. The threshold for clearance of the existing aggregates was determined by both the self-replication efficiencies of the variants and also the dosage of the mutant, indicating that changing dosing regimes might be effective for treating prion variants. In addition to dominant-negative mutant inhibition, prion persistence can also be inhibited by heat shock. Our studies indicate that this inhibition requires the activity of the

deacetylase Sir2, which promotes asymmetric retention of misfolded proteins after cellular stress. Intriguingly, Sir2 mediates its effects through a mating-type specific gene YJL133C-A, which localizes to the mitochondrial membrane. Together, our studies indicate that prion persistence and clearance arise from a complex interplay between prion protein conformation and sequence and the cellular environment in which they reside.

NOTE: Chapter 2 and chapter 3, Which include its separate abstracts, introductions, results, discussion, methods, tables, references and figures, are prepared as manuscripts for submission.

Chapter 1: Introduction

The prion hypothesis

The prion hypothesis was originally raised to explain the molecular basis of the scrapie agent, which causes a class of fatal neurodegenerative diseases (Griffith, 1967; Prusiner, 1982a). The hypothesis posits that the prototypical and perhaps most extensively characterized examples of protein conformation-based inherited phenotypic traits are those defined by the protein infectious particles known as prions (Griffith, 1967; Prusiner, 1982b).

The term prion was proposed by Stanley Prusiner in 1982 to illustrate the protein-based composition of the scrapie agent (Prusiner, 1982b). In support of this proposal, the scrapie agent could be destroyed by protein-denaturing but not by nucleic acid-damaging conditions (Alper et al, 1967; Alper et al, 1966; Bellinger-Kawahara et al, 1987). Prions are now known to be responsible for a multitude of distinct biological phenomena, including several transmissible diseases in mammals and heritable phenotypes in fungi (Tuite & Serio, 2010).

Prions self-replicate by assembling into ordered aggregates, which template the conversion of native-state protein into the prion form (Griffith, 1967). These complexes must then be fragmented to generate small aggregates that serve as additional templates and are delivered transmitted (Griffith, 1967). Studies on prion propagation in mammals and yeast have uncovered striking commonalities and demonstrating an ability to be similarly modulated by both *cis* and *trans* effectors. Understanding the mechanisms by which prion propagation is regulated should illuminate strategies for targeted intervention of prion diseases.

Prion in Mammals

Prions were originally identified as infectious entities that are associated with transmissible spongiform encephalopathies (TSEs) (Prusiner, 1982b; Prusiner, 1998), including Creutzfeldt–Jakob disease (CJD) and kuru in humans, scrapie in sheep and bovine spongiform encephalopathy (BSE) in cattle and others (Table 1) (Benetti & Legname, 2009). Although there are unique symptoms and pathologies associated with each disease, they are all progressively neurodegenerative, and ultimately fatal (Benetti & Legname, 2009).

Prion diseases occur on a sporadic or familial basis (Geschwind, 2015). First, the sporadic form of prion disease is most common, covering almost 85% of cases of prion disease (Appleby & Lyketsos, 2011). The mechanism through which this form of the disease arises is unknown. Second, familial prion diseases arise from mutation of the PrP protein, which could explain 15% of cases of prion disease (Appleby & Lyketsos, 2011). The mutant forms of PrP are more likely to misfold and thereby cause neurodegenerative prion disease (Mastrianni, 2010).

While prion diseases may arise in sporadic and familial forms, the major insight into the disease agent was gained from studies of prion infectivity. Prion infection may occur through many routes, including accidental or experimental inoculation with contaminated material or blood, or by ingestion of contaminated meat (Ironside, 1996). While transmission of prion disease within the same species is most efficient, cross-species transmission is believed to occur naturally in rare circumstances and has been accomplished experimentally in laboratory mice and hamsters (Chandler, 1961; Kimberlin & Walker, 1977; Kimberlin et al, 1975; Will et al, 1996).

The prion protein, PrP, was identified as being the primary agent responsible for these diseases because it co-purified with infectivity (Bolton et al, 1982). There are two conformers of PrP protein: cellular PrP (PrP^{C}), which is the normal conformer, and scrapie PrP (PrP^{Sc}), which is the infectious conformer (Detwiler & Baylis, 2003; Harman & Silva, 2009; Prusiner, 1982b; Prusiner, 1998). PrP^{Sc} was predicted to 'replicate' during infection by contacting specific regions on PrP^{C} to recruit this protein and convert it into PrP^{Sc} (Kocisko et al, 1994).

Supporting a crucial role for PrP in prion disease, PrP knockout mice are resistant to TSEs (White et al, 2008). Although this result seems to favor a gain-of-function model for prion diseases, subsequent studies have shown that a loss-of-function model cannot be completely ruled out. For example, the expression of PrP fragments induces spontaneous neurodegeneration in PrP knockout mice (Aguzzi et al, 2008; Baumann et al, 2007; Shmerling et al, 1998), indicating prion pathology induced by PrP could be explained as a loss of some PrP functions but not of others (Westergard et al, 2007). Current research, therefore, cannot exclude either possibility.

Prion in Yeasts

Prions have also been found in fungi, including the yeast *Saccharomyces cerevisiae* and the multi-cellular fungus *Podospora anserina* (Büeler et al, 1994). Although fungal prions are not infectious, they are transmissible through cell division and mating (Liebman & Derkatch, 1965). Like PrP^{Sc}, fungal prion proteins can adopt conformations that are also self-replicating. These conformers are partitioned to daughter cells during division, leading to the inheritance of the associated phenotypes (Wickner et al, 2007).

There are several known transmissible prion proteins in fungi (Table 2). Indeed, the list of fungal prions continues to grow and includes proteins of various functions. Some of the best-studied examples are the [*URE3*], [*PSI*$^{+}$] and [*PIN*$^{+}$] prions of *Saccharomyces cerevisiae*, which are the prion form of the Ure2, Sup35 and Rnq1 proteins, respectively (Cox, 1965; Derkatch et al, 2001; Osherovich & Weissman, 2001; Sondheimer & Lindquist, 2000; Wickner, 1994). Another well documented example is the [Het-s] prion of *Podospora anserina*, the prion form of the HET-s protein (Coustou et al, 1997).

While the molecular basis of how conformational conversion of PrP leads to prion disease is currently unknown, conversion of fungal prion proteins to the self-replicating conformation results in the alteration of their normal cellular function and thereby new heritable phenotypes. For instance, Ure2 and Sup35, involved in nitrogen catabolism and translation termination respectively, display reduced activity when in their prion form, leading to the use of alternative nitrogen sources and stop codon readthrough respectively (Cox, 1965; Lacroute, 1971; Liebman & Derkatch, 1965; Serio & Lindquist, 1999; Wickner, 1994). Interestingly, Rnq1 has no known non-prion function, but when in the prion form, Rnq1 acquires a gain-of-function phenotype, which allows for the induction of other yeast prions (Derkatch et al, 2001; Derkatch et al, 2000; Derkatch et al, 1997; Sondheimer & Lindquist, 2000). Like Rnq1, the HET-s protein has no known non-prion function, but its prion form mediates heterokaryon incompatibility during cell fusion upon mating with a strain carrying the Het-S allele (Coustou et al, 1997). As is the case in mammals, transfer of self-replicating conformations of recombinant Ure2, Sup35, and Rnq1 protein into yeast leads to the appearance of [*URE3*], [*PSI*$^{+}$], and [*PIN*$^{+}$], directly

linking the heritable phenotypes to a protein-only mechanism (Brachmann et al, 2005; King & Diaz-Avalos, 2004a; Patel & Liebman, 2007).

Although fungal prions are not associated with an infectious disease, they work as epigenetic determinants that alter a range of cellular processes and phenotypes through inheritance.

Prionoids

The coalescence of proteins into highly ordered aggregates is a hallmark of protein misfolding disorders, which lead to progressive neurodegeneration when affecting the central nervous system. Proteins associated with non-transmissible protein misfolding disorders are denoted 'prionoids' (Aguzzi, 2009; Aguzzi & Lakkaraju, 2016; Aguzzi & Rajendran, 2009).

The most common prionoids include Aβ, Tau, α-synuclein, SAA and PolyQ (Table 3). Similar to self-replicating conformations of the prion protein PrP, their alternative conformations also self-replicate and underlie highly prevalent human neurodegenerative diseases with different pathological features. Prionoids are capable of cell-to-cell propagation, which was demonstrated by studies showing that amyloid seeds can be released from affected cells and then re-enter other cells and convert the native protein into the aggregate state (Aguzzi & Rajendran, 2009). However, unlike the case for the prion protein PrP, there is no experimental evidence so far to show that prionoids could be transmitted between individuals.

Conformational self-replication and transmission

Self-replication within cells is required for prion proteins to stably persist and transmit prion phenotypes. A conformational based model was proposed to explain this process, in which prion protein binds and converts non-prion protein into a prion state (Griffith, 1967). According to this model, after initial misfolding of a normal protein into a prion state, prion protein converts newly synthesized, soluble, non-prion protein into highly ordered aggregates. Both *in vitro* and *in vivo* studies support this model for both mammal and yeast prion proteins.

Conformational self-replication in vitro

The "protein-only" hypothesis for prion propagation implies that it should be possible to generate prions *in vitro* from highly purified recombinant PrP. PrP^{C} from uninfected sources can be converted to proteinase K-resistant forms by PrP^{Sc} in a cell-free system (Kirby et al, 2003; Kocisko et al, 1994). This conversion efficiency is very low but can be improved by protein misfolding cyclic amplification (PMCA), which generates more templates by breaking larger aggregates into smaller aggregates (Castilla et al, 2005; Saborio et al, 2001; Soto et al, 2002). Purified yeast prion proteins also form aggregates *in vitro*, which occurs spontaneously after a lag phase or immediately after the addition of preformed fibers or prion aggregate-containing yeast lysates (Glover et al, 1997; Serio et al, 2000; Taylor et al, 1999). Because *in vitro* generated yeast prions induce the prion state when introduced into yeast cells, this process represents the mechanism underlying prion replication and phenotype determination in yeast (King & Diaz-Avalos, 2004b; Maddelein et al, 2002; Patel & Liebman, 2007; Tanaka et al, 2004). Similarly, *in vitro*-generated aggregates of the mammalian prion protein create prion disease when

inoculated into mice, although this process is less efficient than that of brain-derived material (Kim et al, 2010; Wang et al, 2011; Wang et al, 2010).

Prion biogenesis cycle in vivo

Studies of the yeast prion protein Sup35 have been particularly instrumental in advancing our understanding of prion conformational self-replication within living cells. In addition to the conversion reaction that occurs *in vitro*, the self-replication of the prion conformation *in vivo* involves a multi-step pathway of prion biogenesis that is mediated by cellular factors. The importance of these *in vivo* steps and the existence of interacting cellular factors on prion propagation most likely extends to all fungal prions and has been suggested to apply to the mammalian prion protein, as well (Masel et al, 1999). Based on [*PSI*$^{+}$] studies, four critical steps must occur to ensure the growth and transmission of prions within a population.

First, prion protein synthesis is clearly an important contributor to persistence of prion phenotypes. In mammals, continuous PrP expression is required for disease manifestation (Bueler et al, 1993; Büeler et al, 1994; Prusiner et al, 1993). Moreover, the incubation period for clinical disease decreases upon increasing PrP expression (Prusiner et al, 1990; Tremblay et al, 1998), and overexpressing PrP leads to a higher frequency of prion disease (Sandberg et al, 2011; Scott et al, 1989). However, there is an imperfect correlation between PrP^{Sc} accumulation and clinical disease as mice with a heterozygous disruption of PrP show equal levels of PrP^{Sc} accumulation as their wild type counterparts despite delayed clinical symptoms (Scott et al, 1989). In the yeast prion system, prion appearance is also stimulated by transient overexpression of yeast prion proteins (Chernoff et al, 1993; Chernoff et al, 1992; Derkatch et al, 1996), and overexpression of

Sup35 is toxic to [*PSI*$^{+}$] strains, mirroring the enhanced toxicity (i.e. clinical disease) in mammals under the same conditions.

Second, prion protein in the non-prion state must adopt the self-replicating conformation. Like *in vitro*, this process occurs through a templating mechanism in which existing aggregates of prion protein already in the self-replicating form direct the remodeling of the soluble protein coincident with its incorporation into those complexes (Kirby et al, 2003). For PrP, pulse-labeled PrP transits from a protease sensitive to a protease resistant state within celsl (Borchelt et al, 1990; Caughey & Raymond, 1991), indicating conversion of newly made PrP to the prion state. For yeast [*PSI*+], conversion was detected through observing the formation of Sup35-GFP foci after a [*PSI*$^{+}$] cell expressing unmarked Sup35 was mated with a [*psi*$^{-}$] cell expressing the fusion protein Sup35-GFP (Satpute-Krishnan & Serio, 2005). Meanwhile, this conversion was coincident with the emergence of the [*PSI*$^{+}$] phenotype: stop codon readthrough (Satpute-Krishnan & Serio, 2005). Altogether, these studies suggest protein in the non-prion state could be converted to self-replicating prion conformations.

Third, the aggregate template must be fragmented into smaller complexes to create additional surfaces for conversion. The crucial role of fragmentation in prion self-replication has previously been implicated *in vitro*, where sample agitation or sonication accelerates prion polymerization (Saborio et al, 2001), and several lines of evidence also demonstrate that fragmentation is critical *in vivo* for prion self-replication and transmission in both yeast and mammals. For mammalian PrP, prion infectivity greatly increases upon partial disruption of *ex vivo* preparations of PrP (Caughey et al, 1997; Gabizon et al, 1988; Gabizon et al, 1987; Malone et al, 1978) , indirectly highlighting the importance of

fragmentation on prion propagation. Moreover, the yield of *in vitro* conversion reactions is greatly improved by cyclic rounds of polymerization and sonication (Saborio et al, 2001). Thus, although an endogenous fragmentation activity has not been directly identified for PrP, the fragmentation activity is likely crucial for the establishment and progression of disease (Hall & Edskes, 2004).

In contrast to the mammalian prion system, fragmentation is well observed and studied in yeast. The molecular disaggregase Hsp104 and its cochaperones mediate the fragmentation reaction *in vivo*, and these factors are crucial for stable yeast prion propagation (Allen et al, 2005; Chernoff et al, 1995; Higurashi et al, 2008; Ness et al, 2002; Satpute-Krishnan et al, 2007; Tipton et al, 2008). For example, prion loss results from any type of Hsp104 inactivation: deletion, expression of a dominant Hsp104 mutant, or treatment with the inhibitor guanidine hydrochloride (GdnHCl) (Chernoff et al, 1995; Derkatch et al, 1997; Moriyama et al, 2000; Osherovich & Weissman, 2001; Sanchez & Lindquist, 1990). The direct role for Hsp104-dependent fragmentation *in vivo* was supported by several studies. First, prion loss by Hsp104 inactivation causes propagons (heritable prion units or seeds) to decrease, while Hsp104 reactivation allows for propagon to re-amplify (Byrne et al, 2007). Second, Sup35 aggregate size becomes larger upon Hsp104 inactivation (Kryndushkin et al, 2003; Satpute-Krishnan et al, 2007; Wegrzyn et al, 2001). Lastly, when new protein synthesis is inhibited to block conversion in cells with wild type Hsp104 activity, existing prion aggregates represented by Sup35-GFP foci become diffuse (Kawai-Noma et al, 2006; Satpute-Krishnan et al, 2007). Thus, fragmentation mediated by Hsp104 is crucial for stable propagation of yeast prion [*PSI*$^{+}$].

Fourth, prion aggregates must be transmitted for progression of disease in mammals and for maintenance of the associated phenotype in a yeast population. In yeast, fragmentation of prion aggregates *in vivo* is also crucial for efficient prion transmission. When Sup35 aggregates grew too large upon Hsp104 inactivation they became immobile and preferentially became retained in mother cells, leading to prion loss upon cell division (Bailleul et al, 1999; Byrne et al, 2007; Eaglestone et al, 2000; Kawai-Noma et al, 2009; Ness et al, 2002; Satpute-Krishnan et al, 2007). During the course of mammalian prion disease, PrP^{Sc} must spread throughout the central nervous system to produce symptoms (Beekes et al, 1998). Although several mechanisms by which prions spread transcellularly have been suggested, it is possible that once prion aggregates are released to the extracellular space they can simply diffuse throughout neural tissues (Aguzzi & Rajendran, 2009; Beekes et al, 1998). This could also explain the higher infectivity when prion aggregates are smaller, as they might have a higher mobility and/or ability to enter cells (Masel et al, 1999; Zampieri et al, 2009).

Each step of this *in vivo* prion cycle must be undertaken with high precision to maintain a strong link between protein state and phenotype in order for the prion mechanism to serve as an effective alternate route for the inheritance of traits.

Prion variants

The misfolding of PrP has been linked to a family of related disorders with unique phenotypes in mammals (Basler et al, 1986; Goldfarb et al, 1994; Harrison et al, 2010; Prusiner, 1994). Several studies on mammalian and yeast prions explain phenotypic variability through conformational flexibility of the prion protein (Tanaka et al, 2006). The

flexibility allows prions to adopt a spectrum of self-replicating conformations (prion variants), which assemble into aggregates with discrete core amyloid structural properties (Tanaka et al, 2006). As might be predicted by the pathway of prion propagation, the properties of these prion complexes impact their efficiency of self-replication and thereby their associated phenotypes (Tanaka et al, 2006).

Prion variants have now been observed in a wide range of natural and experimental settings, but the most extensive information on mammalian prion variants has come from work on inbred mouse lines. Through these and other mammalian prion studies, it has become apparent that prion variants are distinguishable by a variety of distinct and repeatable disease characteristics. The most obvious clinical differences among variants is the incubation time between prion inoculation and illness onset, which is strikingly consistent when the same variant is inoculated into inbred mice (Bessen & Marsh, 1992; Bruce et al, 1991; Dickinson & Fraser, 1969; Dickinson & Meikle, 1969; Outram, 1976; Pattison & Millson, 1961). Other distinguishing characteristics include the type, distribution, and severity of pathological changes in the brain, location of amyloid or protease-resistant PrP deposits, ease of interspecies transmission, and resistance to heat inactivation (Bruce et al, 1989; Bruce et al, 1991; Carp et al, 1984; Dickinson & Taylor, 1978; Fraser, 1976; Kimberlin & Walker, 1978).

Mammalian prion variants

Prion strain variation was first suggested in 1961 by Pattison and Millson, who identified different phenotypes in experimentally infected goats (Pattison & Millson, 1961). This concept was later proven in inbred laboratory rodents, which also showed prion disease-specific phenotypes, brain-lesion profiles, and incubation periods (Bruce,

2003). Current evidence suggests that the main difference between prion strains lies in the different conformational arrangements that PrP^{Sc} acquires (Morales et al, 2007). These infectious particles “transmit” their particular conformational motifs to the normally folded proteins expressed in the host leading to specific disease features.

Mammalian prion variants showed differences in laboratory animal models in both clinical signs and biochemical properties. For example, incubation periods or specific patterns of spongiform degeneration in the brain are consistent when the same variant is inoculated into inbred mice (Bessen & Marsh, 1992; Bruce et al, 1991; Dickinson & Fraser, 1969; Dickinson & Meikle, 1969; Outram, 1976; Pattison & Millson, 1961). At the biochemical level, PrP^{Sc} variants differ in the electrophoretic mobility of their protein fragments generated by proteinase K digestion (Morales et al, 2007) and also glycosylation profiles (Morales et al, 2007).

In addition to disease variations in laboratory animals, naturally occurring human prion infections, such as kuru, Creutzfeldt-Jakob disease (CJD), Gerstmann-Straussler-Scheinker syndrome (GSS), fatal familial insomnia (FFI), and variant Creutzfeldt-Jakob disease (vCJD), also differ in their clinical characteristics, including behavioral abnormalities (Brown & Mastrianni, 2010), neuropathology (McLean, 2008; McLean et al, 1998; Parchi et al, 1998) and PrP^{Sc} proteolytic sensitivity (Parchi et al, 1998). Overall, these diseases may represent unique prion variants, in addition to, or dictated by, changes in PrP sequence.

As predicted by the prion hypothesis, phenotypic differences between prion variants are specified by physical differences in the prion protein. Interestingly, for mouse prion variants, amyloid thermodynamic stability is inversely related to disease severity,

with less thermodynamic stable variants displaying shorter incubation times (Legname et al, 2006; Safar et al, 1998). This intriguing link between aggregate thermodynamic stability and the prion-associated phenotype was initially interpreted as a change in the rate of conformational self-replication that is primarily mediated through differences in aggregate frangibility. However, transmissible mink encephalopathy variants display the reverse trend in the hamster model system (Ayers et al, 2011; Bessen & Marsh, 1992; Bessen & Marsh, 1994), perhaps suggesting a more complicated interplay between aggregate stability and prion-associated phenotype within a cellular context.

Yeast prion variants

Yeast prion variants have also been well studied for the [*PSI*$^{+}$], [URE3] and [*PIN*$^{+}$] prions. Interestingly, [Het-s] variants have never been observed. The [*PSI*$^{+}$] prion system in particular has been especially useful for the study of prion variants.

As introduced earlier, the yeast prion Sup35 is a translational termination factor in its normal soluble form (Cox, 1965; Paushkin et al, 1996). However, in its prion aggregated [*PSI*$^{+}$] state, its ability to terminate translation at stop codons becomes inefficient. [*PSI*$^{+}$] and [*psi*$^{-}$] can be distinguished by the suppression of a nonsense allele *ade1-14*, which has a premature stop codon in laboratory strains (Chernoff et al, 1995; Cox, 1965). The premature stop codon of *ade1-14* is read through in [*PSI*$^{+}$] cells, producing full-length Ade1 protein and therefore white colonies on rich medium (Chernoff et al, 1995; Cox, 1965). In contrast, [*psi*$^{-}$] ade1-14 cells produce a truncated Ade1 protein, resulting in red colonies on rich mediium due to the accumulation of a metabolic intermediate in the adenine synthesis pathway (Chernoff et al, 1995; Cox, 1965).

In addition to the non-prion and prion states, [*PSI*$^+$] variants are also readily detectible based on their phenotypes. [*PSI*$^+$] variants are often referred to as “strong” or “weak” for their respective degree of phenotypic severity, i.e. stop codon read through levels and mitotic stability (Uptain et al, 2001; Zhou et al, 1999). The phenotypic severity of [*PSI*$^+$] is a product of the level of functional (soluble) Sup35, which would promote recognition of the stop codon in *ade1-14*, and also the size distribution of Sup35 aggregates, which vary in their level of functionality. Therefore, weak variants of [*PSI*$^+$] appear pink on rich medium, do not grow as efficiently as strong variants on medium lacking adenine, and have higher frequencies of mitotic prion loss (Derkatch et al, 1996; Uptain et al, 2001; Zhou et al, 1999).

The efficiency of aggregate fragmentation by chaperones relative to polymer growth explains the phenotypic differences between prion variants (Tanaka et al, 2006). Strong [*PSI*$^+$] aggregates are more efficiently fragmented and therefore produce a larger number of propagons per cell, which act as new templates to convert more newly synthesized Sup35 protein into aggregates (Tanaka et al, 2006). In contrast, weak [*PSI*$^+$] aggregates are less efficiently fragmented, resulting in fewer propagons and less efficient capture of new Sup35 molecules. This explains why weak [*PSI*$^+$] variants are characterized by a larger aggregate size (Kryndushkin et al, 2003) with more non-aggregated soluble Sup35 protein (Uptain et al, 2001; Zhou et al, 1999), leading to a ‘weak’ ability to readthrough stop codons (Derkatch et al, 1996) when compared to strong [*PSI*$^+$] variants. The different efficiency of aggregate fragmentation between strong [*PSI*$^+$] and weak [*PSI*$^+$] might be explained by the fact that a large amyloid core (Toyama et al, 2007) makes weak [*PSI*$^+$] variants more physically stable and less accessible to Hsp104

than strong prion variants with a smaller amyloid core. Thus, phenotypic differences in [*PSI*$^{+}$] variants are based on biochemical properties of aggregates.

Prion protein polymorphisms and compatibility with distinct conformations

Prion sequence polymorphisms have been identified and found to impact prion persistence. For example, several PrP polymorphisms affect its susceptibility to prion disease. Moreover, there are also fungal prion mutations that modulate prion-associated phenotype. However, prion variants with different protein conformations show different sensitivities to the inhibition or protection caused by the sequence polymorphisms. Therefore, prion sequence, together with its unique protein conformations, determines the prion-associated phenotypes.

Interspecies transmission

The existence of a species barrier to prion disease has long been noted, as prion infections rarely spread from one species to another (Afanasieva et al, 2011). The interspecies barrier appears to be predominantly a product of the PrP primary sequence of the host and donor proteins, and the conformation of the donor PrP^{Sc} amyloid.

Interspecies prion transmission barriers may be due to the differences in the amino acid sequences of PrP proteins, which was verified experimentally. It was demonstrated that hamster prions efficiently infect transgenic mice with a hamster PrP gene but do not infect wild type mice (Scott et al, 1989). Notably, the prion transmission barrier is not always symmetrical: prion transmission may be robust in one direction but non-existent or very weak in the reverse direction. Barriers of interspecies prion transmission and their

asymmetry can be observed both *in vivo* and *in vitro.* For instance, infection of hamsters with mouse prion resulted in the emergence of pathological symptoms after 378 days (Kimberlin & Walker, 1978; Scott et al, 1989), while infection of mouse with hamster prions did not result in any pathological symptoms even after two years (Kimberlin et al, 1989), indicating that amino acid sequence alone could not explain the interspecies prion transmission barrier.

Besides amino acid sequence, strain conformations have also been reported to contribute to the interspecies prion transmission barriers (Bessen & Marsh, 1992). For example, nvCJD, but not conventional CJD, can be efficiently transmitted to transgenic mice producing human PrP (Hill et al, 1997).

In addition to mammal PrP, prion species barriers are also well documented for the yeast [*PSI*$^{+}$] system and mimic many of the observations made in the mammalian system. For instance, [*PSI*$^{+}$] species barriers demonstrate asymmetry (Chen et al, 2010) and variant dependency (Chen et al, 2007; Chien & Weissman, 2001; Tanaka et al, 2005; Vishveshwara & Liebman, 2009), while species specificity is influenced by the sequence used for initial seeding (Chien & Weissman, 2001). Furthermore, expression of cross-species sequences can generate novel prion variants as well as cause prion loss (Chen et al, 2007).

Altogether, both amino acid sequence and strain conformations affect the interspecies prion transmission barrier.

Prion inhibition and resistance

Variations in the amino acid sequence of prion proteins can affect their phenotypes in both mammals and yeast. For example, naturally occurring PrP polymorphisms in animals and humans or mutations found in yeast prions alter the individual's susceptibility to prion disease (Morales et al, 2007) or yeast prion persistence (Doel et al, 1994), respectively. Numerous studies have demonstrated that these effects can be explained by sequence-dependent changes in the self-replication process we introduced earlier.

The M129V and E219K polymorphisms of the human prion sequence play roles in prion inhibition. Although these polymorphisms are not directly pathogenic, heterozygosity at either of these positions is associated with resistance to sporadic Creutzfeldt-Jakob disease (Palmer et al, 1991; Shibuya et al, 1998b). Conversion of Human PrP (90–231) into mature amyloid fibrils is enhanced if position 129 encodes a valine, whereas methionine in this position promotes formation of soluble oligomers (Baskakov et al, 2005; Lewis et al, 2006; Tahiri-Alaoui et al, 2004). Studies in transgenic mouse, in tissue culture cells, and *in vitro* of these protective alleles demonstrate a dominant-negative effect on prion formation of the heterologous protein (Crozet et al, 2004; Furuya et al, 2006; Hizume et al, 2009; Kaneko et al, 1997; Lee et al, 2007; Perrier et al, 2002). Furthermore, although endogenous PrP and extra-species or chimeric PrP protein in transgenic mice are prion competent alone, they can inhibit prion disease when co-expressed, thereby also exerting dominant-negative inhibition *in vivo* (Priola & Chesebro, 1995; Telling et al, 1994; Telling et al, 1995). Given their dominant effects, it seems likely that these sequence variants perturb some aspects of the prion propagation pathway outlined above, thereby serving as a system to further probe prion self-replication *in vivo*.

To explain their potential mechanism of inhibition, a mathematical model was constructed that suggested that wild type and heterologous PrP could incorporate into the same fiber, thus altering fiber properties. For example, the polymorphic proteins could act as “end-blocking drugs” precluding the additional binding or conversion of heterologous protein onto the fiber and thereby being effective at a lower expression ratio. Alternatively, polymorphic proteins could affect other aspects of prion self-replication such as fragmentation, thus requiring incorporation throughout the complex which requires higher effective concentrations (Masel & Jansen, 2000).

Dominant inhibitory mutations have also been isolated in fungal prions and, as is the case for PrP polymorphisms, these mutations also affect conformational self-replication *in vivo*, thereby changing the protein-based traits (DePace et al, 1998). For the [*PSI*$^{+}$] prion, some substitutions, known as [*PSI*$^{+}$]-no-more (PNM) mutations, induce prion loss (Doel et al, 1994). The most extensively studied PNM mutation is G58D (PNM2), which encodes a Sup35 Gly58Asp mutation (Doel et al, 1994). This mutant Sup35 incorporates into wild type [*PSI*$^{+}$] complexes (Derkatch et al, 1999; DiSalvo et al, 2011) and induces prion loss over many generations (Doel et al, 1994; Osherovich et al, 2004), suggesting that this variant might interfere with the replication of prion complexes and/or their transmission to daughter cells.

Various models have been proposed to explain the dominant-negative activity of prion protein mutants, but controversies persist about the actual mechanism of inhibition. In two recent studies, G58D inhibition was linked to either an enhancement of the fragmentation reaction that led to dissolution of prion aggregates (DiSalvo et al, 2011), or to a failure to transmit existing aggregates to daughter cells upon division that blocked

the spread of the aggregates in the population (Verges et al, 2011). These studies used different conformations of the prion protein, raising the possibility that the mutants could impact prion propagation through distinct pathways depending upon conformation, a hypothesis that will be explored in this dissertation.

Conformational evolution, mutation, adaptation

Prions exhibit metastability allowing for new traits to arise, endure, transmutate, or disappear within the lifetime of an individual due to the dynamics of protein conformations. Favorable prion conformations can be selected and propagate depending on the environmental changes caused either by interspecies transmission or pharmacological treatment.

Interspecies transmission

Interspecies transmission can alter the conformation of the prion. For example, the scrapie symptoms in mice when sheep prion was directly transmitted was different from the scrapie symptoms when sheep scrapie is transmitted to mice with an intermediary passage in white rats (Pattison & Jones, 1968). Prion variants can also be passaged between different species *in vitro* using amyloid seed and monomeric PrP of different species. *In vitro* passaging of amyloid fibers with monomeric PrP of a new species creates amyloids that have increased infectivity to the new species *in vivo* (Castilla et al, 2008; Green et al, 2008). These observations indicated that the infectious agent can experience changes in a new host, though the nature of these induced changes is not clear. As more and more cases of this scrapie “mutation” were observed (Bruce & Dickinson, 1987), it

became apparent that such changes of prion characteristics were not an exceptional occurrence (Bruce & Dickinson, 1987; Kimberlin & Walker, 1986).

Pharmacological treatment

Previous studies indicate that even sensitive conformational variants can develop resistance to anti-prion compounds. For example, swainsonine-sensitive 22L prions could develop resistance to swainsonine (Li et al, 2010; Mahal et al, 2010). An evolutionary conformational selection mechanism for PrP^{Sc} may explain the observed drug-induced evolution of mammalian prions (Oelschlegel & Weissmann, 2013). Different prion-infected cell sub-lines were exposed to swainsonine and both drug-resistant and drug-dependent prion populations that propagated more rapidly in the presence rather than the absence of the drug were observed. Moreover, the new, initially drug-dependent prions became new stable prion variants after drug withdrawal. The prion adaptations are most likely driven by the conformational selection mechanism, and this metastability calls for the reevaluation of different therapeutic strategies that target amyloid-forming aggregates of PrP^{Sc}.

Prion curing

Given the physical differences among prion variants, it is straightforward to predict that aggregates composed of these variants direct distinct biological outcomes through modulating different prion propagation steps. However, predicting the exact way that these alterations will manifest as a new phenotype is quite complicated due to the interdependency of each step in the pathway.

Modulation of prion cycle alters biological outcomes – inhibiting synthesis

It has been reported that blockage of new protein synthesis can reverse established prion phenotypes. Specifically, the neuroinvasive prion infection with spongiform change and prion disease progression in mammals can be reversed through inhibition of new PrP expression (Mallucci et al, 2003; Mallucci et al, 2007; White et al, 2008). For yeast [*PSI*$^{+}$], when the N or NM prion forming domains are deleted, strains that normally propagate [*PSI*$^{+}$] became unable to do so (Ter-Avanesyan et al, 1994). Thus, synthesis of new protein plays an important role in prion persistence.

GdnHCl – inhibit fragmentation

Fragmentation is required to generate templates (Bailleul et al, 1999; Byrne et al, 2007; Cox et al, 2003; Eaglestone et al, 2000; Ness et al, 2002). The loss of fragmentation reduces the number of templates and leads to the growth of aggregates, which them limits their transmissibility. For example, GdnHCl inhibits the activity of Hsp104, which is required for yeast prion propagation as we discussed earlier (Ferreira et al, 2001; Jung & Masison, 2001). [*PSI*$^{+}$] is then lost by dilution of preexisting inheritable [*PSI*$^{+}$] "seeds" among progeny during cell division, eventually leading to [*psi*$^{-}$] cells.

Heat shock – enhance fragmentation

In *Saccharomyces cerevisiae*, a transit heat shock induces [*PSI*$^{+}$]^{Weak} prion loss through disassembly of existing Sup35 amyloids (Klaips et al, 2014). According to recent studies, the increase in Hsp104 expression at elevated temperature (Escusa-Toret et al, 2013; Klaips et al, 2014; Sanchez et al, 1992) alone is not sufficient to induce Sup35 amyloid resolution and [*PSI*$^{+}$]^{Weak} curing (Klaips et al, 2014). Rather, Hsp104 is

asymmetrically retained in mother cells (Klaips et al, 2014), and this increase in chaperone accumulation, along with elevated expression level, promotes curing in the mother cells (Klaips et al, 2014).

Dominant-negative mutants – changes in chaperone: aggregate ratio

At normal levels, Hsp104 is responsible for propagation of the prion polymers via subsequent cycles of breakage and growth. More effective aggregate resolution within cells would be predicted to occur if the chaperone-to-aggregate ratio is higher. For example, expression of the dominant-negative mutant G58D leads to prion loss in daughter cells (DiSalvo et al, 2011; Verges et al, 2011). It is possible that prion loss in daughter cells resulted from imbalance of chaperone: aggregate ratio. As less aggregates were inherited by daughter cells, either by enhanced fragmentation in mother cells (DiSalvo et al, 2011) or by inefficient transmission (Verges et al, 2011), the chaperone-to-aggregate ratio shifted and led to the disassembly of Sup35 aggregates in daughter cells, a hypothesis that will be explored in this dissertation.

Protein inheritance

Similar to prion aggregates, oxidatively damaged protein aggregates are inherited asymmetrically. Although the machinery of aggregated protein transmission was unknown, alterations in transmission can change the associated phenotypes.

Prion aggregate

It was proposed that the propensity of prion transmission to the daughter cell partly depends on the size of the diffuse oligomers (Derdowski et al, 2010). In this model, larger

aggregates are less transmissible to the next generations, whereas smaller oligomers are more transmissible. By contrast, the monomeric form of Sup35 is the easiest to transmit.

The proposal that there is a transmission bias, even in the presence of functional Hsp104, might extend to yeast prion 'strains' and other amyloid-forming protein phenomena. [*PSI*$^{+}$] has multiple phenotypic strains, including strong and weak [*PSI*$^{+}$]. The fibrils that cause the strong [*PSI*+] are known to be fragile, resulting in their smaller size (Tanaka et al, 2006). Size-dependent transmission explains why the strong phenotype is more mitotically stable than the weak phenotype (Derkatch et al, 1996).

In addition, GdnHCl treatment causes prion loss, which could be explained by blockage of transmission, as GdnHCl inhibits fragmentation and thus leads to larger aggregate accumulation within mother cells (Kryndushkin et al, 2003). The preferential retention of the large aggregates in the mother cells results in prion loss upon cell division (Derdowski et al, 2010).

Damaged protein aggregates and chaperones

In addition to prion aggregates, oxidatively damaged proteins that colocalize with Hsp104-GFP (Erjavec et al, 2007) are inherited asymmetrically during yeast cytokinesis (Erjavec et al, 2007; Liu et al, 2010). This phenomenon was revealed by *in situ* detection of protein carbonyls or Hsp104-GFP in single yeast cells (Aguilaniu et al, 2003; Erjavec et al, 2007). A distinctively asymmetrical distribution of carbonylated proteins was found in mother cells during yeast cytokinesis. Also, damaged protein caused by elevated temperature were also asymmetrically distributed between mother and daughter cells (Liu et al, 2010). Once the damaged protein was formed in cells, the cells respond to this stress by elevating the expression of PQC (Protein Quality Control) factors, including

Hsp104 (Morimoto, 2011). Mother cells exposed to heat retain most of the Hsp104, which is associated with the damaged proteins when these cells divide. This retention allows Hsp104 to accumulate to a level required for the breakdown of amyloid aggregates. (Klaips et al, 2014). Various models have been raised to explain the damage asymmetry mechanism (discussed in “Asymmetric inheritance of damaged protein in yeasts”), which is accomplished by a spatial PQC involving Hsp104.

The relationship of Sir2 protein and aggregate inheritance and aging

Sir2 protein was reported to mediate damage asymmetry and thereby the rejuvenation process. Although several studies illustrate the complicated networking regulated by Sir2, little is known about how Sir2 regulates the damage asymmetry process. Identifying the downstream target of Sir2 that is responsible for this process might further our understanding of the machinery of aggregate transmission.

Sir2 protein and chromatin silencing

Sir2 encodes an NAD+-dependent deacetylase involved in chromatin silencing (Blander & Guarente, 2004; Imai et al, 2000; Rusche et al, 2003) that facilitates transcriptional silencing at cryptic mating type loci HML and HMR, at telomeres, and at the rDNA locus (Fritze et al, 1997). This silencing regulates the processes of recombination, genomic stability, and aging. Sir2 is one of four “Silent Information Regulator” genes in yeast but is the only one that is highly conserved from archaea to humans (Dutnall & Pillus, 2001).

Silencing at HML, HMR, and heterochromatic telomeres is mediated by the Sir complex, comprised of the two structural proteins Sir3 and Sir4, and Sir2 which is the enzymatic component (Moazed et al, 1997). The Sir complex does not bind DNA directly; instead it is recruited to regulatory chromosomal domains and the Origin Recognition Complex via other factors (Rusche et al, 2003). Once a silencing complex is bound to a nucleosome, Sir2 deacetylates the histone tails of H3 and H4 of the adjacent nucleosome (Rusche et al, 2003). Because the Sir proteins have a higher affinity for H3 and H4 with reduced acetylation, deacetylation creates a binding site for an additional silencing complex. This process repeats until Sir complexes are spread across the entire chromatin region to be silenced (Rusche et al, 2003).

Sir2 also represses rDNA loci and affects their chromatin structure and silencing in a dose-dependent manner (Fritze et al, 1997; Gottlieb & Esposito, 1989; Smith et al, 1998). Sir2 may play a role in slowing the aging of yeast cells by preventing the formation of extrachromosomal rDNA circles (ERCs) that form through homologous recombination within rDNA arrays, one likely cause of yeast cell aging (Kaeberlein et al, 1999; Park et al, 1999).

Sir2 protein controls asymmetric damage protein retention

As introduced earlier, damaged proteins are inherited asymmetrically during yeast cytokinesis (Aguilaniu et al, 2003; Erjavec et al, 2007). Similar to yeast, accumulating evidence suggests that mammalian cells also asymmetrically segregate cellular components including genomic DNA, organelles, and damaged proteins during cell division (Moore & Jessberger, 2017). Studies investigating the segregation of aggregates in mammalian cells during asymmetric division have suggested that the inheritance of

aggregates to the ‘other’ daughter cell may improve cellular fitness for the proliferating, stem, or longest-lived daughters (Bufalino & van der Kooy, 2014; Ogrodnik et al, 2014; Rujano et al, 2006). However, the question that remains unanswered in both yeast and mammals is the mechanism of asymmetric retention.

The Sir2 protein was reported to control asymmetric damaged-protein retention in yeast cells based on experiments comparing the distribution of carbonylated proteins or Hsp104-GFP aggregates during cell division between wild type and *Δsir2*; these studies found that asymmetric inheritance was disrupted in *Δsir2*. (Aguilaniu et al, 2003; Erjavec et al, 2007). Given the polarized spatial distribution of F-actin during cytokinesis, the actin cytoskeleton was suggested to be required for proper segregation of damaged proteins (Aguilaniu et al, 2003). This idea was supported by additional experimental evidence demonstrating that inhibition of actin assembly by latrunculin A (Lat-A) abolished the ability of wild-type mother cells to retain oxidized proteins (Aguilaniu et al, 2003).

However, the specific mechanism by which damaged proteins are asymmetrically inherited still remains controversial. In the retrograde transport model, protein aggregates formed upon heat shock in emerging buds are transported back to the mother cells, an idea that was proposed based on real-time imaging showing that aggregates formed in the daughter compartment during heat shock relocalized into the mother cells (Liu et al, 2010). Furthermore, screening of mutants suggested that retrograde transport of protein aggregates from daughter cells to mother cells is an actin cable-dependent rather than actin patch-dependent process (Liu et al, 2010). Contradicting the retrograde transport model, the dynamics of Hsp104-associated protein aggregates were examined by video microscopy, particle tracking and image correlation analysis (Zhou et al, 2011). These

studies showed that protein aggregates undergo random walk without directional bias. Moreover, clearance of heat-induced aggregates from the bud does not depend on the formin proteins but occurs mostly through dissolution via Hsp104p chaperone (Zhou et al, 2011). Aggregates formed naturally in aged cells also exhibit random walk but do not dissolve during the observation (Zhou et al, 2011). These data indicate the absence of a role for actin or cell polarity in aggregate segregation; modeling suggests that their asymmetric inheritance can be a predictable outcome of aggregates' slow diffusion and the geometry of yeast cells (Zhou et al, 2011). However, a new study by Spokoini et al. now shows that confinement of protein aggregate motion through association with the JUNQ (juxtanuclear quality control) and IPOD (insoluble protein deposit) compartments on the surface of the nucleus and vacuole, respectively, is important for the asymmetric inheritance of misfolded proteins (Spokoini et al, 2012). Similarly, protein aggregates formed on the ER are frequently also associated with or are later captured by mitochondria, greatly constraining aggregate mobility (Zhou et al, 2014). During mitosis, aggregates are tethered to well-anchored maternal mitochondria, whereas mitochondria acquired by the bud are largely free of aggregates (Zhou et al, 2014).

Although the machinery of damage asymmetry was unknown, this process has been suggested to be important for both aging- and heat shock-induced prion curing as we discussed earlier. However, the role of Sir2 in heat shock induced prion curing was not known, as Sir2 mediates damage asymmetry (Aguilaniu et al, 2003; Erjavec et al, 2007; Liu et al, 2010). Further studies of this system would shed light on the machinery of damage asymmetry and would elucidate the mechanism of prion aggregate dissolution upon thermal stress.

Summary of Dissertation Studies

I. Controversies persist about the actual mechanism of dominant-negative inhibition of prion propagation with either an enhancement of the fragmentation reaction or a failure to transmit existing aggregates to daughter cells upon division proposed as competing models (DiSalvo et al, 2011; Verges et al, 2011). To resolve this controversy, we have compared the mechanism of prion curing in the [*PSI*$^{+}$]^{Sc4}, [*PSI*$^{+}$]^{Sc37} and [*PSI*$^{+}$]^{Weak} Sup35 strains. Our studies indicate that the G58D mutant inhibits propagation of all Sup35 conformations through a common mechanism: an enhancement of fragmentation which leads to Sup35 aggregate disassembly in daughter cells. Despite these mechanistic commonalities, the ratio of mutant to wild type protein required for dominant-negative inhibition correlates with differences in the basal kinetic stabilities of the Sup35 aggregates. Thus, the conformational variation does not modulate the mechanism by which the inhibition occurs but rather modulates the sensitivity of these strains to prion loss by enhanced fragmentation.

II. To further understand the mechanism underlying aggregates asymmetric retention and its impact on heat-induced prion curing, we explored the effect of Sir2, which mediates damage asymmetry, on heat-induced prion curing. Our studies revealed that deletion of Sir2 led to a reduction of heat-induced prion curing. This loss of curing correlated with a disruption of asymmetric inheritance of total Hsp104, which could be explained by the derepression of HM loci. Further studies on mating type-regulated genes controlled by HM loci indicates that *yjl133c-a* was required for the reduction of heat-induced prion curing.

Chapter 2: A dominant-negative mutant inhibits multiple prion variants through a common mechanism

This chapter has been prepared as a manuscript and submitted to *PLoS Genetics*.

Abstract

Prions adopt alternative, self-replicating protein conformations and thereby determine novel phenotypes that are often irreversible. Nevertheless, dominant-negative prion mutants can revert phenotypes associated with some conformations. These observations suggest that, while intervention is possible, distinct inhibitors must be developed to overcome the conformational plasticity of prions. To understand the basis of this specificity, we determined the impact of the G58D mutant of the Sup35 prion on three of its conformational variants, which form amyloids in *S. cerevisiae*. G58D had been previously proposed to have unique effects on these variants, but our studies suggest a common mechanism. All variants, including those reported to be resistant, are inhibited by G58D but at distinct doses. G58D lowers the kinetic stability of the associated amyloid, enhancing its fragmentation by molecular chaperones, promoting Sup35 resolubilization, and leading to amyloid clearance particularly in daughter cells. Reducing the availability or activity of the chaperone Hsp104, even transiently, reverses curing. Thus, the specificity of inhibition is determined by the sensitivity of variants to the mutant dosage rather than mode of action, challenging the view that a unique inhibitor must be developed to combat each variant.

Author Summary

Prion proteins adopt alternative conformations and assemble into amyloid fibers, which have been associated with human disease. These fibers are highly stable and self-replicate, leading to their persistence and resulting in a set of progressive and often fatal disorders. Inhibitors have been shown to interfere with some conformations but not others, suggesting that distinct strategies must be developed to target each. However, we show here that a single dominant-negative mutant can inhibit multiple conformations of the same prion protein through the same pathway but at distinct doses. Thus, the basis of this specificity is sensitivity rather than resistance to the mechanism of inhibition, suggesting that common strategies may be used to target a range of prion conformations.

Introduction

Alternative, self-replicating protein conformations have emerged as *bona fide* parallel protein-folding trajectories with significant biological consequences (Tuite & Serio, 2010). In most cases, these alternative conformations are β-sheet-rich and self-assembling, forming linear amyloid aggregates (Knowles et al, 2014). These amyloids replicate the conformation of their constituent monomers by acting as templates to direct the refolding of other conformers of the same protein as they are bound by and incorporated into the growing aggregate. In so doing, the majority of the protein is converted to the alternative conformation, changing protein activity and thereby inducing new phenotypes, such as neurodegenerative diseases (i.e., Transmissible Spongiform Encephalopathies or prion diseases, Alzheimer's and Huntington's diseases) and organelle biogenesis in mammals and gene expression regulation in single-celled organisms (Knowles et al, 2014; Tuite & Serio, 2010; Yuan & Hochschild, 2017). The high efficiency of this process, when combined with the high kinetic stability of the aggregates (Knowles et al, 2014), contributes to the recalcitrance of amyloids to clearance by protein quality control pathways (Landreh et al, 2016). As a result, the associated phenotypes are frequently difficult - if not impossible - to reverse, especially in the clinic (Trevitt & Collinge, 2006).

One notable exception to the persistence of amyloid-associated phenotypes is their reversal or "curing" by dominant-negative mutants of prion proteins. These sequence variants were first identified by their ability to confer resistance to scrapie in sheep (Q171R or R154H in the mammalian prion protein PrP), sporadic Creutzfeldt-Jakob disease (sCJD) in humans (E219K in PrP), and translation termination infidelity in yeast (G58D in

Sup35) (Belt et al, 1995; Clouscard et al, 1995; Dawson et al, 1998; Doel et al, 1994; Goldmann et al, 1994; Hizume et al, 2009; Ikeda et al, 1995; Jeong et al, 2005; Laplanche et al, 1993; Nozaki et al, 2010; Shibuya et al, 1998a; Tranulis, 2002; Westaway et al, 1994). Subsequently, these mutants were shown to interfere with the assembly of amyloid by the wild type prion protein *in vitro* and to reduce or clear existing amyloid composed of the wild type prion protein when delivered to tissue culture cells, mice, or yeast (Atarashi et al, 2006; Crozet et al, 2004; Doel et al, 1994; Eiden et al, 2011; Furuya et al, 2006; Geoghegan et al, 2009; Hizume et al, 2009; Kishida et al, 2004; Kochneva-Pervukhova et al, 1998; Lee et al, 2007; Paludi et al, 2007; Perrier et al, 2002; Toupet et al, 2008). Given this unique curing ability, elucidating the mechanism(s) by which dominant-negative prion mutants act may reveal potential strategies for reversing amyloid persistence more generally.

Despite the promise of this line of investigation, the inhibition achieved by dominant-negative mutants appears to be conformation-specific. For example, the resistance to sCJD conferred by the E219K PrP mutant in humans is not extended to the conformations, known as variants, responsible for genetic and iatrogenic forms of the disease (Hizume et al, 2009; Kobayashi et al, 2015; Lukic et al, 2010; Noguchi-Shinohara et al, 2007; Nozaki et al, 2010; Shibuya et al, 1998a; Yamada et al, 2009). Similarly, resistance to classical scrapie is not observed for the bovine spongiform encephalopathy (BSE) or atypical scrapie variants in sheep with Q171R or R154H mutations in PrP (Andreoletti et al, 2006; Benestad et al, 2008; Buschmann et al, 2004; Foster et al, 2001; Gavier-Widen et al, 2004; Goldmann et al, 1994; Hope et al, 1999; Houston et al, 2003; Jacobs et al, 2011; Langeveld et al, 2015; Luhken et al, 2004; Madec et al, 2004; Onnasch

et al, 2004; Orge et al, 2004; Orge et al, 2010; Ronzon et al, 2006; Somerville et al, 1997). Finally, the G58D mutation of Sup35 cures the [*PSI*$^{+}$]^{Strong} and [*PSI*$^{+}$]^{Sc4} variants (*n.b.* [*PSI*$^{+}$] denotes the transmissible amyloid state of Sup35) to different extents in different genetic backgrounds but is unable to cure the [*PSI*$^{+}$]^{Sc37} and [*PSI*$^{+}$]^{Weak} variants in yeast (Derkatch et al, 1999; Verges et al, 2011).

What is the molecular basis of this differential inhibition? One possibility is that the distinct recognition surfaces and/or rate-limiting steps in the self-replication process characteristic of the variants make them susceptible to only certain mechanisms of inhibition (Eisenberg & Sawaya, 2017; King, 2001; Sievers et al, 2011; Tanaka et al, 2005; Tanaka et al, 2006; Tessier & Lindquist, 2007; Zampieri et al, 2009). Alternatively, the conformational differences may confer distinct sensitivities to the same mechanism of inhibition. Given the conformational plasticity of amyloidogenic proteins (Ghaemmaghami, 2016; Shorter, 2010), understanding the forces limiting the efficacy of inhibitors can mean the difference between developing an infinite number of individual interventions for each variant or simply different dosing regimes for the same inhibitor.

Here, we exploit the yeast prion Sup35 to gain this insight. We explored the sensitivity of three variants of Sup35 (i.e., [*PSI*$^{+}$]^{Sc4}, [*PSI*$^{+}$]^{Weak}, and [*PSI*$^{+}$]^{Sc37}) to expression of G58D and the impact of this dominant-negative mutant on the self-replication of each variant. Our studies indicate that “resistance” to G58D can be partially overcome at higher dosage of the mutant, revealing differential sensitivity to the inhibition. G58D reduces the kinetic stabilities of the amyloids associated with the variants, which determines their efficiencies of fragmentation by chaperones (Tanaka et al, 2006). Consistent with this correlation, G58D inhibition of the three variants was dependent on

the chaperone Hsp104, as was the case for the previously studied [*PSI*$^{+}$]^{Strong} variant (DiSalvo et al, 2011). In the presence of G58D, Sup35 amyloid was fragmented by Hsp104 with higher efficiency. This increase led to amyloid clearance in daughter cells, which could be reversed by transient inhibition of Hsp104 specifically in this population. Thus, G58D dominant-negative inhibition targets distinct conformational variants through the same mechanism with differing efficacy, suggesting that the observed “resistance” is relative rather than absolute.

Results

[PSI^{+}] variants are inhibited at distinct doses of G58D

To determine if the specificity of G58D on [*PSI*$^{+}$] variants occurs through distinct mechanisms or through distinct sensitivities to the same mechanism of inhibition, we generated diploid [*PSI*$^{+}$]^{Sc4}, [*PSI*$^{+}$]^{Weak} and [*PSI*$^{+}$]^{Sc37} yeast strains expressing wild type Sup35 at different ratios relative to G58D (2:1, 1:1, 1:2; S1 Fig). Inhibition of [*PSI*$^{+}$] propagation can be monitored functionally because the formation of amyloid by Sup35 partially compromises its activity and leads to a defect in translation termination (Patino et al, 1996; Paushkin et al, 1996). [*PSI*$^{+}$] strains carrying the *ade1-14* allele form white colonies on rich medium due to read-through of a premature stop codon in the *ADE1* open reading frame. However, strains with defective prion propagation, or those that have lost the prion state (known as [*psi*$^{-}$]), form red colonies on rich medium as a result of the accumulation of active Sup35 (Chernoff et al, 1995).

Expression of G58D at any ratio in a [*PSI*$^{+}$]^{Sc4} strain promoted the accumulation of red pigment on rich medium, indicating reversal of the prion phenotype (Fig 1A). By colony color, the severity of this effect increased with G58D dosage, with a 1:2 ratio of wild type to G58D leading to a colony phenotype for [*PSI*$^{+}$]^{Sc4} that was indistinguishable from [*psi*$^{-}$] (Fig 1A). For the [*PSI*$^{+}$]^{Sc37} and [*PSI*$^{+}$]^{Weak} variants, which were previously reported to be compatible with G58D expression (Derkatch et al, 1999; Verges et al, 2011), efficient prion propagation was also dependent on the ratio of wild type to G58D, but the critical threshold for phenotypic reversal was distinct in each case. The [*PSI*$^{+}$]^{Sc37} variant formed colonies that were more pink on rich medium at a 1:1 ratio of wild type to G58D relative to a wild type strain and that were indistinguishable from [*psi*$^{-}$] at a 1:2 ratio of wild type to G58D (Fig 1B), mirroring our observations for [*PSI*$^{+}$]^{Sc4} (Fig 1A). In contrast, the [*PSI*$^{+}$]^{Weak} variant phenotype was only partially reversed at the highest ratio of wild type to G58D tested (1:2), where the pinker colonies on rich medium relative to the wild type [*PSI*$^{+}$]^{Weak} strain indicated a mild inhibition by G58D (Fig 1C). Thus, the three [*PSI*$^{+}$] variants are each dominantly inhibited by G58D expression in a dose-dependent manner, but the dose required for inhibition of [*PSI*$^{+}$]^{Sc4} and [*PSI*$^{+}$]^{Sc37} is lower than that of [*PSI*$^{+}$]^{Weak}.

To assess whether reversal of the [*PSI*$^{+}$] phenotype upon G58D expression reflected prion loss (i.e., curing), we determined the frequencies of [*psi*$^{-}$] appearance during mitotic division for each strain. [*PSI*$^{+}$] propagation was largely stable at the 2:1 (~0% curing) and 1:1 (~1% curing) ratios of wild type to G58D for both [*PSI*$^{+}$]^{Sc4} and [*PSI*$^{+}$]^{Sc37}, where the colony phenotype was only mildly reversed (Fig 1A, 1B, 1D, 1E). At a 1:2 ratio of wild type to G58D, both [*PSI*$^{+}$]^{Sc4} (~9% curing, Fig 1D) and [*PSI*$^{+}$]^{Sc37} (~8%

curing, Fig 1E) were more unstable, consistent with the stronger reversal of their prion phenotypes at this ratio (Fig 1A, 1B). For the [*PSI*$^{+}$]^{Weak} variant, which is less sensitive to G58D inhibition (Fig 1C), [*PSI*$^{+}$] propagation was stable at all wild type:G58D ratios tested (Fig 1F). Thus, [*PSI*$^{+}$] curing in diploids expressing G58D parallels the severity of the phenotypic reversal in all three variants and, for the most sensitive strains (i.e., [*PSI*$^{+}$]^{Sc4} and [*PSI*$^{+}$]^{Sc37}), arises in a dose-dependent manner. Together, these observations indicate that the previously described "resistance" of [*PSI*$^{+}$]^{Sc37} and [*PSI*$^{+}$]^{Weak} to curing by G58D expression reflected their higher threshold for sensitivity rather than their absolute recalcitrance to inhibition by this mutant.

G58D reduces the kinetic stability of Sup35 aggregates from all [PSI^{+}] variants

Although the three [*PSI*$^{+}$] variants studied here, in addition to the previously studied [*PSI*$^{+}$]^{Strong} variant (DiSalvo et al, 2011), differ in their sensitivities to G58D inhibition (Fig 1), the dose dependence of this inhibition suggests a common underlying mechanism (DiSalvo et al, 2011; Masel et al, 1999). We previously linked G58D inhibition to a reduction in the kinetic stability of Sup35 aggregates and a resulting increase in their fragmentation by the chaperone Hsp104, which led to their disassembly (DiSalvo et al, 2011). In this model, the distinct effective inhibitory ratios of G58D on [*PSI*$^{+}$] variants may reflect the impact that this mutant has on the kinetic stability of each. While it has been well-established that Sup35 aggregates in the [*PSI*$^{+}$]^{Sc4} conformation are of lower stability than those in the [*PSI*$^{+}$]^{Sc37} conformation, the relative stabilities of the four variants have not been previously reported (Dong et al, 2010; Tanaka et al, 2006; Toyama et al, 2007).

To gain this insight, we first determined the kinetic stabilities of Sup35 aggregates, in the absence of G58D, by their sensitivity to disruption with 2% SDS at different

temperatures as a baseline comparison (Manning & Colon, 2004). Solubilized protein is then quantified by entry into a SDS-polyacrylamide gel and immunoblotting (DiSalvo et al, 2011). For wild type strains, Sup35 was efficiently released from aggregates between 65°C and 75°C in lysates from strains propagating the [*PSI*$^{+}$]^{Strong} and [*PSI*$^{+}$]^{Sc4} variants (Fig 2A) or between 70°C and 90°C in lysates from strains propagating the [*PSI*$^{+}$]^{Weak} and [*PSI*$^{+}$]^{Sc37} variants (Fig 2B). The higher kinetic stability of the latter variants is consistent with their lower efficiency of fragmentation, which leads to a larger steady-state size for their associated amyloids as assessed by semi-denaturing agarose gel electrophoresis (SDD-AGE) and immunoblotting for Sup35 (Fig S2) (Derdowski et al, 2010; Tanaka et al, 2006).

To sensitize the assay in an attempt to reveal biochemical differences between the variants in each group, we deleted the *NATA* N-terminal acetyltransferase, which reduces the kinetic stability of Sup35 amyloid in [*PSI*$^{+}$] strains (Holmes et al, 2014; Pezza et al, 2009). In this genetic background, the fraction of soluble Sup35 released from amyloid of the [*PSI*$^{+}$]^{Strong} variant in the presence of SDS was significantly increased relative to that from the [*PSI*$^{+}$]^{Sc4} variant over the same temperature range (Fig 2C), indicating that the aggregates are less kinetically stable in the [*PSI*$^{+}$]^{Strong} than the [*PSI*$^{+}$]^{Sc4} variant. Similarly, a significantly larger fraction of Sup35 was released from amyloid in the presence of SDS from the [*PSI*$^{+}$]^{Sc37} variant than from the [*PSI*$^{+}$]^{Weak} variant (Fig 2D), indicating that the aggregates are less kinetically stable in the [*PSI*$^{+}$]^{Sc37} than the [*PSI*$^{+}$]^{Weak} variant. Thus, the kinetic stability of Sup35 aggregates in [*PSI*$^{+}$] variants increases in the order [*PSI*$^{+}$]^{Strong}, [*PSI*$^{+}$]^{Sc4}, [*PSI*$^{+}$]^{Sc37}, [*PSI*$^{+}$]^{Weak}.

If G58D inhibits these variants through a common mechanism, we would expect the kinetic stabilities of each of the variants to decrease in the presence of the mutant. To test this possibility, we assessed the sensitivity of Sup35 aggregates, isolated from diploid strains expressing a 1:1 ratio of wild type to G58D, to disruption with 2% SDS at different temperatures. Soluble protein was then quantified by entry into an SDS-polyacrylamide gel and immunoblotting for Sup35. For the [*PSI*$^{+}$]^{Sc4} strain, G58D expression increased the amount of soluble Sup35 released from aggregates at all temperatures assayed (65°C, 70°C and 75°C) in comparison with a wild type strain (Fig 3A). G58D similarly promoted Sup35 release from aggregates isolated from the [*PSI*$^{+}$]^{Sc37} (Fig 3B) and [*PSI*$^{+}$]^{Weak} (Fig. 3C) strains at 80°C and 85°C, but the magnitude of this effect was greater for the former. Thus, G58D incorporation destabilizes Sup35 aggregates from [*PSI*$^{+}$] variants in a manner that correlates directly with the severity of their phenotypic inhibition (Fig 1). These observations are consistent with the idea that G58D acts through a similar mechanism to inhibit the [*PSI*$^{+}$] variants.

Dominant inhibition of [PSI^{+}] variants by G58D depends on Hsp104

A decrease in the kinetic stability of amyloid should increase its efficiency of fragmentation and potentially lead to its clearance. To begin to determine the effects of G58D on the fragmentation of Sup35 amyloid associated with these [*PSI*$^{+}$] variants, we first assessed the steady-state size distributions of these complexes by SDD-AGE and immunoblotting for Sup35. As we have previously observed for [*PSI*$^{+}$]^{Strong} (DiSalvo et al, 2011), expression of G58D at any ratio relative to wild type Sup35 in a [*PSI*$^{+}$]^{Sc4} strain led to a decrease in the accumulation of slowly migrating aggregates in comparison to the same dose of wild type protein alone (Fig 3D). For [*PSI*$^{+}$]^{Sc37}, similar decreases were

observed (Fig 3E), but for [*PSI*$^{+}$]^{Weak}, Sup35 aggregates were only shifted to smaller complexes at the lowest wild type to G58D ratio tested (1:2, Fig 3F). Together, these observations suggest that the kinetic destabilization of Sup35 aggregates by G58D results in a higher efficiency of fragmentation *in vivo*, and these effects correlate directly with the severity of their phenotypic inhibition (Fig 1).

To determine how the kinetic destabilization of Sup35 aggregates by G58D impacts the number of heritable prion units (propagons) in [*PSI*$^{+}$]^{Sc4}, [*PSI*$^{+}$]^{Sc37} and [*PSI*$^{+}$]^{Weak} strains, we used a genetic assay [75]. Specifically, diploid strains expressing either two copies of wild type *SUP35* or one copy each of wild type *SUP35* and *G58D* were treated with guanidine HCl (GdnHCl), a potent inhibitor of the fragmentation catalyst Hsp104 [67,76-81], allowed to dilute existing aggregates through cell division, and plated in the absence of the inhibitor to quantify the number of cells inheriting an aggregate. As we have previously observed in a [*PSI*$^{+}$]^{Strong} strain (DiSalvo et al, 2011), G58D expression in either [*PSI*$^{+}$]^{Sc4} and [*PSI*$^{+}$]^{Sc37} diploids reduced propagon number by factors of ~2 and ~4, respectively (Fig 3G, H), consistent with the reversal of the [*PSI*$^{+}$] phenotype and the loss of [*PSI*$^{+}$] that we observed in these strains (Fig 1A, B, D, E). In contrast, G58D expression in [*PSI*$^{+}$]^{Weak} increased propagon number by a factor of ~2.5 (Fig 3I). Although we did not detect any changes in the severity or stability of the [*PSI*$^{+}$]^{Weak} phenotype at this ratio (Fig 1C, F), this increase in propagon count provides an explanation for the previously reported strengthening of the [*PSI*$^{+}$]^{Weak} phenotype upon G58D expression to much higher levels (Derkatch et al, 1999). Phenotypic strengthening is associated with a decrease in soluble Sup35, which would result from an increase in amyloid templates, detected as propagons in this assay, through enhanced fragmentation

(Tanaka et al, 2006). Thus, the phenotypic consequences of G58D expression, both inhibition and enhancement, can be directly explained by changes in the steady-state accumulation of Sup35 propagons. Given the distinct kinetic stabilities of Sup35 amyloid in the [*PSI*$^{+}$] variants studied here (Fig 2), the specificity of G58D inhibition and enhancement likely reflect thresholds for fragmentation activity that result in changes in the steady-state accumulation of Sup35 forms *in vivo*.

If enhanced fragmentation is indeed the mechanism underlying G58D effects, these changes should be Hsp104-dependent. To determine if this is the case, we constructed heterozygous disruptions of *HSP104* in diploid strains expressing G58D at different ratios (Fig S3). In strains expressing only wild type Sup35, heterozygous disruption of *HSP104* significantly decreased the number of propagons in the [*PSI*$^{+}$]^{Sc4} and [*PSI*$^{+}$]^{Sc37} variants tested (Fig 3G-H, compare lanes 1 and 3), consistent with its catalytic role in fragmentation (Ness et al, 2002; Satpute-Krishnan et al, 2007) and the size threshold for Sup35 aggregate transmission (Derdowski et al, 2010). In contrast, heterozygous disruption of *HSP104* in [*PSI*$^{+}$] variant strains expressing both wild type and G58D Sup35 increased the number of propagons (Fig 3G-I, compare lanes 2 and 4). Thus, the reduction in propagon number associated with G58D is suppressed by lowering the dosage of *HSP104* and thereby fragmentation activity, suggesting that enhanced fragmentation is the underlying mechanism.

Next, we determined if these changes in propagon number upon heterozygous disruption of *HSP104* impacted the severity and stability of the [*PSI*$^{+}$] phenotype. Heterozygous disruption of *HSP104* restored the [*PSI*$^{+}$] phenotype (Fig 1A) and efficiently suppressed [*PSI*$^{+}$] loss (Fig 1D) in the [*PSI*$^{+}$]^{Sc4} strains expressing any ratio of G58D. For

the [*PSI*$^{+}$]^{Sc37} and [*PSI*$^{+}$]^{Weak} variants, similar although attenuated trends were apparent. Heterozygous disruption of Hsp104 partially reversed the pinker colony color on rich medium for both [*PSI*$^{+}$]^{Sc37} and [*PSI*$^{+}$]^{Weak} (Fig 1B, C). For [*PSI*$^{+}$]^{Sc37}, heterozygous disruption of Hsp104 increased [*PSI*$^{+}$] loss in all strains, indicating that wild type fragmentation levels must be close to the threshold required for efficient propagation of the amyloid state (Fig 1E). Nonetheless, in the strain expressing the 1:2 ratio of wild type to G58D, the frequency of [*PSI*$^{+}$] loss was suppressed by heterozygous disruption of Hsp104 (Fig 1E). Thus, reduction of Hsp104 reverses the G58D-induced inhibition of the [*PSI*$^{+}$] phenotype. Together, these observations are consistent with the idea that the downstream effect of G58D is identical for all [*PSI*$^{+}$] variants: an enhancement of the fragmentation efficiencies of their Sup35 amyloid.

Hsp104 mediates G58D inhibition by promoting Sup35 aggregate disassembly

The enhanced efficiency of fragmentation of Sup35 aggregates in the presence of G58D (Fig 3D, E) and the reduction in propagon levels (Fig 3G, H) suggests that Sup35 aggregates are being destroyed in strains propagating the [*PSI*$^{+}$]^{Sc4} and [*PSI*$^{+}$]^{Sc37} variants. For [*PSI*$^{+}$]^{Strong}, we previously detected this disassembly by monitoring the soluble pool of Sup35 in response to cycloheximide treatment to follow the fate of existing protein (DiSalvo et al, 2011). However, [*PSI*$^{+}$]^{Strong} is more sensitive to G58D expression than [*PSI*$^{+}$]^{Sc4}, [*PSI*$^{+}$]^{Sc37} and [*PSI*$^{+}$]^{Weak} (Fig 1) (DiSalvo et al, 2011), suggesting that release of soluble Sup35 from aggregates by enhanced fragmentation may be less readily detected in the latter variants. Specifically, the individual steps in prion propagation *in vivo* (e.g. conversion, fragmentation, and transmission) are variant-specific and difficult to monitor in isolation in a living system (Satpute-Krishnan et al, 2007; Tanaka et al, 2006).

Moreover, the accumulation of soluble Sup35 is impacted not only by the inherent rate of conversion on fibers ends but also by the cumulative effect of each of the steps of prion propagation on the number of those ends (Derdowski et al, 2010; Tanaka et al, 2006). Because the cumulative effects of each event on soluble Sup35 levels are not intuitive to qualitatively predict from those rates, we developed a deterministic model of Sup35 dynamics to deconstruct this complexity and gain additional mechanistic insight into the differential effects of G58D on the variants. This model uses a range of conversion and fragmentation rates that support [*PSI*$^{+}$] maintenance to capture different variants (see Supplementary Information). In addition, we have incorporated the concept of nucleation, which specifies a minimum size for a thermodynamically stable aggregate and has been previously established as a key event in Sup35 aggregation *in vitro* (Glover et al, 1997; King et al, 1997; Serio et al, 2000).

The steady-state size and number of Sup35 aggregates reflects a balance between conversion, which depends on continuous synthesis of Sup35, and fragmentation (Derdowski et al, 2010); when Sup35 synthesis is halted, aggregates are predicted to increase in number (Fig 4A) and decrease in size (Fig 4B) because fragmentation is proposed to exert a greater influence on the equilibrium state (Derdowski et al, 2010). In line with this observation, our model predicts that cycloheximide treatment will decrease soluble Sup35 levels for prion variants that are stably propagating [*PSI*$^{+}$] (Fig 4C) because additional templates have been created (Fig 4A).

Intriguingly, the extent of this decrease is predicted in our model to correspond inversely with the rate of fragmentation: that is, the slowest rate of fragmentation induces the largest decrease in soluble Sup35 (Fig 4B, black), relative to the steady-state levels

prior to the manipulation. If fragmentation produces more templates, which in turn promotes Sup35 conversion to the amyloid state, why would we predict a lower rate of fragmentation to have the most significant effect on soluble Sup35 levels? The reason is, as we have previously demonstrated under heat shock conditions (Klaips et al, 2014), fragmentation resolubilizes Sup35 in addition to creating new templates. Thus, high rates of fragmentation will push the balance between conversion and fragmentation toward the latter, causing a shift from aggregated to soluble Sup35. Consistent with this logic, our model predicts an increase in aggregate number that corresponds inversely with fragmentation rate (i.e. the largest increase in aggregate number corresponds to the slowest fragmentation rate; Fig 4A, black). This correlation can be explained directly by changes in the rate of Sup35 resolubilization from aggregates: the slowest fragmentation rate leads to the slowest rate of resolubilization (Fig 4D, black) and thereby the largest increase in aggregate number (Fig 4A, black).

These predictions correlate with our observations of the [*PSI*$^{+}$]^{Sc4}, [*PSI*$^{+}$]^{Sc37}, and [*PSI*$^{+}$]^{Weak} variants upon treatment with cycloheximide. For strains where wild type Sup35 was the only form present, the average size of Sup35 aggregates decreased (Fig 5A-C). In addition, the level of soluble Sup35 decreased upon cycloheximide treatment for the [*PSI*$^{+}$]^{Weak} and [*PSI*$^{+}$]^{Sc37} variants, but no significant decrease was observed for [*PSI*$^{+}$]^{Sc4} variant (Fig 5D-F, lane 1). According to our model, these observations are consistent with a nucleation-dependent aggregation process, which permits resolubilization of aggregates that are fragmented below the minimum thermodynamically stable size (Fig. 4D, compare solid and dashed lines), and a higher rate of fragmentation for [*PSI*$^{+}$]^{Sc4}, which would release more aggregated Sup35 into the soluble pool (Fig 4D, red). In the

presence of G58D, soluble Sup35 levels in [*PSI*$^{+}$]^{Sc37} and [*PSI*$^{+}$]^{Weak} are no longer reduced (Fig 5E, F, compare lanes 1 and 3), suggesting that G58D expression promotes aggregate fragmentation and thereby resolubilization. Consistent with this idea, treatment of the variants with both cycloheximide and guanidine HCl led to an increase in aggregate size (Fig 5A-C) and a decrease in soluble Sup35 levels in the presence of G58D (Fig 5D-F, compare lanes 3 and 4), indicating that Hsp104-catalyzed fragmentation promotes Sup35 resolubilization.

The ability of our mathematical model to capture the behavior of Sup35 in response to these manipulations strongly supports the idea that G58D destabilizes Sup35 aggregates to promote their increased fragmentation by Hsp104 and thereby their resolubilization. However, a more nuanced evaluation indicates that the threshold for inhibition cannot be explained by fragmentation efficiency alone. For example, [*PSI*$^{+}$]^{Sc37} has a similar phenotypic sensitivity to G58D dosage as the [*PSI*$^{+}$]^{Sc4} variant (Fig 1) but a kinetic stability, size, and likely fragmentation efficiency closer to the [*PSI*$^{+}$]^{Weak} variant (Fig 2 and Fig S2). A bulk shift in Sup35 from aggregate to soluble requires that the resolubilized Sup35 does not efficiently reconvert to the aggregated state; thus, conversion efficiencies will also impact the outcome of the G58D effects on aggregate kinetic stability, fragmentation and resolubilization. Sup35 aggregates in the [*PSI*$^{+}$]^{Sc37} conformation direct conversion at a higher rate than those in the [*PSI*$^{+}$]^{Sc4} conformation (Tanaka et al, 2006), but the relative rates of conversion for [*PSI*$^{+}$]^{Sc37} and [*PSI*$^{+}$]^{Weak} have not been reported. To compare these variants, we transiently treated strains with GdnHCl in liquid culture to reduce propagon number and then monitored propagon recovery as a function of time after removal of GdnHCl by plating cells and assessing their colony-color

phenotype. The [*PSI*$^{+}$]^{Weak} variant amplified its propagons at a faster rate than the [*PSI*$^{+}$]^{Sc37} variant (Fig S4). This recovery rate is a function of the product of the conversion and fragmentation rates (Tanaka et al, 2006). Because Sup35 aggregates in the [*PSI*$^{+}$]^{Sc37} conformation are less kinetically stable than those in the [*PSI*$^{+}$]^{Weak} conformation (Fig 2B, D) and thereby likely fragmented at a higher rate, this observation suggests that the conversion rate of [*PSI*$^{+}$]^{Sc37} is much lower than that of [*PSI*$^{+}$]^{Weak}. As a result, resolubilized Sup35 would be less likely to reconvert to the aggregated state in the [*PSI*$^{+}$]^{Sc37} variant than in the [*PSI*$^{+}$]^{Weak} variant. Thus, the higher rate of resolution and the lower rate of conversion combine to increase the sensitivity of [*PSI*$^{+}$]^{Sc37} to G58D inhibition relative to [*PSI*$^{+}$]^{Weak}.

G58D promotes Sup35 aggregate disassembly in daughter cells

Together, our studies are consistent with the ideas that resolubilization of aggregated Sup35 is the mechanism of G58D inhibition and that the variant-specific rates of conversion and fragmentation dictate the threshold for phenotypic reversal. However, Weissman and colleagues previously reported that loss of [*PSI*$^{+}$]^{Sc4} propagated by G58D alone was associated with propagon loss from daughter but not mother cells (Verges et al, 2011). This observation was interpreted as a G58D-dependent defect in Sup35 aggregate transmission to daughter cells, but using a direct fluorescence-based microscopy assay for Sup35-GFP transmission, we were unable to detect a transmission defect in [*PSI*$^{+}$]^{Strong} strains expressing wild type and G58D Sup35 (DiSalvo et al, 2011). The appearance of daughter cells without propagons could also arise if Sup35 aggregates were transmitted but subsequently disassembled by Hsp104 in this compartment. If this scenario is correct, inhibition of Hsp104 will lead to an increase in [*PSI*$^{+}$] propagons in

daughter cells. To test this hypothesis, we constructed [*PSI*$^{+}$]^{Sc4} diploid strains expressing only G58D Sup35 and compared prion propagation in wild type and *HSP104* heterozygous disruption versions of this strain by plating on rich medium and observing colony-color phenotype. Consistent with previous observations (Verges et al, 2011), [*PSI*$^{+}$]^{Sc4} propagation is unstable in a wild type strain (~50% prion loss), but we found that this instability is strongly suppressed by heterozygous disruption of *HSP104* (~5% prion loss; Fig 6A).

Propagons are normally distributed between mother and daughter cells in a 2:1 ratio (Cox et al, 2003). However, analysis of propagon numbers in mother and daughter cells showed an even stronger bias in the distribution of propagons toward the mothers in the presence of G58D (Fig 6B, black diamonds), including a population of pairs in which the mother but not the daughter retained a large number of propagons (Fig 6B, red diamonds). By contrast, heterozygous disruption of *HSP104* reduced the stronger mother bias associated with G58D expression, and more propagons were detected in daughter cells (Fig 6B, white triangles). Notably, daughter cells lacking propagons were not isolated from the *HSP104* heterozygous disruption strain, indicating that the suppression of prion loss (Fig 6A) correlated with an increase in propagons in daughter cells (Fig 6B).

Given the suppression of these phenotypes by heterozygous disruption of Hsp104, we next directly determined if Hsp104 inhibition specifically in daughter cells is sufficient to suppress [*PSI*$^{+}$] loss. To do so, we isolated daughter cells from [*PSI*$^{+}$]^{Sc4} diploids expressing one copy each of wild type and *G58D SUP35* by FACS, based on the staining of bud scars with Alexa-647 WGA. The absence of bud scars in cells with the lowest fluorescence intensity indicates that this fraction contains the newborn population, in

contrast to a mixed population before sorting (Fig 6C and Fig S5). The isolated daughters were then incubated on rich medium in the presence or absence of GdnHCl for three hours to transiently inhibit Hsp104 activity and then plated to determine the frequency of prion loss. Strikingly, GdnHCl treatment of daughter cells suppressed the frequency of prion loss (Fig 6D). Because daughter cells were biochemically isolated before treatment, the GdnHCl suppression of prion loss cannot be explained by an increased transmission of Sup35 aggregates to daughter cells upon Hsp104 inhibition. Rather, Sup35 aggregates must have already been present, with the transient inhibition of Hsp104 blocking their resolubilization after transfer, consistent with the idea that G58D inhibits the propagon of all [*PSI*$^{+}$] variants through the same mechanism.

Discussion

Together, our studies indicate that a single inhibitor, the dominant-negative G58D mutant of Sup35, can perturb the propagation of four different variants of the [*PSI*$^{+}$] prion, [*PSI*$^{+}$]^{Strong}, [*PSI*$^{+}$]^{Sc4}, [*PSI*$^{+}$]^{Sc37}, and [*PSI*$^{+}$]^{Weak}, through the same mechanism. The effects of G58D expression are most easily detected at the protein level, as kinetic destabilization of Sup35 amyloid (Fig 3A-C) and related reductions in the size of their SDS-resistant core polymers (Fig 3D-F). These changes only become apparent at the phenotypic and inheritance levels when the impact on Sup35 amyloid rises above a threshold dictated by the rates of conversion and fragmentation for the variants, allowing disassembly to dominate over reassembly.

The G58D mutation lies in the second oligopeptide repeat of Sup35, a region of the protein that is essential for prion propagation (Osherovich et al, 2004; Parham et al,

2001; Ter-Avanesyan et al, 1994) and that impacts the ability of the Hsp104 chaperone to thread monomers through its central pore during the fragmentation process (Langlois et al, 2016). Position 58 is located within the amyloid core of Sup35 in the [*PSI*$^{+}$]^{Sc37} variant but is more accessible in the [*PSI*$^{+}$]^{Sc4} variant (Toyama et al, 2007). Nonetheless, the kinetic destabilization of the four variants by G58D (Fig 3A-C) (DiSalvo et al, 2011) suggests this region contributes directly to associations within each of the aggregates. Structural studies on the isolated second repeat revealed that the G58D substitution introduced a turn into the otherwise extended conformation of the wild type repeat, suggesting that packing and thereby amyloid kinetic stability could be altered by this conformational change (Marchante et al, 2013).

Previous studies on the [*PSI*$^{+}$]^{Strong} and [*PSI*$^{+}$]^{Sc4} conformational variants suggested two different mechanisms for G58D-induced curing. For [*PSI*$^{+}$]^{Strong}, curing depended not only on the dosage of *G58D* but also of *HSP104*, suggesting that prion propagation was inhibited by amyloid disassembly. Indeed, in the presence of G58D, previously aggregated Sup35 transitioned to the soluble fraction (DiSalvo et al, 2011). For [*PSI*$^{+}$]^{Sc4}, curing correlated with the loss of heritable aggregates in daughter cells, interpreted as a G58D-induced defect in amyloid transmission (Verges et al, 2011). These distinct models for inhibition are consistent with the idea that different conformational variants must be cured through different molecular mechanisms (Ghaemmaghami, 2016; Shorter, 2010). However, our studies resolve this controversy: G58D inhibits both variants by promoting amyloid disassembly in daughter cells. This model is supported by both the Hsp104-dependence of the curing of both variants (Fig 1D) (DiSalvo et al, 2011) and of the reduction in propagons (Fig 3H) (DiSalvo et al, 2011). In addition, overexpression of

Hsp104 cures [*PSI*$^{+}$]^{Sc4} propagated by G58D but not wild type Sup35, suggesting the former is more sensitive to higher fragmentation rates than the latter (Verges et al, 2011). Consistent with this interpretation, overexpression of an N-terminally truncated Hsp104 mutant (Verges et al, 2011), which is deficient in substrate processing (Sweeny et al, 2015), is unable to cure [*PSI*$^{+}$]^{Sc4} propagated by G58D.

We have previously drawn parallels between the dominant-negative inhibition of [*PSI*$^{+}$] propagation by Sup35 G58D and that of protease-resistant PrP by hamster Q219K (corresponding to E219K in humans and Q218K in mouse). In both cases, the mutant is incorporated into wild type aggregates but capable of destabilizing the amyloid state only when present in excess to wild type protein, and the efficacy of dominant-negative inhibition is greater for less kinetically stable conformational variants (DiSalvo et al, 2011; Geoghegan et al, 2009; Hizume et al, 2009; Lee et al, 2007; Safar et al, 1998). Given the likelihood that the mechanisms of inhibition are similar between the yeast and mammalian dominant-negative mutants, the “resistance” of sCJD to E219K in humans and of 22L to Q219K in mice may be possible to overcome by increasing the dosage of the mutant, as we have demonstrated here for G58D and [*PSI*$^{+}$]^{Sc37} (Fig 1B, E). For G58D, inhibition occurs at a dosage far below that at which the prion state is induced to appear (Derkatch et al, 1999), indicating that the threshold between curing and induction is wide enough to accommodate switches in one direction or the other specifically. A similar analysis in mammals would be prudent before pursuing increased dosage of dominant-negative mutants as a therapeutic strategy.

How can the absence of heritable aggregates in some daughter cells be reconciled with amyloid disassembly as a common mechanism of inhibition for G58D? Our previous

studies have revealed that increasing chaperone levels by heat shock, leads to amyloid disassembly in a [*PSI*$^{+}$]^{Weak} strain (Klaips et al, 2014), suggesting that the ratio of chaperones:amyloid is a key contributor to the balance between amyloid assembly and disassembly. A similar skew in this ratio likely occurs during G58D curing but through a distinct mechanism. Our previous studies uncovered a size threshold for amyloid transmission during yeast cell division: larger aggregates were preferentially retained in mother cells (Derdowski et al, 2010). This asymmetry created an age-dependent difference in aggregate load, with newborn daughters taking several generations to return to the steady-state level of propagons observed in mother cells (Derdowski et al, 2010). This observation suggests that the chaperone:substrate ratio could be skewed toward the former in daughter cells. This altered ratio, when combined with the decrease in the kinetic stability of Sup35 amyloid induced by G58D (Fig 3A-C), likely creates a niche where amyloid disassembly dominates. Indeed, the normally resistant [*PSI*$^{+}$]^{Strong} variant is cured by transient heat shock when G58D is expressed (Klaips et al, 2014). Consistent with the idea that G58D cures [*PSI*$^{+}$] by promoting amyloid disassembly, curing is reduced (Fig 5A), and propagon numbers increase in daughters (Fig 5B) when Hsp104 levels are reduced. Most importantly, transiently blocking Hsp104 activity in daughter cells after division also greatly reduces prion loss (Fig 5D). Thus, G58D–containing Sup35 amyloid is transmitted to daughter cells, but, once there, these aggregates are at greater risk of clearance by Hsp104-mediated disassembly.

Beyond dominant-negative mutants, conformational variants of PrP and Sup35 also differ in their sensitivities to small molecule inhibitors (Ghaemmaghami, 2016; Shorter, 2010). Unfortunately, even sensitive conformational variants can develop

resistance to these compounds, further complicating attempts to develop therapeutic interventions for these diseases. For example, treatment of prion-infected mice or tissue culture cells with quinacrine or swainsonine reduced the kinetic stability of protease-resistant PrP and altered its tropism in cell lines, but these properties were reversed when treatment was removed (Ghaemmaghami et al, 2009; Li et al, 2010; Mahal et al, 2010). Although it remains unclear whether the emerging conformational variants were minor components that were selected or newly induced by the treatment, this conformational plasticity creates a moving target that is impossible to manage if a unique inhibitor must be developed in each case. Our studies suggest that as prion conformational variants evolve, adapt or mutate, changes in dosing regimes could be effective countermeasures. Indeed, quinacrine can eliminate the RML conformational variant of PrP from CAD5 cells at a 5-fold lower dosage than is required to eliminate an IND24-resistant variant (Berry et al, 2013).

Much research is focused on the appearance and self-replicating amplification of amyloid, yet these processes are clearly counteracted by disassembly pathways *in vivo*. This balance between assembly and disassembly contributes strongly to prion persistence, even in mammals. For example, inhibition of PrP expression can reverse accumulation of protease-resistant PrP, pathological changes and clinical progression of prion disease in mice, presumably by allowing clearance pathways to dominate, if initiated before extensive damage arises (Mallucci et al, 2003). While mammals lack an Hsp104 homolog, a chaperone system, composed of mammalian Hsp70, Hsp110, and class A and B J-proteins, possesses strong disaggregase activity (Nillegoda et al, 2015), capable of directing amyloid disassembly, although this activity has yet to be tested against

protease-resistant PrP (Gao et al, 2015). Nevertheless, natural variations in the accumulation of prion and chaperone proteins may also serve as a new framework in which to consider phenotypic differences among variants. For example, tropism and clinical progression are likely to be impacted by the balance between assembly and disassembly pathways, as we have observed for mitotic stability and heat shock-induced prion curing in yeast (Derdowski et al, 2010; Klaips et al, 2014). Moreover, the steady-state ratio of chaperones:amyloid may be a key consideration in screening potential therapeutics and in their ultimate efficacy *in vivo*, particularly for small molecules proteostasis regulators that perturb the assembly/disassembly balance.

Methods

Plasmids. All plasmids used in this study are listed in S1 Table. pRS306-P_{ADH} contains P_{ADH}-Multiple Cloning Site-T_{CYC1} as a *Kpn*I-*Sac*I fragment from pSM556 (a gift from F.U. Hartl) in a similarly digested pRS306. The *SUP35(G58D*) ORF was then subcloned into pRS306-P_{ADH} as a *Bam*HI-*Eco*RI fragment isolated from pRS306-SUP35(G58D) to create pRS306-P_{ADH}SUP35(G58D) (SB468).

Oligonucleotides. Oligonucleotides used in this study are listed in S2 Table.

Yeast strains. All strains are derivatives of 74-D694 and are listed in S3 Table. [*PSI*$^{+}$]^{Sc4} (SY2085) and [*PSI*$^{+}$]^{Sc37} (SY2086) haploid wild type strains were gifts from J. Weissman. Yeast strains expressing ectopic copies of *SUP35* or *G58D* from *URA3* (pRS306) or *TRP1* (pRS304)-marked plasmids were constructed by transforming yeast strains with plasmids that were linearized with *Bst*BI or *Bsu*361, respectively, and by selecting for transformants on the appropriate minimal medium. In all cases, expression was confirmed by quantitative immunoblotting for Sup35. Disruptions of *SUP35* (FP35, FP36) were generated by transformation of PCR-generated cassettes using pFA6aKanMX4 as a template with the indicated oligonucleotide primers (S2 Table) and selection on rich medium supplemented with G418. *HSP104* disruptions were generated by transformation with a *Pvu*I-*Bam*HI fragment of pYABL5 (a gift from S. Lindquist) and selection on minimal medium lacking leucine. Disruption of *NAT1* (FP29, FP30) were generated by transformation of PCR-generated cassettes using pFA6a-hphMX4 as a template with the indicated primers (S2 Table) and selection on complete medium supplemented with hygromycin. All the disruptions were verified by PCR and 2:2 segregation of the appropriate marker.

Prion loss. Exponentially growing cultures of the indicated strain were plated on YPD for single colonies, and the frequency of [*PSI*$^+$] loss was determined by the number of red colonies arising.

Protein analysis. Semidenaturing detergent agarose gel electrophoresis (SDD-AGE), SDS-PAGE, quantitative immunoblotting and SDS-sensitivity experiments were performed as previously described (Pezza et al, 2009). To analyze the fate of aggregated Sup35, cultures were grown to midlog phase and treated with cycloheximide (CHX) or both CHX and guanidine HCl (GdnHCl) for 1.7 hours. Yeast lysates were collected before and after treatment and incubated at 53°C and 100°C in the presence of 2% SDS before analysis by SDS-PAGE. Lysates were also prepared from the same cultures and analyzed by SDD-AGE.

Propagon counts. The number of propagons per cell was determined using a previously described *in vivo* dilution, colony-based method (Cox et al, 2003). For propagon counting in mothers and daughters, a pair of mother and daughter cells was separated by micromanipulation onto minimal medium (SD-complete with 2.5mM adenine and 4% dextrose) with 3mM GdnHCl. After growing at 30°C for about 48 h, whole colonies were isolated using a cut pipette tip, resuspended in a small volume of water and plated onto YPD plates. The number of white colonies was then counted.

Daughter-specific assays. Daughters were separated by FACS based on bud-scar labeling. Yeast cells were incubated for 1 h at room temperature in 1µg/ml Alexa-647 wheat germ agglutinin (WGA) in PBS. After washing twice in PBS, cells with the lowest fluorescence intensity (5%) were sorted as newborn daughter cells, and a sample of this fraction was viewed by fluorescence microscopy to confirm bud scar number. This

fraction was also moved to rich medium (1/4 YPD) for color development. For Hsp104 inhibition, sorted fractions were first moved to a minimal medium with 3mM GdnHCl for three hours before being transferred to rich medium. In each case only completely red colonies were counted as [*psi*$^-$].

Fluorescence Microscopy. Fluorescence microscopy was performed on a DeltaVision deconvolution microscope equipped with a 100x objective. WGA Alexa-647 fluorescence was collected using 650nm excitation and 668nm emission wavelengths and with an exposure of 50ms. Images were processed in ImageJ software.

Propagon Recovery Cultures were grown in YPAD medium to an OD_{600} of 0.1 at 30°C. GdnHCl was added to 3mM, and the culture was returned to 30°C for 5 hours to decrease the propagon number. Cultures were then collected by centrifugation, washed and transferred to YPAD medium without GdnHCl for recovery. Samples were plated on YPD, and the number of propagons per cell was counted at the indicated timepoints.

Acknowledgements

We thank F.U. Hartl and S. Lindquist for reagents, J. Laney and members of the Serio lab for helpful discussions and comments on the manuscript.

Table 1: Plasmids

Name	Description	Reference
6686	pRS306-P_{SUP35}SUP35	DiSalvo et al. 2011
SB467	pRS306-P_{SUP35}SUP35(G58D)	DiSalvo et al. 2011
SB468	pRS306-P_{ADH}SUP35(G58D)	This study
SB645	pRS304-P_{SUP35}SUP35(G58D)	DiSalvo et al. 2011
SB657	pRS306-P_{tet02}SUP35	DiSalvo et al. 2011
SB658	pRS306-P_{tet02}SUP35(G58D)	DiSalvo et al. 2011

Table 2: Oligonucleotide Sequences

Name	Description	Sequence (5’-3’)
FP29	5’NAT1 KO	GACAAATACCATTGAGGAAGGCGATTGACC CTAACGAAGTCAGCTGAAGCTTCGTACGC
FP30	3’NAT1 KO	AATTAAGTAAGAGTTAATTGACACATTGAGG AGTTGCAGGGCATAGGCCACTAGTGGATCT G
FP31	5’NAT1 KO CHK	AAGCAGTAGGAAAATTGGTGTGG
FP32	3’NAT1 KO CHK	CTGATCGCGTCTTTATCTTGTG
FP33	PTEF CHK	GCACGTCAAGACTGTCAAGG
FP34	pFA6a	TGCCCAGATGCGAAGTTAAGTG
FP35	5’SUP35 KO	ACTTGCTCGGAATAACATCTATATCTGCCCA CTAGCAACACGGATCCCCGGGTTAATTAA
FP36	3’SUP35 KO	GGTATTATTGTGTTTGCATTTACTTATGTTT GCAAGAAATGAATTCGAGCTCGTTTAAAC
FP75	5'HSP104 promoter	CCATCGATTCAAAGGCGTTATT
FP76	3'HSP104	TCATACTTTGGTTGCAGAC
FP77	5'LEU2 test	CACATGAACAAGGAAGTACAG
FP78	3'LEU2 test	AGAAACGGCCTTAACGAC
FP93	5'SUP35 KO CHK	CACAAAAATCATACAACGAATGG
FP108	3’SUP35 KO CHK	CTAAATGATGTTGACAAACTTATG

Table 3: Yeast Strains

Strains	Genotype	Plasmids Integrated	Figure	Reference
SLL2606	*MATa* [*PSI*$^{+}$]^{Strong} *ade1-14 his3Δ200 trp1-289 ura3-52 leu2-3, 112*	-	2A, S2	Chernoff et al. 1995
SLL2600	*MATa* [*PSI*$^{+}$]^{Weak} *ade1-14 his3Δ200 trp1-289 ura3-52 leu2-3, 112*	-	2B, S2, S4	Derkatch et al. 1996
SLL3261	*MATa/α* [*psi*$^{-}$] *ade1-14/ade1-14 his3Δ200/his3Δ200 trp1-289/ trp1-289 ura3-52/ura3-52 leu2-3, 112/ leu2-3, 112*	-	1A, 1B, 1C, 3D, 3E, 3F	DiSalvo et al. 2011
SY320	*MATα* [*PSI*$^{+}$]^{Strong} *ade1-14 his3Δ200 trp1-289 ura3-52 leu2-3, 112 nata::hphMX4*	-	2C	This study
SY1773	*MATa/α* [*PSI*$^{+}$]^{Weak} *ade1-14/ade1-14 his3Δ200/his3Δ200 trp1-289/ trp1-289 ura3-52/ura3-52::URA3::*P_{SUP35}*SUP35 leu2-3, 112/ leu2-3, 112*	6686	1C, 1F, 3F, S1C	This study
SY1774	*MATa/α* [*PSI*$^{+}$]^{Weak} *ade1-14/ade1-14 his3Δ200/his3Δ200 trp1-289/ trp1-289 ura3-52/ura3-52::URA3::*P_{SUP35}*SUP35(G58D) leu2-3, 112/ leu2-3, 112*	SB467	1C, 1F, 3F, S1C	This study
SY1776	*MATa/α* [*PSI*$^{+}$]^{Weak} *ade1-14/ade1-14 his3Δ200/his3Δ200 trp1-289/ trp1-289 ura3-52/ura3-52::URA3::*P_{SUP35}*SUP35 leu2-3, 112/ leu2-3, 112 SUP35/sup35::kanMX4*	6686	1C, 1F, 3C, 3F, 3I, S1C	This study
SY1777	*MATa/α* [*PSI*$^{+}$]^{Weak} *ade1-14/ade1-14 his3Δ200/his3Δ200 trp1-289/ trp1-289 ura3-52/ura3-52::URA3::*P_{SUP35}*SUP35(G58D) leu2-3, 112/ leu2-3, 112 SUP35/sup35::kanMX4*	SB467	1C, 1F, 3C, 3F, 3I, S1C	This study
SY1780	*MATa/α* [*PSI*$^{+}$]^{Weak} *ade1-14/ade1-14 his3Δ200/his3Δ200 trp1-289/ trp1-289::TRP1::* P_{SUP35}*SUP35(G58D) ura3-52/ura3-52::URA3::*P_{SUP35}*SUP35(G58D) leu2-3, 112/ leu2-3, 112 SUP35/sup35::kanMX6*	SB467, SB645	1C, 1F, 3F, S1C	This study
SY2085	*MATa* [*PSI*$^{+}$]^{Sc4} *ade1-14 his3Δ200 trp1-289 ura3-52 leu2-3, 112*	-	2A, S2	Tanaka et al. 2006

SY2086	*MATa* [*PSI*$^{+}$]^{Sc37} *ade1-14 his3Δ200 trp1-289 ura3-52 leu2-3, 112*	-	2B, S2, S4	Tanaka et al. 2006
SY2248	*MATα* [*PSI*$^{+}$]^{Sc4} *ade1-14 his3Δ200 trp1-289 ura3-52 leu2-3, 112 nata::LEU2*	-	2C	This study
SY2257	*MATa/α* [*PSI*$^{+}$]^{Sc4} *ade1-14/ade1-14 his3Δ200/his3Δ200 trp1-289/ trp1-289 ura3-52/ura3-52::URA3::*P_{SUP35}*SUP35 leu2-3, 112/ leu2-3, 112*	6686	1A, 1D, 3D, S1A	This study
SY2258	*MATa/α* [*PSI*$^{+}$]^{Sc4} *ade1-14/ade1-14 his3Δ200/his3Δ200 trp1-289/ trp1-289 ura3-52/ura3-52 leu2-3, 112/ leu2-3, 112*	-	1A, 1D, 3A, 3D, 3G, S1A	This study
SY2259	*MATa/α* [*PSI*$^{+}$]^{Sc4} *ade1-14/ade1-14 his3Δ200/his3Δ200 trp1-289/ trp1-289 ura3-52/ura3-52::URA3::*P_{SUP35}*SUP35(G58D) leu2-3, 112/ leu2-3, 112 SUP35/sup35::kanMX4*	SB467	1A, 1D, 3A, 3D, 3G, 6C, 6D, S1A, S5	This study
SY2260	*MATa/α* [*PSI*$^{+}$]^{Sc4} *ade1-14/ade1-14 his3Δ200/his3Δ200 trp1-289/ trp1-289::TRP1::* P_{SUP35}*SUP35(G58D) ura3-52/ura3-52::URA3::*P_{SUP35}*SUP35(G58D) leu2-3, 112/ leu2-3, 112 SUP35/sup35::kanMX6*	SB467, SB645	1A, 1D, 3D, S1A	This study
SY2261	*MATa/α* [*PSI*$^{+}$]^{Sc4} *ade1-14/ade1-14 his3Δ200/his3Δ200 trp1-289/ trp1-289 ura3-52/ura3-52::URA3::*P_{SUP35}*SUP35(G58D) leu2-3, 112/ leu2-3, 112*	SB467	1A, 1D, 3D, S1A	This study
SY2281	*MATa/α* [*PSI*$^{+}$]^{Sc4} *ade1-14/ade1-14 his3Δ200/his3Δ200 trp1-289/ trp1-289 ura3-52/ura3-52::URA3::*P_{SUP35}*SUP35 leu2-3, 112/ leu2-3, 112 HSP104/hsp104::LEU2*	6686	1A, 1D, S3A	This study
SY2283	*MATa/α* [*PSI*$^{+}$]^{Sc4} *ade1-14/ade1-14 his3Δ200/his3Δ200 trp1-289/ trp1-289 ura3-52/ura3-52 leu2-3, 112/ leu2-3, 112 HSP104/hsp104::LEU2*	-	1A, 1D, 3G, S3A	This study
SY2285	*MATa/α* [*PSI*$^{+}$]^{Sc4} *ade1-14/ade1-14 his3Δ200/his3Δ200 trp1-289/ trp1-289 ura3-52/ura3-52::URA3::*P_{SUP35}*SUP35(G58D) leu2-3, 112/ leu2-3, 112 HSP104/hsp104::LEU2*	SB467	1A, 1D, S3A	This study

SY2287	*MATa/α* [*PSI*$^{+}$]^{Sc4} *ade1-14/ade1-14 his3Δ200/his3Δ200 trp1-289/ trp1-289 ura3-52/ura3-52::URA3::*P_{SUP35}*SUP35(G58D) leu2-3, 112/ leu2-3, 112 SUP35/sup35::kanMX4 HSP104/hsp104::LEU2*	SB467	1A, 1D, 3G, S3A	This study
SY2289	*MATa/α* [*PSI*$^{+}$]^{Sc4} *ade1-14/ade1-14 his3Δ200/his3Δ200 trp1-289/ trp1-289::TRP1::* P_{SUP35}*SUP35(G58D) ura3-52/ura3-52::URA3::*P_{SUP35}*SUP35(G58D) leu2-3, 112/ leu2-3, 112 SUP35/sup35::kanMX6 HSP104/hsp104::LEU2*	SB467, SB645	1A, 1D, 3G, S3A	This study
SY2535	*MATa/α* [*PSI*$^{+}$]^{Weak} *ade1-14/ade1-14 his3Δ200/his3Δ200 trp1-289/ trp1-289 ura3-52/ura3-52::URA3::*P_{SUP35}*SUP35 leu2-3, 112/ leu2-3, 112 HSP104/hsp104::LEU2*	6686	1C, 1F, S3C	This study
SY2536	*MATa/α* [*PSI*$^{+}$]^{Weak} *ade1-14/ade1-14 his3Δ200/his3Δ200 trp1-289/ trp1-289 ura3-52/ura3-52 leu2-3, 112/ leu2-3, 112 HSP104/hsp104::LEU2*	-	1C, 1F, 3I, S3C	This study
SY2537	*MATa/α* [*PSI*$^{+}$]^{Weak} *ade1-14/ade1-14 his3Δ200/his3Δ200 trp1-289/ trp1-289 ura3-52/ura3-52::URA3::*P_{SUP35}*SUP35(G58D) leu2-3, 112/ leu2-3, 112 HSP104/hsp104::LEU2*	SB467	1C, 1F, S3C	This study
SY2538	*MATa/α* [*PSI*$^{+}$]^{Weak} *ade1-14/ade1-14 his3Δ200/his3Δ200 trp1-289/ trp1-289 ura3-52/ura3-52::URA3::*P_{SUP35}*SUP35(G58D) leu2-3, 112/ leu2-3, 112 SUP35/sup35::kanMX4 HSP104/hsp104::LEU2*	SB467	1C, 1F, 3I, S3C	This study
SY2539	*MATa/α* [*PSI*$^{+}$]^{Weak} *ade1-14/ade1-14 his3Δ200/his3Δ200 trp1-289/ trp1-289::TRP1::* P_{SUP35}*SUP35(G58D) ura3-52/ura3-52::URA3::*P_{SUP35}*SUP35(G58D) leu2-3, 112/ leu2-3, 112 SUP35/sup35::kanMX6 HSP104/hsp104::LEU2*	SB467, SB645	1C, 1F, S3C	This study
SY2812	*MATα* [*PSI*$^{+}$]^{Sc37} *ade1-14 his3Δ200 trp1-289 ura3-52 leu2-3, 112 nata::hphMX4*	-	2D	This study
SY2847	*MATa/α* [*PSI*$^{+}$]^{Sc37} *ade1-14/ade1-14 his3Δ200/his3Δ200 trp1-289/ trp1-289 ura3-52/ura3-52::URA3::*P_{SUP35}*SUP35 leu2-3, 112/ leu2-3, 112*	6686	1C, 1E, 3E, S1B	This study
SY2848	*MATa/α* [*PSI*$^{+}$]^{Sc37} *ade1-14/ade1-14 his3Δ200/his3Δ200 trp1-289/ trp1-289 ura3-52/ura3-52 leu2-3, 112/ leu2-3, 112*	-	1B, 1E, 3B, 3E, 3H, 5B, 5E, S1B	This study

SY2849	*MATa/α* [*PSI*$^{+}$]^{Sc37} *ade1-14/ade1-14 his3Δ200/his3Δ200 trp1-289/ trp1-289 ura3-52/ura3-52::URA3::*P_{SUP35}*SUP35(G58D) leu2-3, 112/ leu2-3, 112*	SB467	1B, 1E, 3E, S1B	This study
SY2850	*MATa/α* [*PSI*$^{+}$]^{Sc37} *ade1-14/ade1-14 his3Δ200/his3Δ200 trp1-289/ trp1-289 ura3-52/ura3-52::URA3::*P_{SUP35}*SUP35(G58D) leu2-3, 112/ leu2-3, 112 SUP35/sup35::kanMX4*	SB467	1B, 1E, 3B, 3E, 3H, 5B, 5E, S1B	This study
SY2851	*MATa/α* [*PSI*$^{+}$]^{Sc37} *ade1-14/ade1-14 his3Δ200/his3Δ200 trp1-289/ trp1-289::TRP1::* P_{SUP35}*SUP35(G58D) ura3-52/ura3-52::URA3::*P_{SUP35}*SUP35(G58D) leu2-3, 112/ leu2-3, 112 SUP35/sup35::kanMX6*	SB467, SB645	1B, 1E, 3E, S1B	This study
SY2856	*MATa/α* [*PSI*$^{+}$]^{Sc37} *ade1-14/ade1-14 his3Δ200/his3Δ200 trp1-289/ trp1-289 ura3-52/ura3-52::URA3::*P_{SUP35}*SUP35 leu2-3, 112/ leu2-3, 112 HSP104/hsp104::LEU2*	6686	1B, 1E, S3B	This study
SY2857	*MATa/α* [*PSI*$^{+}$]^{Sc37} *ade1-14/ade1-14 his3Δ200/his3Δ200 trp1-289/ trp1-289 ura3-52/ura3-52 leu2-3, 112/ leu2-3, 112 HSP104/hsp104::LEU2*	-	1B, 1E, 3H, S3B	This study
SY2858	*MATa/α* [*PSI*$^{+}$]^{Sc37} *ade1-14/ade1-14 his3Δ200/his3Δ200 trp1-289/ trp1-289 ura3-52/ura3-52::URA3::*P_{SUP35}*SUP35(G58D) leu2-3, 112/ leu2-3, 112 HSP104/hsp104::LEU2*	SB467	1B, 1E, S3B	This study
SY2859	*MATa/α* [*PSI*$^{+}$]^{Sc37} *ade1-14/ade1-14 his3Δ200/his3Δ200 trp1-289/ trp1-289 ura3-52/ura3-52::URA3::*P_{SUP35}*SUP35(G58D) leu2-3, 112/ leu2-3, 112 SUP35/sup35::kanMX4 HSP104/hsp104::LEU2*	SB467	1B, 1E, 3H, S3B	This study
SY2860	*MATa/α* [*PSI*$^{+}$]^{Sc37} *ade1-14/ade1-14 his3Δ200/his3Δ200 trp1-289/ trp1-289::TRP1::* P_{SUP35}*SUP35(G58D) ura3-52/ura3-52::URA3::*P_{SUP35}*SUP35(G58D) leu2-3, 112/ leu2-3, 112 SUP35/sup35::kanMX6 HSP104/hsp104::LEU2*	SB467, SB645	1B, 1E, S3B	This study
SY2862	*MATα* [*PSI*$^{+}$]^{Weak} *ade1-14 his3Δ200 trp1-289 ura3-52 leu2-3, 112 nata::hphMX4*	-	2D	This study
SY2878	*MATa/α* [*PSI*$^{+}$]^{Weak} *ade1-14/ade1-14 his3Δ200/his3Δ200 trp1-289/ trp1-289 ura3-52/ura3-52::URA3::*P_{tet02}*SUP35 leu2-3, 112/ leu2-3, 112 SUP35/sup35::kanMX4*	SB657	5C, 5F	This study

SY2879	*MATa/α* [*PSI*$^{+}$]^{Weak} *ade1-14/ade1-14 his3Δ200/his3Δ200 trp1-289/ trp1-289 ura3-52/ura3-52::URA3::*P_{tet02}*SUP35(G58D) leu2-3, 112/ leu2-3, 112 SUP35/sup35::kanMX4*	SB658	5C, 5F	This study
SY2957	*MATa/α* [*PSI*$^{+}$]^{Sc4} *ade1-14/ade1-14 his3Δ200/his3Δ200 trp1-289/ trp1-289 ura3-52::URA3::*P_{ADH}*SUP35(G58D)/ura3-52::URA3::*P_{SUP35}*SUP35(G58D) leu2-3, 112/ leu2-3, 112 sup35::kanMX4/sup35::kanMX4*	SB467 , SB468	6A, 6B	This study
SY2976	*MATa/α* [*PSI*$^{+}$]^{Sc4} *ade1-14/ade1-14 his3Δ200/his3Δ200 trp1-289/ trp1-289 ura3-52::URA3::*P_{ADH}*SUP35(G58D)/ura3-52::URA3::*P_{SUP35}*SUP35(G58D) leu2-3, 112/ leu2-3, 112 sup35::kanMX4/sup35::kanMX4 HSP104/hsp104::LEU2*	SB467 , SB468	6A, 6B	This study
SY3044	*MATa/α* [*PSI*$^{+}$]^{Sc4} *ade1-14/ade1-14 his3Δ200/his3Δ200 trp1-289/ trp1-289 ura3-52/ura3-52::URA3::*P_{tet02}*SUP35 leu2-3, 112/ leu2-3, 112 SUP35/sup35::kanMX4*	SB657	5A, 5D	This study
SY3045	*MATa/α* [*PSI*$^{+}$]^{Sc4} *ade1-14/ade1-14 his3Δ200/his3Δ200 trp1-289/ trp1-289 ura3-52/ura3-52::URA3::*P_{tet02}*SUP35(G58D) leu2-3, 112/ leu2-3, 112 SUP35/sup35::kanMX4*	SB658	5A, 5D	This study

References

Andreoletti O, Morel N, Lacroux C, Rouillon V, Barc C, Tabouret G, Sarradin P, Berthon P, Bernardet P, Mathey J, Lugan S, Costes P, Corbiere F, Espinosa JC, Torres JM, Grassi J, Schelcher F, Lantier F (2006) Bovine spongiform encephalopathy agent in spleen from an ARR/ARR orally exposed sheep. The Journal of general virology 87: 1043-6

Atarashi R, Sim VL, Nishida N, Caughey B, Katamine S (2006) Prion strain-dependent differences in conversion of mutant prion proteins in cell culture. J Virol 80: 7854-62

Belt PB, Muileman IH, Schreuder BE, Bos-de Ruijter J, Gielkens AL, Smits MA (1995) Identification of five allelic variants of the sheep PrP gene and their association with natural scrapie. The Journal of general virology 76 (Pt 3): 509-17

Benestad SL, Arsac JN, Goldmann W, Noremark M (2008) Atypical/Nor98 scrapie: properties of the agent, genetics, and epidemiology. Veterinary research 39: 19

Berry DB, Lu D, Geva M, Watts JC, Bhardwaj S, Oehler A, Renslo AR, DeArmond SJ, Prusiner SB, Giles K (2013) Drug resistance confounding prion therapeutics. Proceedings of the National Academy of Sciences of the United States of America 110: E4160-9

Buschmann A, Luhken G, Schultz J, Erhardt G, Groschup MH (2004) Neuronal accumulation of abnormal prion protein in sheep carrying a scrapie-resistant genotype (PrPARR/ARR). The Journal of general virology 85: 2727-33

Chernoff YO, Lindquist SL, Ono B, Inge-Vechtomov SG, Liebman SW (1995) Role of the chaperone protein Hsp104 in propagation of the yeast prion-like factor [psi+]. Science 268: 880-4

Clouscard C, Beaudry P, Elsen JM, Milan D, Dussaucy M, Bounneau C, Schelcher F, Chatelain J, Launay JM, Laplanche JL (1995) Different allelic effects of the codons 136 and 171 of the prion protein gene in sheep with natural scrapie. The Journal of general virology 76 (Pt 8): 2097-101

Cox B, Ness F, Tuite M (2003) Analysis of the generation and segregation of propagons: entities that propagate the [PSI+] prion in yeast. Genetics 165: 23-33

Crozet C, Lin YL, Mettling C, Mourton-Gilles C, Corbeau P, Lehmann S, Perrier V (2004) Inhibition of PrPSc formation by lentiviral gene transfer of PrP containing dominant negative mutations. Journal of cell science 117: 5591-7

Dawson M, Hoinville LJ, Hosie BD, Hunter N (1998) Guidance on the use of PrP genotyping as an aid to the control of clinical scrapie. Scrapie Information Group. The Veterinary record 142: 623-5

Derdowski A, Sindi SS, Klaips CL, DiSalvo S, Serio TR (2010) A size threshold limits prion transmission and establishes phenotypic diversity. Science 330: 680-3

Derkatch IL, Bradley ME, Zhou P, Liebman SW (1999) The PNM2 mutation in the prion protein domain of SUP35 has distinct effects on different variants of the [PSI+] prion in yeast. Current genetics 35: 59-67

DiSalvo S, Derdowski A, Pezza JA, Serio TR (2011) Dominant prion mutants induce curing through pathways that promote chaperone-mediated disaggregation. Nature structural & molecular biology 18: 486-92

Doel SM, McCready SJ, Nierras CR, Cox BS (1994) The dominant PNM2- mutation which eliminates the psi factor of Saccharomyces cerevisiae is the result of a missense mutation in the SUP35 gene. Genetics 137: 659-70

Dong J, Castro CE, Boyce MC, Lang MJ, Lindquist S (2010) Optical trapping with high forces reveals unexpected behaviors of prion fibrils. Nature structural & molecular biology 17: 1422-30

Eiden M, Soto EO, Mettenleiter TC, Groschup MH (2011) Effects of polymorphisms in ovine and caprine prion protein alleles on cell-free conversion. Veterinary research 42: 30

Eisenberg DS, Sawaya MR (2017) Structural Studies of Amyloid Proteins at the Molecular Level. Annual review of biochemistry 86: 69-95

Foster JD, Parnham D, Chong A, Goldmann W, Hunter N (2001) Clinical signs, histopathology and genetics of experimental transmission of BSE and natural scrapie to sheep and goats. The Veterinary record 148: 165-71

Furuya K, Kawahara N, Yamakawa Y, Kishida H, Hachiya NS, Nishijima M, Kirino T, Kaneko K (2006) Intracerebroventricular delivery of dominant negative prion protein in a mouse model of iatrogenic Creutzfeldt-Jakob disease after dura graft transplantation. Neuroscience letters 402: 222-6

Gao X, Carroni M, Nussbaum-Krammer C, Mogk A, Nillegoda NB, Szlachcic A, Guilbride DL, Saibil HR, Mayer MP, Bukau B (2015) Human Hsp70 Disaggregase Reverses Parkinson's-Linked alpha-Synuclein Amyloid Fibrils. Mol Cell 59: 781-93

Gavier-Widen D, Noremark M, Benestad S, Simmons M, Renstrom L, Bratberg B, Elvander M, af Segerstad CH (2004) Recognition of the Nor98 variant of scrapie in the Swedish sheep population. Journal of veterinary diagnostic investigation : official publication of the American Association of Veterinary Laboratory Diagnosticians, Inc 16: 562-7

Geoghegan JC, Miller MB, Kwak AH, Harris BT, Supattapone S (2009) Trans-dominant inhibition of prion propagation in vitro is not mediated by an accessory cofactor. PLoS pathogens 5: e1000535

Ghaemmaghami S (2016) Biology and Genetics of PrP Prion Strains. Cold Spring Harbor perspectives in medicine

Ghaemmaghami S, Ahn M, Lessard P, Giles K, Legname G, DeArmond SJ, Prusiner SB (2009) Continuous quinacrine treatment results in the formation of drug-resistant prions. PLoS pathogens 5: e1000673

Glover JR, Kowal AS, Schirmer EC, Patino MM, Liu JJ, Lindquist S (1997) Self-seeded fibers formed by Sup35, the protein determinant of [PSI+], a heritable prion-like factor of S. cerevisiae. Cell 89: 811-9

Goldmann W, Hunter N, Smith G, Foster J, Hope J (1994) PrP genotype and agent effects in scrapie: change in allelic interaction with different isolates of agent in sheep, a natural host of scrapie. The Journal of general virology 75 (Pt 5): 989-95

Hizume M, Kobayashi A, Teruya K, Ohashi H, Ironside JW, Mohri S, Kitamoto T (2009) Human prion protein (PrP) 219K is converted to PrPSc but shows heterozygous inhibition in variant Creutzfeldt-Jakob disease infection. The Journal of biological chemistry 284: 3603-9

Holmes WM, Mannakee BK, Gutenkunst RN, Serio TR (2014) Loss of amino-terminal acetylation suppresses a prion phenotype by modulating global protein folding. Nature communications 5: 4383

Hope J, Wood SC, Birkett CR, Chong A, Bruce ME, Cairns D, Goldmann W, Hunter N, Bostock CJ (1999) Molecular analysis of ovine prion protein identifies similarities between BSE and an experimental isolate of natural scrapie, CH1641. The Journal of general virology 80 (Pt 1): 1-4

Houston F, Goldmann W, Chong A, Jeffrey M, Gonzalez L, Foster J, Parnham D, Hunter N (2003) Prion diseases: BSE in sheep bred for resistance to infection. Nature 423: 498

Ikeda T, Horiuchi M, Ishiguro N, Muramatsu Y, Kai-Uwe GD, Shinagawa M (1995) Amino acid polymorphisms of PrP with reference to onset of scrapie in Suffolk and Corriedale sheep in Japan. The Journal of general virology 76 (Pt 10): 2577-81

Jacobs JG, Bossers A, Rezaei H, van Keulen LJ, McCutcheon S, Sklaviadis T, Lantier I, Berthon P, Lantier F, van Zijderveld FG, Langeveld JP (2011) Proteinase K-resistant material in ARR/VRQ sheep brain affected with classical scrapie is composed mainly of VRQ prion protein. J Virol 85: 12537-46

Jeong BH, Lee KH, Kim NH, Jin JK, Kim JI, Carp RI, Kim YS (2005) Association of sporadic Creutzfeldt-Jakob disease with homozygous genotypes at PRNP codons 129 and 219 in the Korean population. Neurogenetics 6: 229-32

King CY (2001) Supporting the structural basis of prion strains: induction and identification of [PSI] variants. Journal of molecular biology 307: 1247-1260

King CY, Tittmann P, Gross H, Gebert R, Aebi M, Wuthrich K (1997) Prion-inducing domain 2-114 of yeast Sup35 protein transforms in vitro into amyloid-like filaments. Proceedings of the National Academy of Sciences of the United States of America 94: 6618-22

Kishida H, Sakasegawa Y, Watanabe K, Yamakawa Y, Nishijima M, Kuroiwa Y, Hachiya NS, Kaneko K (2004) Non-glycosylphosphatidylinositol (GPI)-anchored recombinant prion protein with dominant-negative mutation inhibits PrPSc replication in vitro. Amyloid 11: 14-20

Klaips CL, Hochstrasser ML, Langlois CR, Serio TR (2014) Spatial quality control bypasses cell-based limitations on proteostasis to promote prion curing. eLife 3

Knowles TP, Vendruscolo M, Dobson CM (2014) The amyloid state and its association with protein misfolding diseases. Nature reviews Molecular cell biology 15: 384-96

Kobayashi A, Teruya K, Matsuura Y, Shirai T, Nakamura Y, Yamada M, Mizusawa H, Mohri S, Kitamoto T (2015) The influence of PRNP polymorphisms on human prion disease susceptibility: an update. Acta neuropathologica 130: 159-70

Kochneva-Pervukhova NV, Paushkin SV, Kushnirov VV, Cox BS, Tuite MF, Ter-Avanesyan MD (1998) Mechanism of inhibition of Psi+ prion determinant propagation by a mutation of the N-terminus of the yeast Sup35 protein. EMBO J 17: 5805-10

Landreh M, Sawaya MR, Hipp MS, Eisenberg DS, Wuthrich K, Hartl FU (2016) The formation, function and regulation of amyloids: insights from structural biology. J Intern Med 280: 164-76

Langeveld JP, Jacobs JG, Hunter N, van Keulen LJ, Lantier F, van Zijderveld FG, Bossers A (2015) Prion Type-Dependent Deposition of PRNP Allelic Products in Heterozygous Sheep. J Virol 90: 805-12

Langlois CR, Pei F, Sindi SS, Serio TR (2016) Distinct Prion Domain Sequences Ensure Efficient Amyloid Propagation by Promoting Chaperone Binding or Processing In Vivo. PLoS genetics 12: e1006417

Laplanche JL, Chatelain J, Westaway D, Thomas S, Dussaucy M, Brugere-Picoux J, Launay JM (1993) PrP polymorphisms associated with natural scrapie discovered by denaturing gradient gel electrophoresis. Genomics 15: 30-7

Lee CI, Yang Q, Perrier V, Baskakov IV (2007) The dominant-negative effect of the Q218K variant of the prion protein does not require protein X. Protein science : a publication of the Protein Society 16: 2166-73

Li J, Browning S, Mahal SP, Oelschlegel AM, Weissmann C (2010) Darwinian evolution of prions in cell culture. Science 327: 869-72

Luhken G, Buschmann A, Groschup MH, Erhardt G (2004) Prion protein allele A136 H154Q171 is associated with high susceptibility to scrapie in purebred and crossbred German Merinoland sheep. Archives of virology 149: 1571-80

Lukic A, Beck J, Joiner S, Fearnley J, Sturman S, Brandner S, Wadsworth JD, Collinge J, Mead S (2010) Heterozygosity at polymorphic codon 219 in variant creutzfeldt-jakob disease. Archives of neurology 67: 1021-3

Madec JY, Simon S, Lezmi S, Bencsik A, Grassi J, Baron T (2004) Abnormal prion protein in genetically resistant sheep from a scrapie-infected flock. The Journal of general virology 85: 3483-6

Mahal SP, Browning S, Li J, Suponitsky-Kroyter I, Weissmann C (2010) Transfer of a prion strain to different hosts leads to emergence of strain variants. Proceedings of the National Academy of Sciences of the United States of America 107: 22653-8

Mallucci G, Dickinson A, Linehan J, Brandner S, Collinge J, Mallucci G, Dickinson A, Linehan J (2003) Depleting Neuronal PrP in Prion Infection Prevents Disease and Reverses Spongiosis Published by : American Association for the Advancement of Science Stable URL : http://www.jstor.org/stable/3835558 Your use of the JSTOR archive indicates your acceptance. Science 302: 871-874

Manning M, Colon W (2004) Structural basis of protein kinetic stability: resistance to sodium dodecyl sulfate suggests a central role for rigidity and a bias toward beta-sheet structure. Biochemistry 43: 11248-54

Marchante R, Rowe M, Zenthon J, Howard MJ, Tuite MF (2013) Structural definition is important for the propagation of the yeast [PSI+] prion. Mol Cell 50: 675-85

Masel J, Jansen VA, Nowak MA (1999) Quantifying the kinetic parameters of prion replication. Biophysical chemistry 77: 139-52

Ness F, Ferreira P, Cox BS, Tuite MF (2002) Guanidine hydrochloride inhibits the generation of prion "seeds" but not prion protein aggregation in yeast. Molecular and cellular biology 22: 5593-605

Nillegoda NB, Kirstein J, Szlachcic A, Berynskyy M, Stank A, Stengel F, Arnsburg K, Gao X, Scior A, Aebersold R, Guilbride DL, Wade RC, Morimoto RI, Mayer MP, Bukau B (2015) Crucial HSP70 co-chaperone complex unlocks metazoan protein disaggregation. Nature 524: 247-51

Noguchi-Shinohara M, Hamaguchi T, Kitamoto T, Sato T, Nakamura Y, Mizusawa H, Yamada M (2007) Clinical features and diagnosis of dura mater graft associated Creutzfeldt Jakob disease. Neurology 69: 360-7

Nozaki I, Hamaguchi T, Sanjo N, Noguchi-Shinohara M, Sakai K, Nakamura Y, Sato T, Kitamoto T, Mizusawa H, Moriwaka F, Shiga Y, Kuroiwa Y, Nishizawa M, Kuzuhara S, Inuzuka T, Takeda M, Kuroda S, Abe K, Murai H, Murayama S et al. (2010) Prospective 10-year surveillance of human prion diseases in Japan. Brain : a journal of neurology 133: 3043-57

Onnasch H, Gunn HM, Bradshaw BJ, Benestad SL, Bassett HF (2004) Two Irish cases of scrapie resembling Nor98. The Veterinary record 155: 636-7

Orge L, Galo A, Machado C, Lima C, Ochoa C, Silva J, Ramos M, Simas JP (2004) Identification of putative atypical scrapie in sheep in Portugal. The Journal of general virology 85: 3487-91

Orge L, Oliveira A, Machado C, Lima C, Ochoa C, Silva J, Carvalho R, Tavares P, Almeida P, Ramos M, Pinto MJ, Simas JP (2010) Putative emergence of classical scrapie in a background of enzootic atypical scrapie. The Journal of general virology 91: 1646-50

Osherovich LZ, Cox BS, Tuite MF, Weissman JS (2004) Dissection and design of yeast prions. PLoS Biol 2: E86

Paludi D, Thellung S, Chiovitti K, Corsaro A, Villa V, Russo C, Ianieri A, Bertsch U, Kretzschmar HA, Aceto A, Florio T (2007) Different structural stability and toxicity of PrP(ARR) and PrP(ARQ) sheep prion protein variants. Journal of neurochemistry 103: 2291-300

Parham SN, Resende CG, Tuite MF (2001) Oligopeptide repeats in the yeast protein Sup35p stabilize intermolecular prion interactions. EMBO J 20: 2111-9

Patino MM, Liu JJ, Glover JR, Lindquist S (1996) Support for the prion hypothesis for inheritance of a phenotypic trait in yeast. Science 273: 622-6

Paushkin SV, Kushnirov VV, Smirnov VN, Ter-Avanesyan MD (1996) Propagation of the yeast prion-like [psi+] determinant is mediated by oligomerization of the SUP35-encoded polypeptide chain release factor. EMBO J 15: 3127-34

Perrier V, Kaneko K, Safar J, Vergara J, Tremblay P, DeArmond SJ, Cohen FE, Prusiner SB, Wallace AC (2002) Dominant-negative inhibition of prion replication in transgenic mice. Proceedings of the National Academy of Sciences of the United States of America 99: 13079-84

Pezza JA, Langseth SX, Raupp Yamamoto R, Doris SM, Ulin SP, Salomon AR, Serio TR (2009) The NatA acetyltransferase couples Sup35 prion complexes to the [PSI+] phenotype. Molecular biology of the cell 20: 1068-80

Ronzon F, Bencsik A, Lezmi S, Vulin J, Kodjo A, Baron T (2006) BSE inoculation to prion diseases-resistant sheep reveals tricky silent carriers. Biochemical and biophysical research communications 350: 872-7

Safar J, Wille H, Itri V, Groth D, Serban H, Torchia M, Cohen FE, Prusiner SB (1998) Eight prion strains have PrP(Sc) molecules with different conformations. Nature medicine 4: 1157-65

Satpute-Krishnan P, Langseth SX, Serio TR (2007) Hsp104-dependent remodeling of prion complexes mediates protein-only inheritance. PLoS Biol 5: e24

Serio TR, Cashikar AG, Kowal AS, Sawicki GJ, Moslehi JJ, Serpell L, Arnsdorf MF, Lindquist SL (2000) Nucleated conformational conversion and the replication of conformational information by a prion determinant. Science 289: 1317-21

Shibuya S, Higuchi J, Shin RW, Tateishi J, Kitamoto T (1998) Codon 219 Lys allele of PRNP is not found in sporadic Creutzfeldt-Jakob disease. Annals of neurology 43: 826-8

Shorter J (2010) Emergence and natural selection of drug-resistant prions. Molecular bioSystems 6: 1115-30

Sievers SA, Karanicolas J, Chang HW, Zhao A, Jiang L, Zirafi O, Stevens JT, Munch J, Baker D, Eisenberg D (2011) Structure-based design of non-natural amino-acid inhibitors of amyloid fibril formation. Nature 475: 96-100

Somerville RA, Birkett CR, Farquhar CF, Hunter N, Goldmann W, Dornan J, Grover D, Hennion RM, Percy C, Foster J, Jeffrey M (1997) Immunodetection of PrPSc in spleens of some scrapie-infected sheep but not BSE-infected cows. The Journal of general virology 78 (Pt 9): 2389-96

Sweeny EA, Jackrel ME, Go MS, Sochor MA, Razzo BM, DeSantis ME, Gupta K, Shorter J (2015) The Hsp104 N-terminal domain enables disaggregase plasticity and potentiation. Mol Cell 57: 836-49

Tanaka M, Chien P, Yonekura K, Weissman JS (2005) Mechanism of cross-species prion transmission: an infectious conformation compatible with two highly divergent yeast prion proteins. Cell 121: 49-62

Tanaka M, Collins SR, Toyama BH, Weissman JS (2006) The physical basis of how prion conformations determine strain phenotypes. Nature 442: 585-9

Ter-Avanesyan MD, Dagkesamanskaya AR, Kushnirov VV, Smirnov VN (1994) The SUP35 omnipotent suppressor gene is involved in the maintenance of the non-Mendelian determinant [psi+] in the yeast Saccharomyces cerevisiae. Genetics 137: 671-6

Tessier PM, Lindquist S (2007) Prion recognition elements govern nucleation, strain specificity and species barriers. Nature 447: 556-61

Toupet K, Compan V, Crozet C, Mourton-Gilles C, Mestre-Frances N, Ibos F, Corbeau P, Verdier JM, Perrier V (2008) Effective gene therapy in a mouse model of prion diseases. PloS one 3: e2773

Toyama BH, Kelly MJ, Gross JD, Weissman JS (2007) The structural basis of yeast prion strain variants. Nature 449: 233-7

Tranulis MA (2002) Influence of the prion protein gene, Prnp, on scrapie susceptibility in sheep. APMIS 110: 33-43

Trevitt CR, Collinge J (2006) A systematic review of prion therapeutics in experimental models. Brain : a journal of neurology 129: 2241-65

Tuite MF, Serio TR (2010) The prion hypothesis: from biological anomaly to basic regulatory mechanism. Nature reviews Molecular cell biology 11: 823-833

Verges KJ, Smith MH, Toyama BH, Weissman JS (2011) Strain conformation, primary structure and the propagation of the yeast prion [PSI+]. Nature structural & molecular biology 18: 493-9

Westaway D, Zuliani V, Cooper CM, Da Costa M, Neuman S, Jenny AL, Detwiler L, Prusiner SB (1994) Homozygosity for prion protein alleles encoding glutamine-171 renders sheep susceptible to natural scrapie. Genes & development 8: 959-69

Yamada M, Noguchi-Shinohara M, Hamaguchi T, Nozaki I, Kitamoto T, Sato T, Nakamura Y, Mizusawa H (2009) Dura mater graft-associated Creutzfeldt-Jakob disease in Japan: clinicopathological and molecular characterization of the two distinct subtypes. Neuropathology : official journal of the Japanese Society of Neuropathology 29: 609-18

Yuan AH, Hochschild A (2017) A bacterial global regulator forms a prion. Science 355: 198-201

Zampieri M, Legname G, Altafini C (2009) Investigating the conformational stability of prion strains through a kinetic replication model. PLoS computational biology 5: e1000420

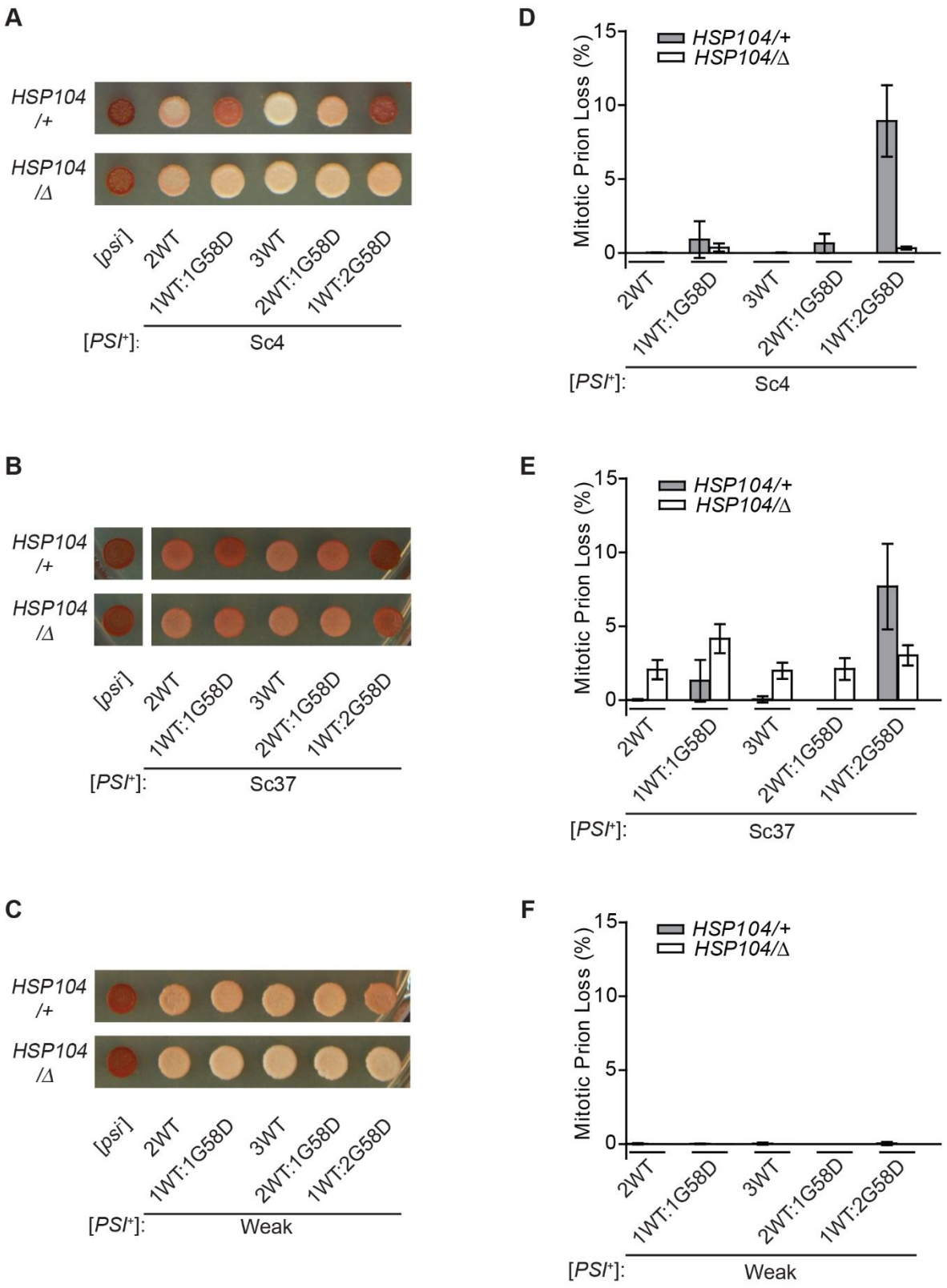

Fig 1. Dose-dependent effects of G58D expression on [*PSI*$^{+}$] variants. [*PSI*$^{+}$]^{Sc4} (*A*), [*PSI*$^{+}$]^{Sc37} (*B*) and [*PSI*$^{+}$]^{Weak} (*C*) wild type (*HSP104*/+) or heterozygous-disruption

(*HSP104/Δ*) diploid strains expressing wild type (WT) and G58D Sup35 from P_{SUP35} at the indicated ratios were spotted on rich medium to analyze the [*PSI*$^{+}$] phenotype. [*psi*$^{-}$] diploids were included as controls. Spontaneous frequencies of [*PSI*$^{+}$]^{Sc4} (*D*), [*PSI*$^{+}$]^{Sc37} (*E*) and [*PSI*$^{+}$]^{Weak} (*F*) loss during mitotic division were determined by counting the percentage of [*psi*$^{-}$] colonies. For each strain, >3000 colonies were scored. Error bars represent standard deviations from 12 biological replicates.

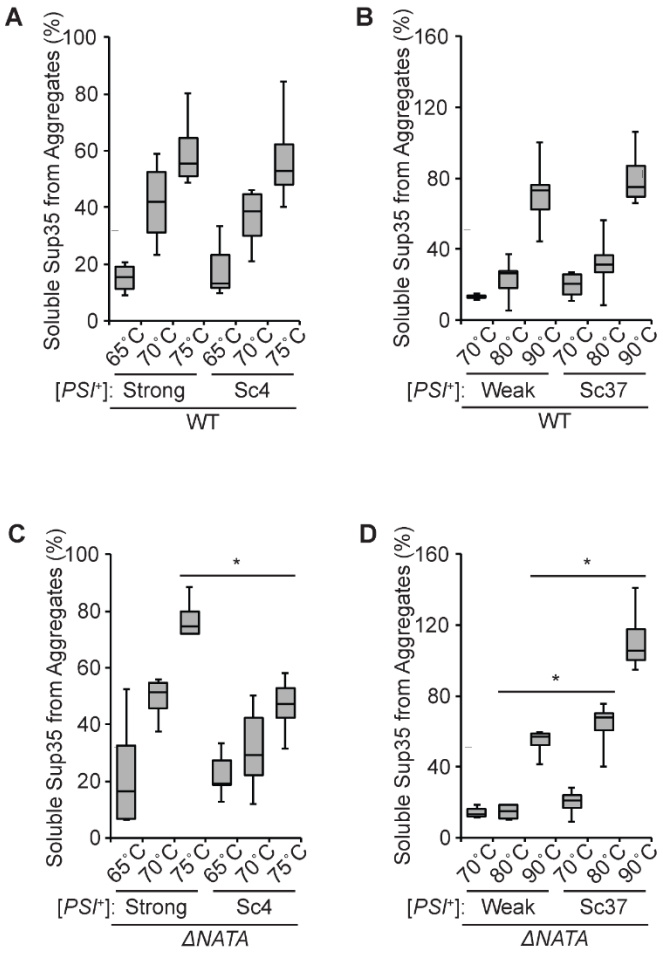

Fig 2. Analysis of aggregate properties for [*PSI*$^{+}$] variants. Lysates from [*PSI*$^{+}$]^{Strong} and [*PSI*$^{+}$]^{Sc4} WT (*A*), [*PSI*$^{+}$]^{Weak} and [*PSI*$^{+}$]^{Sc37} WT (*B*), [*PSI*$^{+}$]^{Strong} and [*PSI*$^{+}$]^{Sc4} *ΔNATA* (*C*) or [*PSI*$^{+}$]^{Weak} and [*PSI*$^{+}$]^{Sc37} *ΔNATA* (*D*) haploid strains were incubated in SDS at the indicated temperatures before SDS-PAGE and quantitative immunoblotting for Sup35 (percentage of Sup35 released from aggregates at the indicated temperatures). Horizontal lines on boxes indicate 25th, 50th and 75th percentiles; whiskers indicate 10th and 90th percentiles. Horizontal lines indicate pair-wise comparisons (n≥4; paired t-test, *P<0.05).

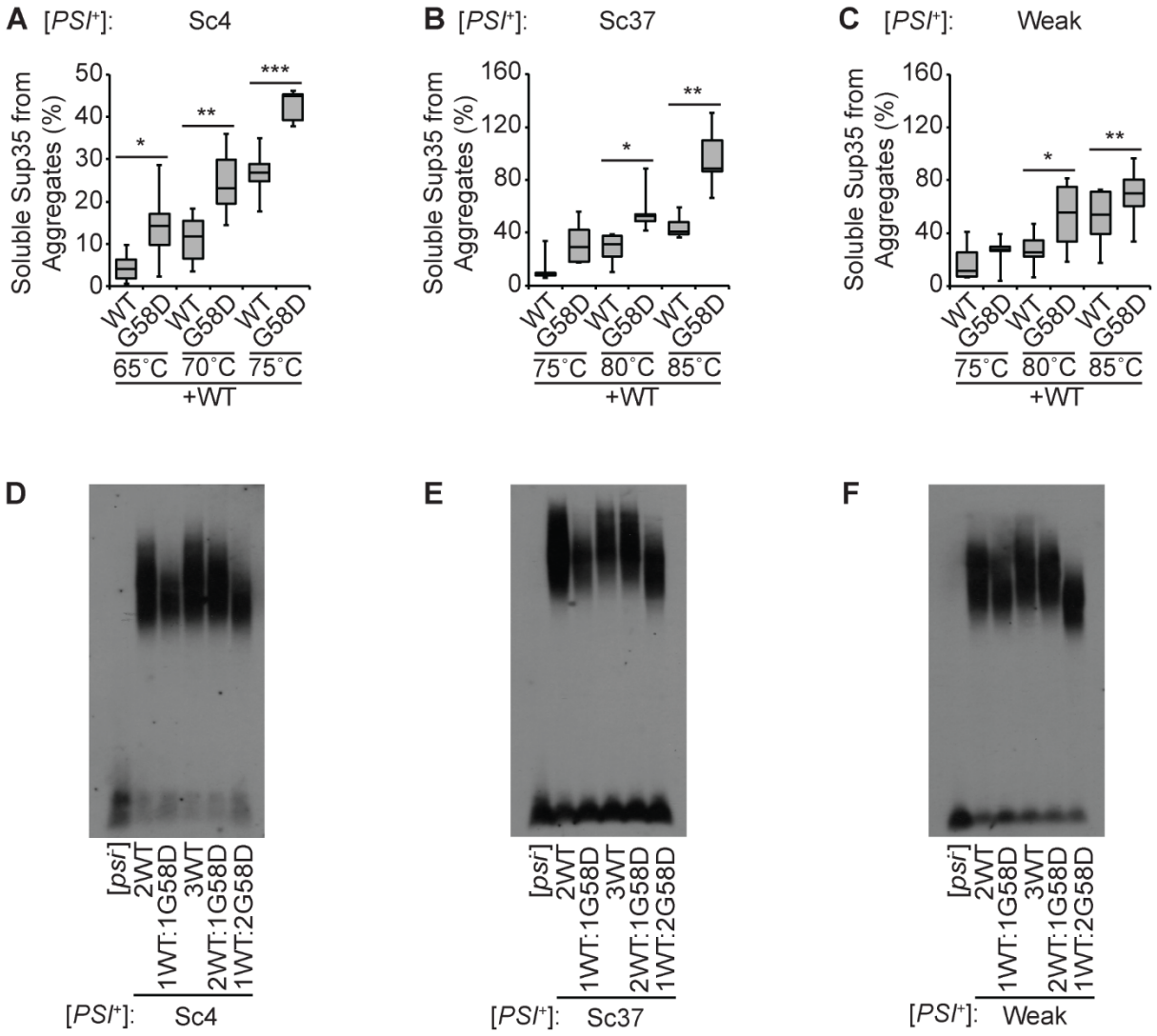
A [PSI+]: Sc4
Soluble Sup35 from Aggregates (%)
50
40
30
20
10
0
*
**
***
WT
G58D
WT
G58D
WT
G58D
65˚C
70˚C
75˚C
+WT
B [PSI+]: Sc37
Soluble Sup35 from Aggregates (%)
160
120
80
40
0
*
**
WT
G58D
WT
G58D
WT
G58D
75˚C
80˚C
85˚C
+WT
C [PSI+]: Weak
Soluble Sup35 from Aggregates (%)
160
120
80
40
0
*
**
WT
G58D
WT
G58D
WT
G58D
75˚C
80˚C
85˚C
+WT
D
[psi-]
2WT
1WT:1G58D
3WT
2WT:1G58D
1WT:2G58D
[PSI+]: Sc4
E
[psi-]
2WT
1WT:1G58D
3WT
2WT:1G58D
1WT:2G58D
[PSI+]: Sc37
F
[psi-]
2WT
1WT:1G58D
3WT
2WT:1G58D
1WT:2G58D
[PSI+]: Weak
G [PSI+]: Sc4
Propagon per Cell (Relative to WT+WT)
2.5
2.0
1.5
1.0
0.5
0.0
***
*
***
***
WT
G58D
WT
G58D
HSP104: +
Δ
+WT
H [PSI+]: Sc37
Propagon per Cell (Relative to WT+WT)
1.5
1.2
0.9
0.6
0.3
0.0
***
***
***
***
WT
G58D
WT
G58D
HSP104: +
Δ
+WT
I [PSI+]: Weak
Propagon per Cell (Relative to WT+WT)
5.0
4.0
3.0
2.0
1.0
0.0
***
*
***
WT
G58D
WT
G58D
HSP104: +
Δ
+WT

Fig 3. Effects of *G58D* and *HSP104* dosage on Sup35 aggregate properties. Lysates from [*PSI*$^{+}$]^{Sc4} (*A*), [*PSI*$^{+}$]^{Sc37} (*B*) or [*PSI*$^{+}$]^{Weak} (*C*) diploid strains expressing one endogenous copy of *SUP35* and a second copy of *SUP35* (WT or G58D) from P_{SUP35} were incubated in SDS at the indicated temperatures before SDS-PAGE and quantitative immunoblotting for Sup35 (percentage of Sup35 released from aggregates at the indicated temperatures). Box plots are as described in the legend to Fig. 2. Horizontal lines indicate pair-wise comparisons (n≥5; paired t-test, **P*<0.05, ***P*<0.05, ****P*<0.001). Lysates of [*PSI*$^{+}$]^{Sc4} (*D*), [*PSI*$^{+}$]^{Sc37} (*E*) or [*PSI*$^{+}$]^{Weak} (*F*) diploid strains expressing Sup35 (WT) and G58D in the indicated ratios were analyzed by SDD-AGE and immunoblotting for Sup35. For [*PSI*$^{+}$]^{Sc4} (*G*), [*PSI*$^{+}$]^{Sc37} (*H*) or [*PSI*$^{+}$]^{Weak} (*I*), the number of propagons present in individual cells was counted in wildype (+) and heterozygous *HSP104* disruption (Δ) strains, and the ratio of propagons relative to WT was determined in diploid strains expressing one endogenous copy of *SUP35* and one copy of *SUP35* (WT or G58D) from P_{SUP35}. Box plots are as described in the legend to Fig. 2. Horizontal lines indicate pair-wise comparisons (n≥10 cells per strain; unpaired t-test, **P*<0.05, ****P*<0.001).

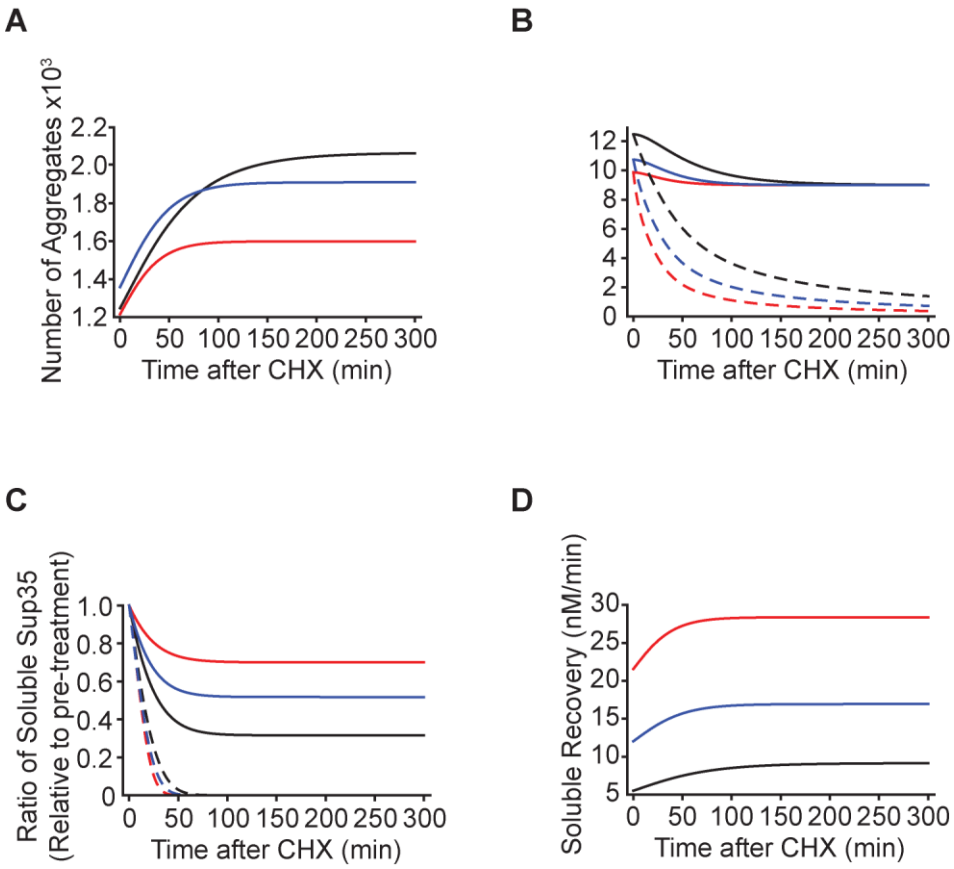

Fig 4. Mathematical model predicts fragmentation-dependent changes in soluble Sup35 levels in response to protein synthesis inhibition. Cycloheximide (CHX) treatment leads to an increase in the number of aggregates (*A*), and increase in average aggregate size (*B*), and a decrease in the ratio of soluble Sup35 (*C*) according to the results of stochastic simulations of a mathematical model of prion propagation. The yields (*A, C*) and the rate at which protein resolubilizes (*D*) vary with the rates of fragmentation: high (red), medium (blue), or low (black). The predicted changes in Sup35 average aggregate size (*B*) and soluble levels (*C*) are lost when nucleation is removed from the model (dashed lines).

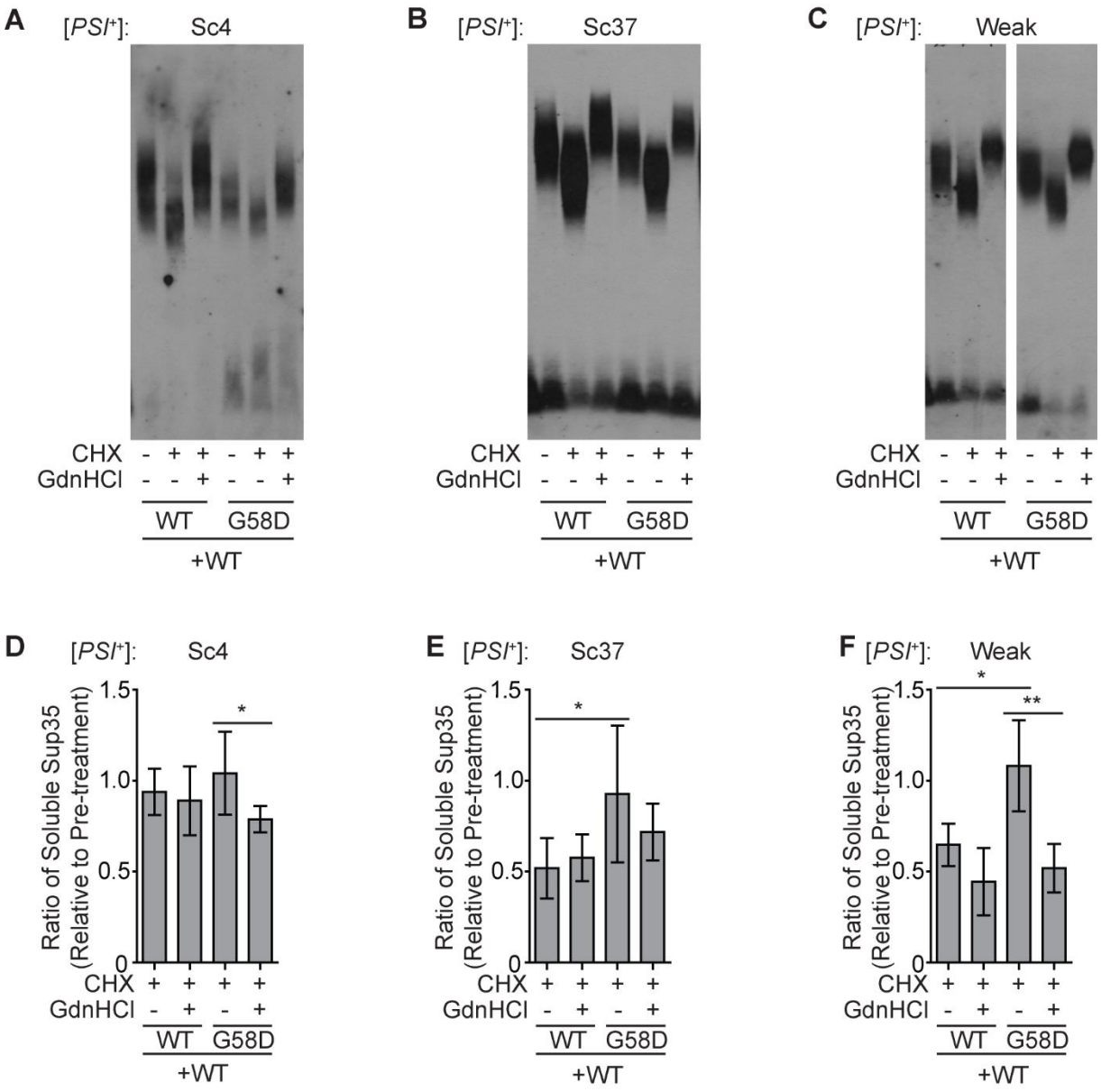

Fig 5. G58D expression promotes Hsp104-mediated resolubilization of aggregates. Lysates of [*PSI*$^{+}$]^{Sc4} (*A*), [*PSI*$^{+}$]^{Sc37} (*B*) or [*PSI*$^{+}$]^{Weak} (*C*) strains expressing two copies of *SUP35* (WT) or one wild-type and one *G58D* copy of *SUP35* were treated with CHX or both CHX and GdnHCl and then analyzed by SDD-AGE and immunoblotting for Sup35. Lysates from diploid [*PSI*$^{+}$]^{Sc4} (*D*), [*PSI*$^{+}$]^{Sc37} (*E*) or [*PSI*$^{+}$]^{Weak} (*F*) strains expressing two copies of *SUP35* (WT) or one wild-type and one *G58D* copy of *SUP35* from P_{tetO2} were

incubated in SDS at 53°C or 100°C before SDS-PAGE and quantitative immunoblotting for Sup35, and the ratio of signal before and after treatment with CHX or both CHX and GdnHCl treatment were determined. Error bars represent standard deviations. Horizontal lines indicate pair-wise comparisons (n ≥ 5; paired t-test, *P<0.05, **P<0.01).

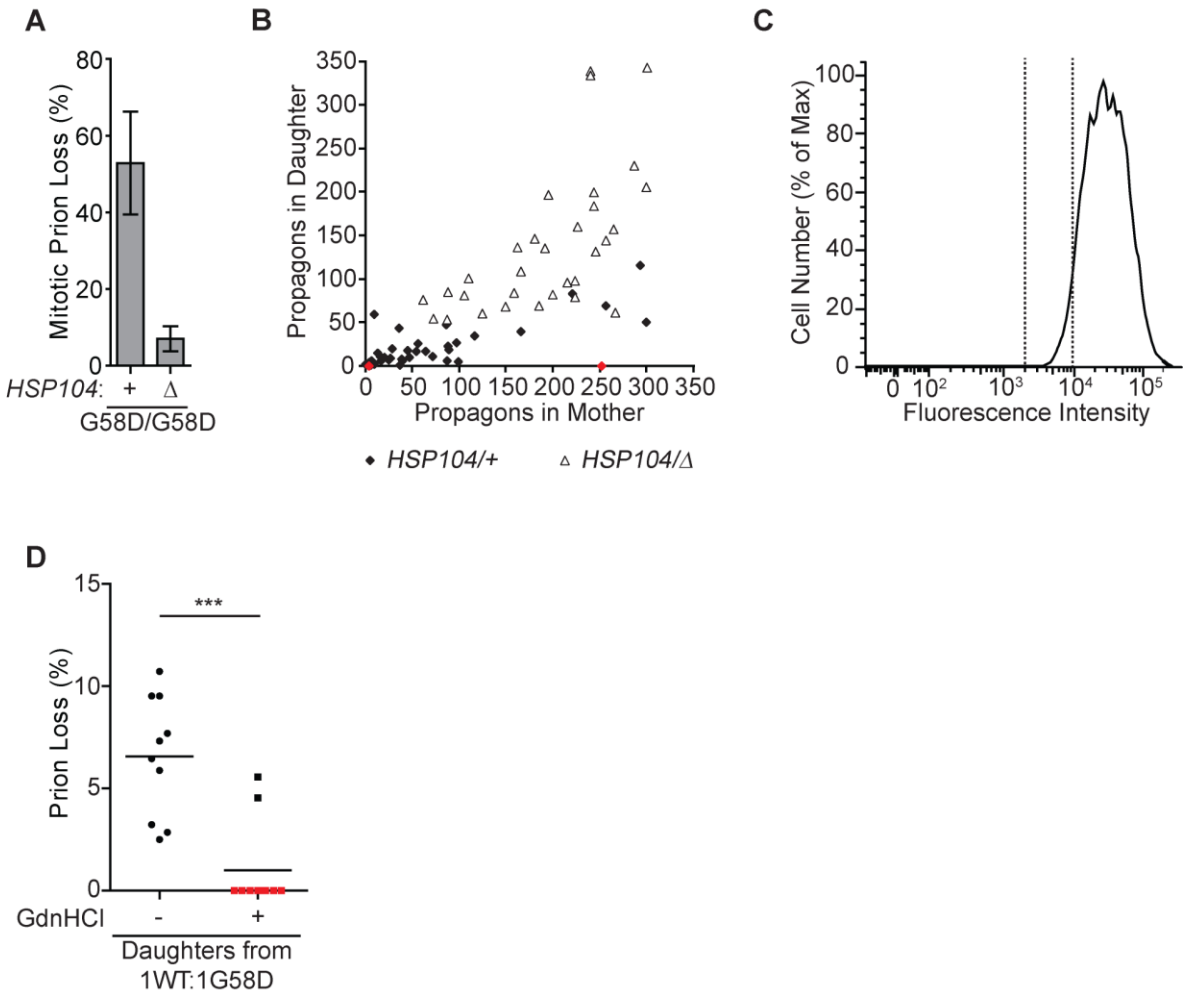

Fig 6. Hsp104 promotes [*PSI*$^{+}$] curing in daughter cells expressing G58D. (*A*) Spontaneous frequencies of [*PSI*$^{+}$]^{Sc4} loss during mitotic division were determined by counting the percentage of [*psi*$^{-}$] colonies for strains that were wild type (+) or heterozygous disruptions for *HSP104* (Δ). For each strain, >3000 colonies were scored. Error bars represent standard deviations from 10 biological replicates. (*B*) The number of propagons in daughter cells was plotted against the number of propagons in mother cells for wild type (*HSP104*/+, black or red diamonds) or heterozygous *HSP104* disruption (*HSP104/Δ,* white triangles) diploid strains expressing one copy of G58D from P_{SUP35} and another copy of G58D from P_{ADH} in an [*PSI*$^{+}$]^{Sc4} strain. Red diamonds represent mother-

daughter pairs in the wild type strain in which the mother contained propagons but the daughter did not. (*C*) The distribution of fluorescence intensities for a population of [*PSI*$^{+}$]^{Sc4} diploid cells expressing one endogenous copy of *SUP35* and a second copy of *SUP35* (*G58D*) from P_{SUP35} stained with Alexa-647 WGA was obtained by flow cytometry. Vertical dotted lines indicate least fluorescent 5%, which was sorted as daughters. (*D*) The daughters isolated in (*C*) were plated onto minimal medium containing 3mM GdnHCl for three hours and then transferred to rich medium. The frequency of [*PSI*$^{+}$] loss was then determined relative to that from daughters isolated from the same culture plated directly onto rich medium. Horizontal lines indicate pair-wise comparisons (n≥10 cells per strain; paired t-test, ***P<0.001).

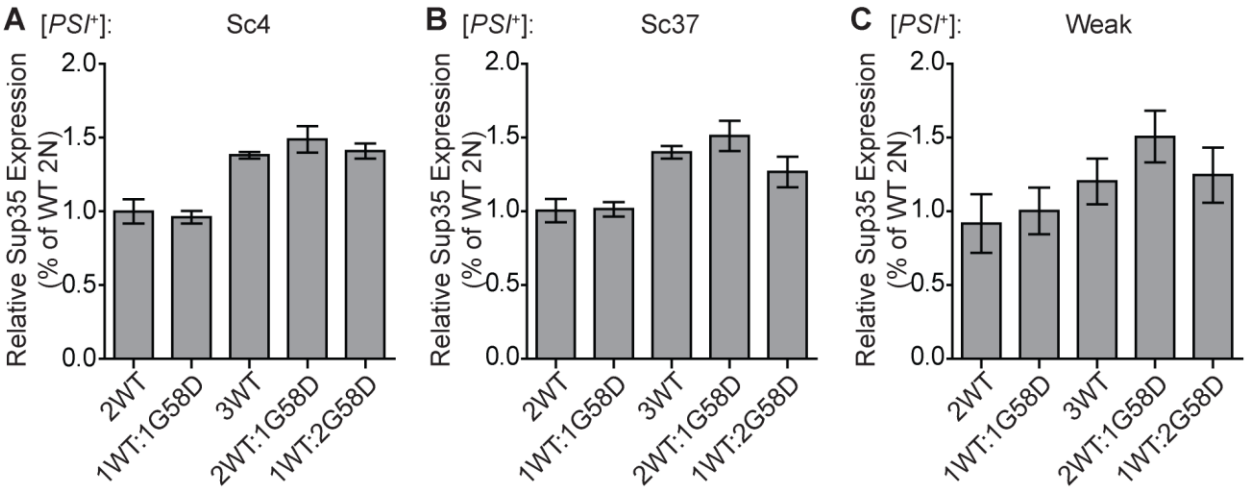

Fig S1. Sup35 expression level is consistent with copy number. Lysates isolated from [*PSI*$^{+}$]^{Sc4} (*A*), [*PSI*$^{+}$]^{Sc37} (*B*) or [*PSI*$^{+}$]^{Weak} (*C*) strains described in Fig. 1A-C were analyzed by SDS-PAGE and quantitative immunoblotting for Sup35. The ratio of Sup35 relative to a wild type diploid is shown. Error bars represent standard deviation.

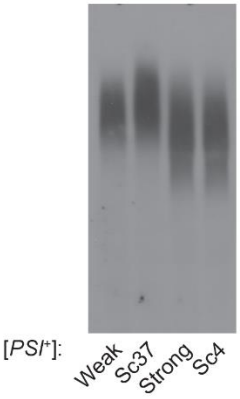

Fig S2. [*PSI*$^{+}$] variants differ in the size of their Sup35 aggregates. Lysates from the indicated [*PSI*$^{+}$] variant haploid yeast strains were analyzed by SDD-AGE and immunoblotting for Sup35.

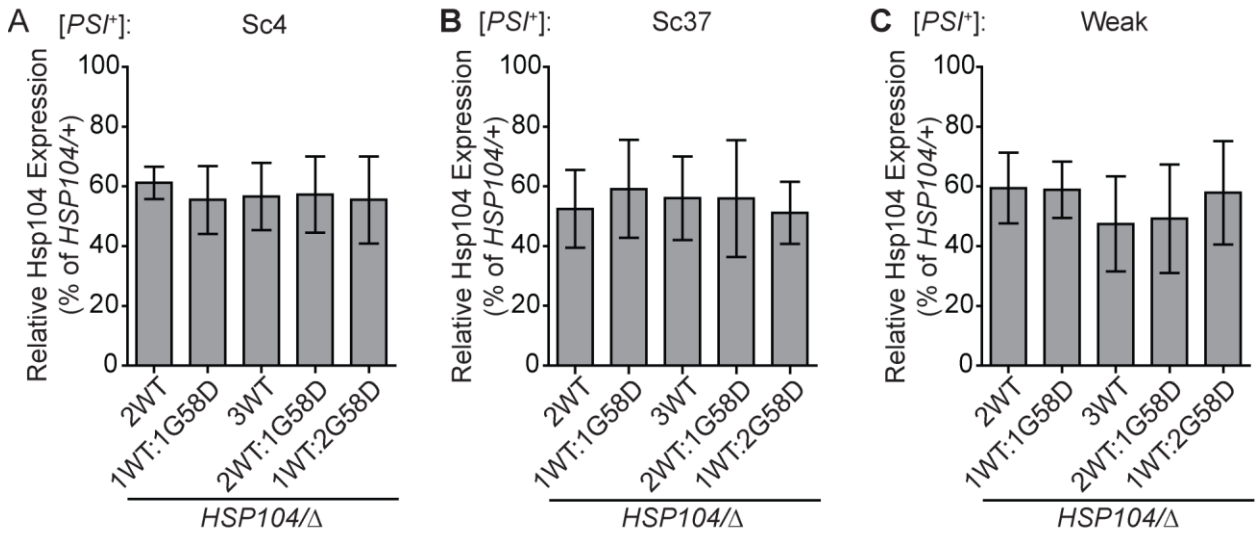

Fig S3**.** Hsp104 expression level is consistent with copy number. Lysates isolated from [*PSI*$^{+}$]^{Sc4} (*A*), [*PSI*$^{+}$]^{Sc37} (*B*) or [*PSI*$^{+}$]^{Weak} (*C*) strains described in Fig. 1A-C were analyzed by SDS-PAGE and quantitative immunoblotting for Hsp104. The ratio of Hsp104 relative to a wild-type diploid is shown. Error bars represent standard deviation.

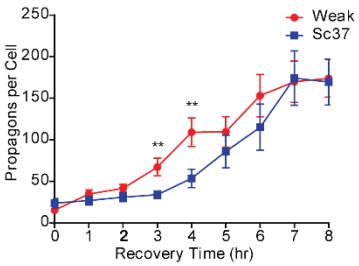

Fig S4. [*PSI*$^{+}$]^{Sc37} and [*PSI*$^{+}$]^{Weak} recover propagons at different rates. The rate of propagon recovery was determined for [*PSI*$^{+}$]^{Sc37} (blue) and [*PSI*$^{+}$]^{Weak} (red) after treatment with GdnHCl. Error bars represent standard deviation. (n ≥ 12 cells per strain per time point; unpaired t-test, ***P*<0.01).

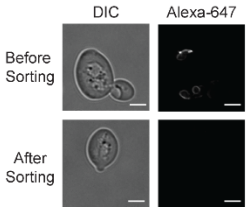

Fig S5. Analysis of FACS-sorted daughter cells. DIC and Alexa-647 WGA fluorescence of bud scars of cells both before and after FACS sorting. Scale bars represent 3μm.

Chapter 3:

Determining the Role of Sir2 in Heat-Induced Prion Curing

Abstract

Mitosis in the yeast *Saccharomyces cerevisiae* is distinctively asymmetrical and encompasses mother cell-specific aging. This asymmetry arises from the retention of oxidized proteins in mother cells during cell division, leading to a reset of the aging clock in daughter cells. Although the underlying mechanism of damage asymmetry is still controversial, the studies all agree that the process involves Sir2 and the Hsp104 chaperone network. Previously, both damage asymmetry and the Hsp104 chaperone network have been reported to contribute to the heat-induced dissolution of amyloid in prion-containing cell; however, the role of Sir2 in this process was not examined. To examine this relationship, we focused on the effect of Sir2 on heat-induced curing of the yeast prion [*PSI*$^{+}$], the alternative, self-templating, amyloid form of Sup35 protein. Remarkably, Sup35 amyloid is not effectively disassembled at elevated temperatures by the molecular chaperone Hsp104 in the *Δsir2* background. This suppression of curing could be explained by Sir2-mediated derepression of mating-type specific loci, specifically a mitochondria-localized protein YJL133C-A. Since the changes in heat-induced prion curing correlated with the efficiency of damage asymmetry, YJL133C-A might be the downstream target of Sir2 in this process, implicating mitochondria as a crucial component.

Introduction

Asymmetric inheritance upon cell division, which produces two daughter cells with different fates, plays an important role in maintaining cellular fitness and potency (Gotz & Huttner, 2005; Henderson & Gottschling, 2008; Homem & Knoblich, 2012; Inaba & Yamashita, 2012; Morrison & Kimble, 2006; Pelletier & Yamashita, 2012). This process has been extensively studied over the past decades in a variety of model organisms, especially in budding yeast *Saccharomyces cerevisiae*. Mitosis of budding yeast is an asymmetrical process, with both cell volume and the transmission efficiencies of cellular components asymmetrically distributed to reset the aging clock in daughter cells (Kennedy et al, 1994).

One of the best known asymmetrical components is damaged protein aggregates, like protein carbonyls. Such species, which are associated with a large number of age-related disorders in humans, including Parkinson's disease, Alzheimer's disease, and diabetes, progressively accumulate during aging (Aguilaniu et al, 2003; Dukan & Nystrom, 1998; Grune et al, 2004; Reverter-Branchat et al, 2004; Stadtman, 1992). Many evidence suggest that damaged protein aggregates are asymmetrically segregated during cytokinesis, which is accomplished by a spatial protein quality control system involving Hsp104 (Erjavec et al, 2007). However, the underlying mechanism that mediates damage asymmetry is unknown.

Sir2, which is highly conserved from archaea to humans (Dutnall & Pillus, 2001), is required for mitotic segregation of damaged protein aggregates in yeast (Aguilaniu et al, 2003; Erjavec et al, 2007; Liu et al, 2010). Sir2 is an NAD+-dependent deacetylase that facilitates transcriptional silencing at cryptic mating type loci HML and HMR, at telomeres,

and at the rDNA locus (Blander & Guarente, 2004; Imai et al, 2000; Rusche et al, 2003). A screen for mutants with a more symmetrical distribution of carbonylated proteins identified Sir2, as an essential component in maintaining damage asymmetry during mitosis (Aguilaniu et al, 2003; Erjavec et al, 2007). Since the spatial distribution of F-actin during cytokinesis also became atypical with deletion of Sir2, the actin cytoskeleton was suggested to be required for proper segregation of damaged proteins. This idea was supported by additional experimental evidence demonstrating that inhibition of actin assembly by latrunculin A (Lat-A) abolished the ability of wild type mother cells to retain oxidized proteins (Aguilaniu et al, 2003). However, little is known about the machineries involved in establishing asymmetrical inheritance of damaged protein aggregates.

Three different models have been proposed to explain the mechanism of damage asymmetry: retrograde transport, diffuse confinement, and organelle confinement. In the retrograde transport model, damaged protein aggregates formed upon heat shock in emerging buds are transported back to the mother cells in an actin cable-dependent rather than an actin patch-dependent process (Liu et al, 2010). However, based on the diffuse confinement model, damaged protein aggregates undergo a random walk without directional bias (Zhou et al, 2011). The asymmetric inheritance is a predictable outcome of aggregates' slow diffusion and the geometry of yeast cells, but the process depends on Hsp104 through an unclear mechanism (Zhou et al, 2011). Another study by Spokoini et al. showed that confinement of protein aggregate motion through association with the JUNQ (juxtanuclear quality control) and IPOD (insoluble protein deposit) compartments on the surface of the nucleus and vacuole, respectively, is important for the asymmetric inheritance of misfolded proteins (Spokoini et al, 2012). Similarly, protein aggregates

formed on the endoplasmic reticulum are frequently also associated with or later captured by mitochondria, greatly constraining aggregate mobility. During mitosis, aggregates are tethered to well-anchored maternal mitochondria, whereas mitochondria acquired by the bud are largely free of aggregates (Zhou et al, 2014).

Similar to the rejuvenation process, heat-induced prion loss is also accomplished by both damaged protein asymmetry and a spatial protein quality control system involving Hsp104 (Klaips et al, 2014). Specifically, a sub-lethal thermal stress converts [*PSI*$^{+}$]^{Weak}, the alternative, self-templating, amyloid form of the Sup35, to non-prion [*psi*$^{-}$] state through the disassembly of existing Sup35 amyloid by Hsp104 (Klaips et al, 2014). The increase in Hsp104 expression upon thermal stress alone is not sufficient to induce Sup35 amyloid resolution and thus [*PSI*$^{+}$]^{Weak} curing (i.e. converted to [*psi*$^{-}$] state). Rather, Hsp104 must also be asymmetrically localized to mother cells through its engagement with heat-induced protein aggregates in order to induce [*PSI*$^{+}$]^{Weak} curing in mother cells (Klaips et al, 2014). However, the effect of Sir2 on heat-induced prion curing via thermal stress had not been previously addressed.

To explore that relationship, we assessed the effect of Sir2 on heat-induced prion curing. Our studies revealed that deletion of Sir2 leads to a reduction of heat-induced prion curing, which corresponded to loss of Hsp104 asymmetry. This curing defect, along with the relatively symmetrical inheritance of Hsp104 compared to wild type cells, could be reversed by deletion of the HM loci, indicating that Sir2-dependent gene regulation mediated these effects. Further studies on mating-type regulated genes controlled by the HM loci indicate that misregulation of a single gene *yjl133c-a* was required for the reduction of heat-induced prion curing.

Results

Disruption of Sir2 reduces heat-induced prion curing and Hsp104 asymmetry

[*PSI*$^{+}$]^{Weak} is cured at an elevated temperature (Klaips et al, 2014; Newnam et al, 2011). This observation could be explained by the increase in Hsp104 expression at elevated temperature and by its asymmetric retention in mother cells through its engagement with heat-induced protein aggregates (Klaips et al, 2014). Since Sir2 has been reported to mediate the aggregate asymmetry (Aguilaniu et al, 2003; Liu et al, 2010), we hypothesized that Sir2 might also affect heat-induced prion curing.

To monitor transitions from the prion [*PSI*$^{+}$] to the non-prion [*psi*$^{-}$] state, we used yeast strains encoding a premature termination codon in the *ade1-14* gene. In [*PSI*$^{+}$] strains, Sup35 forms into aggregates and thus the translational termination function is compromised, leading to the premature stop-codon read-through and the formation of white or pink colonies on rich medium, while in [*psi*$^{-}$] strains, translation is faithfully terminated at the premature stop codon leading to the formation of red colonies on rich medium (Chernoff et al, 1995). Transiently elevating the growth temperature from 30°C to 40°C induced 70% of [*PSI*$^{+}$]^{Weak} curing in wild type cells with both fully red and sectored colonies observed, while only 18% of heat-induced [*PSI*$^{+}$]^{Weak} curing was observed in *Δsir2* cells (Figure 1A). Consistent with previous reports, thermal stress induced curing through resolution of existing Sup35 aggregates in the wild type strain, which was indicated by the decrease in the size of SDS-resistant Sup35 aggregates immediately after thermal stress (Figure 1B, lane 1 and 2) and by their decreased accumulation during recovery from the stress (Figure 1B, lane 1 and 3), as assessed by semi-denaturing

detergent agarose gel electrophoresis (SDD-AGE) (Kryndushkin et al, 2003). In Δ*sir2* cells, thermal stress also leads to an immediate reduction in Sup35 aggregate size (Figure 2B, lane 4 and 5), but Sup35 aggregates remained abundant during recovery (Figure 1B, lane 3 and 6), consistent with the decrease in heat-induced prion curing in *Δsir2* cells (Figure 1A). Thus, disruption of Sir2 reduces the efficiency of Sup35 amyloid resolution following thermal stress.

Because the heat-induced disassembly of Sup35 amyloid is an Hsp104-dependent process (Klaips et al, 2014), we assessed both Hsp104 levels and their partitioning during cell division to determine the molecular basis of the reduced curing efficiency in Δ*sir2* cells. By SDS-PAGE and quantitative immunoblotting, Hsp104 expression levels were elevated to a similar extend in both wild type and *Δsir2* cells following heat shock (Figure S1A), indicating that differences in gene expression could not explain the reduction in curing efficiency in Δ*sir2* cells.

Next, we assessed both the accumulation of misfolded proteins and Hsp104 asymmetry following thermal stress. By differential centrifugation, protein aggregates accumulated to similar extents in both wild type and *Δsir2* cells (Figure S1B). Correspondingly, the aggregation retention efficiency (ARE: percentage of mother cells capable of retaining all aggregates during cytokinesis), detected by microfluidics, was also similar between wild type and *Δsir2* cells (Figure 1C). This observation is at odds with a previous report (Liu et al, 2010), and we cannot currently explain the discrepancy. To further examine Hsp104 partitioning using a less subjective assay, we monitored the distribution of total Hsp104-GFP, detected by microfluidics, during cell division following thermal stress. Disruption of *Sir2*, significantly decreased the asymmetric retention of

Hsp104 in comparison with wild type cells (Figure 1D). This change corresponds to the decrease in curing efficiency in ∆*sir2* cells (Figure 1A), raising the possibility that it is the causative event.

Sir2 modulates prion curing through its regulation of mating-type specific gene expression

In addition to its role in establishing asymmetry, Sir2 facilitates transcriptional silencing at the cryptic mating type loci (HM loci: HML and HMR) (Aparicio et al, 1991; Klar et al, 1979; Rine & Herskowitz, 1987; Rine et al, 1979). To test whether these activities are related, we explored the possibility that the reduction in heat-induced prion curing in *Δsir2* cells resulted from derepression of HM loci. We constructed *MATa ΔHML* and *Δsir2ΔHML* strains and compared the heat-induced prion curing in these strains to that of wild type yeast. *ΔHML* cells had similar levels of heat-induced curing as wild type cells (Figure 1A), consistent with the fact that HM loci are silenced in wild type cells (Rine & Herskowitz, 1987). However, disruption of *HML* restored heat-induced prion curing in the *Δsir2* background cells back to wild type levels (Figure 1A). Moreover, the accumulation of Sup35 aggregates was reduced in *Δsir2ΔHML* cells compared to *Δsir2* cells during recovery (Figure 1B, lane 6 and 9), suggesting that these complexes were being disassembled in the double mutant. Together, these observations suggest that the reduction in heat-induced prion curing in *Δsir2* cells resulted from the derepression of HM loci.

To ensure that the restoration of prion curing occurred through the same pathway, we examined the subpopulation of cells being cured. Heat-induced prion curing occurs in wild type mother cells (Klaips et al, 2014). We incubated [*PSI*$^{+}$]^{Weak} wild type and *Δsir2ΔHML* cultures at 40°C and then isolated single unbudded cells on rich solid medium

at 30°C. Following budding and cell division, mother and daughter cells were separated by micromanipulation and grown into colonies, which were then dispersed on rich solid medium to quantify prion curing. Mother cells in both wild type and *Δsir2ΔHML* strains were more likely to be cured than their daughters (Figure 1E), indicating curing in both genetic backgrounds proceeded through the same mechanism.

To determine the molecular mechanism of heat-induced prion curing in *Δsir2ΔHML* cells, we also monitored the levels of Hsp104 protein expression (Figure S1A), the accumulation of misfolded proteins (Figure S1B) and ARE (Figure 1C) and found no differences among wild type, *Δsir2* and *Δsir2ΔHML* cells. However, the asymmetric partitioning of Hsp104-GFP in *Δsir2ΔHML* cells during cell division following thermal stress was significantly reversed back to wild type levels (Figure 1D), which is consistent with the curing efficiency. Thus, disruption of asymmetric retention in *Δsir2* cells could also be explained by derepression of HM loci.

Actin cable state could not explain Hsp104-GFP asymmetric retention

It was reported that the actin cytoskeleton helped retain protein aggregates and maintain asymmetric inheritance, as this structure was disrupted in *Δsir2* cells (Aguilaniu et al, 2003; Erjavec et al, 2007; Liu et al, 2010). To test whether the actin cable state could explain total Hsp104-GFP asymmetric retention, we compared the distribution of the actin-binding protein Abp140, tagged with GFP, as this fusion was reported to be a more sensitive detector of actin cables than phalloidin staining (Yang & Pon, 2002). No differences were detected among wild type, *Δsir2* and *Δsir2ΔHML* cells (Figure 2), indicating that the actin cable presence could not explain Hsp104-GFP asymmetric retention.

Cell size but not budding pattern has some effect on heat-induced prion curing

Deletion of *SIR*2 leads to changes of both cell size and budding pattern, as derepression of HM loci changes cell morphology from the haploid to the diploid phenotype (Wright & Schneider, 2013; Yang et al, 2011). Compared to wild type cells, *Δsir2* cells are larger and spindle shaped, reflecting a switch in budding pattern from axial to bipolar budding (Figure 3A) (Haber, 2012); these changes are reversed by the additional deletion of HML in the *MAT*a *Δsir2* strain (Figure 3A), suggesting that the restoration of heat-induced prion curing in the double mutant could be mediated by one or both of these characteristics.

To determine whether changes in budding pattern affect heat-induced prion curing, we disrupted *AXL1, BUD3, or BUD4*; deletion of these genes switches haploids from an axial to a bipolar budding pattern without altering cell size (Figure 3B) (Bi & Park, 2012). No differences in heat-induced prion curing were found among these strains (Figure 3C), indicating budding pattern changes could not explain the reduction in heat-induced prion curing in *Δsir2* cells.

To determine whether changes in cell size affect heat-induced prion curing, we constructed wild type diploids (2N), triploids (3N), and tetraploids (4N) cells to create a series of cells with bipolar budding patterns (Figure 3D) but with varying sizes (Figure 3E). Heat-induced prion curing was slightly reduced as cell size increased (Figure 3F), but this effect did not approach the level seen in *Δsir2* cells (Figure 1A), indicating changes in cell size were not sufficient to explain the differences in heat-induced prion curing.

yjl133c-a could explain heat-induced prion curing in Δsir2 cells

The restoration of heat-induced prion curing to wild type levels in Δ*sir2* cells by disruption of HM loci suggested that this effect was mediated through transcriptional derepression of mating-type regulated genes. To determine whether repression of these targets alone is sufficient to reduce heat-induced prion cuing, we expressed *MATα* in wild type *MATa* cells to create a pseudo-diploid phenotype. As expected, expression of *MAT*α inhibited mating by *MATa* cells (Figure 4A) (Hall & Johnson, 1987), which was shown by the absence of growth on solid media lacking amino acids compared to wild type *MATa* cells, but it was unable to reduce heat-induced prion curing in wild type cells to the level seen in Δ*sir2* cells (Figure 4B). In addition, we found that disruption of Sir3 but not Sir4 phenocopied the reduction in heat-induced prion curing in *Δsir2* cells (Figure 4C), although silencing at *HML*, *HMR*, and heterochromatic telomeres is mediated by the Sir2/3/4 complex (Moazed et al, 1997). Overall, our results show that the repression of mating-type specific genes was required but not sufficient to explain the reduction in heat-induced prion curing observed in Δ*sir2* cells.

To determine which mating type-regulated gene was specifically required for the reduction of heat-induced prion curing in *Δsir2* cells, we constructed a series of double-mutant cells, containing a deletion of *SIR2* and a deletion of a mating-type specific gene, rationalizing that deletion of the latter would restore heat-induced prion curing to wild type levels. Of 17 genes tested, we found that disruption of one, *YJL133c-a*, restored heat-induced prion curing to wild type levels (Figure 4D, 4E). Notably, disruption of *YJL133c-a* alone does not alter heat-induced prion curing levels (Figure 4E), indicating that

derepression of this factor in Δ*sir2* cells is required for the suppression of heat-induced prion curing by disruption of *Δsir2*.

Discussion

In *Saccharomyces cerevisiae*, thermal stress induces [*PSI*$^{+}$]^{Weak} prion curing (Klaips et al, 2014). However, deletion of *SIR2* reduces heat-induced curing through derepression of the HM loci. This effect correlates with the efficiency of Hsp104 asymmetric retention, uncovering a role for mating identity in this process. We eliminated cell size, budding pattern, actin cytoskeleton integrity, and Hsp104 expression levels as contributing factors. Instead, we found that derepression of *YJL133C-A*, one of the mating-type regulated genes, was required for the *Δsir2* heat-induced prion curing phenotype. Thus, YJL133C-A might mediate the establishment of damage asymmetry as a downstream target of Sir2.

Sir2 was reported to mediate damaged protein aggregate asymmetry (Aguilaniu et al, 2003; Erjavec et al, 2007; Liu et al, 2010). However, surprisingly, no differences in the retention of visible foci of Hsp104-GFP (ARE) were detected between wild type and *Δsir2* cells, which was not consistent with previous reports (Liu et al, 2010). While we currently cannot explain this difference, we cannot rule out differences in cell populations, thermal stress conditions, yeast genetic backgrounds, or the presence of the [*PSI*$^{+}$] prion as mitigating factors. For example, we used a milder thermal stress condition (40°C vs 42°C) and a different genetic background for our studies to maintain viability while examining propagation of the [*PSI*$^{+}$] prion. And we only quantified ARE immediately after cytokinesis in cells that experienced thermal stress at their small-budded stage. Further studies are

required to elucidate the basis for the differences between these two studies which would further our understanding of the Sir2-mediated damage asymmetry process.

Since the ARE assay is subjective, we instead examined Hsp104 partitioning after cytokinesis by quantifying total protein levels using a GFP fusion and microfluidics. Previously it was shown that overproduction of Hsp104 in *Δsir2* cells markedly increased the mean lifespan to almost the same value as wild type cells, suggesting that limits on Hsp104 activity contribute to the lifespan reduction of Δ*sir2* cells (Erjavec et al, 2007). Our studies on heat-induced prion curing extend these observations by directly demonstrating that Hsp104 function is reduced in Δ*sir2* cells, presumably due to its increased partitioning. Although deletion of *HML* restored Hsp104 asymmetry and heat shock-induced prion curing, it could not reverse the shorter replicative life span in *Δsir2* cells (Kaeberlein et al, 1999), suggesting that the limitation of Hsp104 function is only partly responsible for the latter effect.

Our studies reveal the involvement of HM loci in asymmetric inheritance. The Sir2/3/4 complex is known to be required for transcriptional silencing of the HM loci in haploid yeast cells (Schlissel et al, 2017; Smeal et al, 1996). Our studies imply a connection between this activity and the establishment of damage asymmetry in yeast cells. These observations raise the possibility that disruption of asymmetric inheritance in older cells might also result from derepression of HM loci during aging.

Our genetic analysis indicates that of the 17 known mating-type specific genes, a single gene, *YJL133C*-A, is required for the reduction in heat-induced prion curing observed in the Δ*sir2* strain. YJL133C-A localizes to the mitochondria, implying that this organelle might play a crucial role in damage asymmetry. Protein aggregates have been

reported to tether to well-anchored maternal mitochondria, whereas mitochondria acquired by the bud are largely free of aggregates upon cell division (Zhou et al, 2014) YJL133C-A, which localizes at outer membrane of mitochondria (Reinders et al, 2006), might mediate the association of aggregates with mitochondria.

Our results indicate that derepression of the HM loci was required but not sufficient to reduce heat-induced prion curing, which suggests that the effect of Sir2 on heat-induced prion curing could also be affected by other functions of Sir2. Although disruption of Sir2, Sir3 and Sir4 all derepress HM mating type loci expression and thus YJL133C-A expression, heat-induced prion curing in *Δsir4* cells was not reduced as in *Δsir2* and *Δsir3* cells, implicating other gene(s) not affected by disruption of Sir4 but affected by disruption of Sir2 or Sir3 was also required for reduce heat-induced prion curing. Further comparison of gene profiles of three different strains (Ellahi et al, 2015) suggests that YFL063W might be the other downstream target of Sir2 that was required to affect heat-induced prion curing.

Together, our observations suggest the downstream targets of Sir2, HM loci and YJL133C-A mediate damage asymmetry in *Saccharomyces cerevisiae*. Within this framework, our studies provide evidence to further support that asymmetric retention of Hsp104 was required for heat-induced prion curing. Our studies raise the possibility that the attachment of aggregates to mitochondria might explain the asymmetric retention mechanism.

Materials

Plasmids. All plasmids used in this study are listed in Table 1. The HMLKO-his3MX6 as a *Xho*I fragment PCR amplified from pFA6a-his3MX6 using primer FP83 and FP84 (Table 2) was then subcloned into pGEM3 as a *Xho*I fragment to create pGEM3-HMLKO-his3MX6 (SB1076). pRS306-$P_{MAT\alpha}$MATα (SB1174) was made by removing the 2-micron sequence from Yep352- $P_{MAT\alpha}$MATα (a gift from J. Laney).

Oligonucleotides. Oligonucleotides used in this study are listed in Table 2.

Yeast strains. All strains are derivatives of 74-D694 and are listed in Table 3. All of the [*PSI*$^{+}$]^{Weak} knockout strains except the HML knockout were constructed by transformation of PCR-generated cassettes using different knockout cassettes as templates with corresponding primers listed in Table 2 and selection on appropriate media. For the HML knockout, SB1076 linearized with *BamH*I was transformed and selected on minimal medium lacking histidine. The ABP140-GFP [*PSI*$^{+}$]^{Weak} strain (SY3184) was created by transforming a PCR-generated cassette using pFA6a-GFP(S65T)-KanMX6 as a template with primers FP71 and FP72 (Table 2) into a wild type [*PSI*$^{+}$]^{Weak} strain (SLL2600) and selecting on medium containing 300 µg/ml G418. Using this strain, SIR2 and HML were disrupted as described above to create ABP140-GFP in the *Δsir2* and *Δsir2ΔHML* backgrounds. All the disruptions and integrations were verified by PCR. The [*PSI*$^{+}$]^{Weak} wild type (*MATa* or *MATα,* 2n) was constructed through overexpressing HO endonuclease in wild type [*PSI*$^{+}$]^{Weak} diploid strain (SY945) followed by FOA counter-selection; single colonies following sporulation were subsequently isolated and tested for mating type. The [*PSI*$^{+}$]^{Weak} wild type (*MATa/α*, 3n) (SY3612) was constructed through mating wild type (*MATa*, n) (SLL2600) with wild type (*MATα*, 2n).

And the [*PSI*$^{+}$]^{Weak} wild type (*MATa/α*, 4n) (SY3613) was constructed through mating wild type (*MATa*, 2n) (SY945) with wild type (*MATα*, 2n).

Growth conditions and phenotypic analysis. Unless otherwise specified, yeast cultures were grown in rich YPD medium supplemented with 0.3 mM adenine. Cultures were maintained at an OD_{600} of less than 0.5 at 30°C for at least 10 doublings to ensure exponential growth. Where indicated, cultures were then transferred to 40°C for the specified period. To analyze colony-color phenotype, aliquots of cultures were diluted in water as needed to ensure well-separated single colonies upon plating on solid YPD medium. After growth at 30°C, each colony was scored based on colony-color phenotype: fully cured (completely red, [*psi*$^{-}$]), sectored (part red and part white), or [*PSI*$^{+}$] (completely white). For all colony-counting assays, at least 150 colonies were counted for each experimental condition/time point.

Protein analysis. Semi-denaturing detergent agarose gel electrophoresis (SDD-AGE), SDS-PAGE and quantitative immunoblotting were performed as previously described (Pezza et al, 2009).

Imaging and microfluidics. Static images were obtained on a DeltaVision deconvolution microscope equipped with a 100x objective. Images were processed in ImageJ software (National Institutes of Health, Bethesda, USA). Microfluidics experiments were performed on a Zeiss Axio Observer Z1 using a CellAsics microfluidics plate with temperature controls and media flow of 1 psi on a Y04C yeast perfusion plate. Imaging was performed in complete minimal medium supplemented with 2% glucose and 2.5 mM adenine. Fluorescence intensity was analyzed using the Zen software package (Zeiss, Germany).

Mating efficiency test. Strains were mated with mating tester strains to complement each other's amino acid auxotrophy. The mating efficiency was measured by the growth of diploid colonies on plate lacking amino acid supplements.

Table 1: Plasmids

Name	**Description**	**Reference**
SB1076	pGEM3-HMLKO-his3MX6	This study
SB1174	pRS306-$P_{MAT\alpha}$MATα	This study

Table 2: Oligonucleotide Sequences

Name	Description	Sequence (5'-3')
FP33	PTEF CHK	GCACGTCAAGACTGTCAAGG
FP34	pFA6a	TGCCCAGATGCGAAGTTAAGTG
FP45	5'SIR2 KO CHK	AGCAGTCTTTCTCCCTTG
FP46	3'SIR2 KO CHK	CGACATGTGCATTGTATTAC
FP54	5'HML KO CHK	ACTTGGAAGAAGCGTTGGATAG
FP69	5'ABP140-GFP CHK	CTTGAGGATAATAGCCGCAGAT
FP70	3'ABP140-GFP CHK	TGGACTGCAAAGAGTTTAGCGC
FP71	5'ABP140-GFP	GTACCGCTGCTGGGTACAAGCTGTGTTTGACGTT CCTCAAGCTGCTGCTGCTGCTCGGATCCCCGGGT TAATTAA
FP72	3'ABP140-GFP	ATGATGAGAGAGGAGGTGGTACTTGTCTCAGAAC TTCCTAGAATTCGAGCTCGTTTAAAC
FP83	5' HML-HI3MX6	CTCGAGGGTTAATTAAGGCGCGCCAGAT
FP84	3' HML-HI3MX6	CTCGAGGCATAGGCCACTAGTGGATCTG
FP96	3'HML KO CHK	CATAGGTTTCCAGCATAGTCTC
FP100	5'AXL1 KO	CTGGCGTTAAAAAATAGCAACTGAATAAGTTTTTTT ACTGCAGCTGAAGCTTCGTACGC
FP101	3'AXL1 KO	TAACAAAAACGTGGAAAGGCTGGAACGAGCAAAA TACGGTGCATAGGCCACTAGTGGATCTG
FP102	5'AXL1 KO CHK	TATGTTGTTCTACCTTAAAAATTTG
FP103	3'AXL1 KO CHK	CTGTCTTGGATGCACTAGACAT
FP112	5'SIR2 KO	CATTCAAACCATTTTTCCCTCATCGGCACATTAAA GCTGGCAGCTGAAGCTTCGTACGC
FP113	3'SIR2 KO	TATTAATTTGGCACTTTTAAATTATTAAATTGCCTT CTACGCATAGGCCACTAGTGGATCTG
FP116	5'HSP104-GFP	CGATAATGAGGACAGTATGGAAATTGATGATGACC TAGATGGTAGTGGTAGTGGTAGTCGGATCCCCGG GTTAATTAA
FP117	3'HSP104-GFP	ATTCTTGTTCGAAAGTTTTTAAAAATCACACTATAT TAAAGAATTCGAGCTCGTTTAAAC
FP118	5'HSP104-GFP CHK	CAAGAATCTACCAAGAATTTGGT
FP119	3'HSP104-GFP CHK	TGTTCGCTGTAACATTATATTGGC
FP141	5'BUD3 KO	TGTTATCTGGTTGCTAAAAGAGTATATTTACACCTC ACCACAGCTGAAGCTTCGTACGC
FP142	3'BUD3 KO	TTGCATTAAATTAAAAAGAAAAAAAAAATCAATAAA ACACGCATAGGCCACTAGTGGATCTG

FP143	5’BUD3 KO CHK	GGTACAGGATTATTAGTGAGCAA
FP144	3’BUD3 KO CHK	TTGCTCCTCTGGGTTGTGCTAT
FP145	5’BUD4 KO	TTTAGTTCATTAAATTATATAAAAACAAAAGTACAG AAGCCAGCTGAAGCTTCGTACGC
FP146	3’BUD4 KO	TCATCAGATTATATGCTGTTTTCATTCCATTAATCA CCTTGCATAGGCCACTAGTGGATCTG
FP147	5’BUD4 KO CHK	CAAGTTGTTGATGTTCATCTGCT
FP148	3’BUD4 KO CHK	TACCTGGATGGAGTATTTACATA
FP267	5’P_{GPD}-HOG1	ATTTTCTCTTTCTTCTATATTGGTAAATACTAGACT CGAAGAATTCGAGCTCGTTTAAAC
FP268	3’P_{GPD}-HOG1	TACCGAATATCTGTGTCCTAATGAATTCCTCGTTA GTGGTCATTCGAAACTAAGTTCTTGGTGTTT
FP269	5’P_{GPD}-HOG1 CHK	CTTCATTACGGCATAACGTATTA
FP270	3’P_{GPD}-HOG1 CHK	CGAAATCGCAAATCTTCAAATCA
FP284	5’P_{GPD}-DDR2 CHK	CAGACCACCCCTGAGCTAAGG
FP285	3’P_{GPD}-DDR2 CHK	GTATACGGGTCGTTCAAGTACG
FP399	5’YJL047C-A KO	CCAAAGATGCATAGTTCAACTGATTGAACATACTA TCGAACAGCTGAAGCTTCGTACGC
FP400	3’YJL047C-A KO	AGTACGCGCTGGGTCCGTTACGATTCGTGCTGCA AGAGGTGCATAGGCCACTAGTGGATCTG
FP401	5’YJL047C-A KO CHK	CTAGGGACGAATCAACAGCAAC
FP402	3’YJL047C-A KO CHK	CCTGACATCTCGTACATTTCTG
FP403	5’YER053C-A KO	TAAAAACAAACAATAGCTTTACTACACAGTACACA CTACACAGCTGAAGCTTCGTACGC
FP404	3’YER053C-A KO	TACCTCTCTTGGCGGCAGTAAGCAGATTAGCTGAT TTAAAGCATAGGCCACTAGTGGATCTG
FP405	5’YER053C-A KO CHK	GCTTCAGTTTGAAATGTAAGGGA
FP406	3’YER053C-A KO CHK	TTGTGCCTTCCTCGAATGTCTA
FP407	5’SFC1 KO	TTTAGCCGTAAGATAACATAACAAAGAAGAAGAAA GAAAACAGCTGAAGCTTCGTACGC
FP408	3’SFC1 KO	TTTTTTCTTTATTTCATTTTGTAGTCCCATTGTTCAT CATGCATAGGCCACTAGTGGATCTG
FP409	5’SFC1 KO CHK	AACGGACCTTAATTGTGACGAA
FP410	3’SFC1 KO CHK	GTTTGTAAAACTTAGGAACCATG
FP411	5’FMP43 KO	AAGCATTCAAGACACATAGAAACACAAACCTATAT TTTTACAGCTGAAGCTTCGTACGC
FP412	3’FMP43 KO	AAAAAAATGCGAGTTCAGGAACATATTATCGTTTA CGTAAGCATAGGCCACTAGTGGATCTG

FP413	5’FMP43 KO CHK	AGGTTACCCTGCAGTTTGGATA
FP414	3’FMP43 KO CHK	ATCGTAAGATGTGACTATGTTGC
FP415	5’JID1 KO	TATCTACACACCATAGGTCACTACTTGCAATATATT TGTTCAGCTGAAGCTTCGTACGC
FP416	3’JID1 KO	ATTTAGTAATTGTATTCCGCGAGCGGCGCAATAGG TGATTGCATAGGCCACTAGTGGATCTG
FP417	5’JID1 KO CHK	CGTCTTTGTTATTGATAAGACATC
FP418	3’JID1 KO CHK	TCCATTCTAACTAATTCATCTCT
FP419	5’GTO3 KO	TATTCCATCTCTCTCTTGCAACCACGGCAAAGCTG GAGCTCAGCTGAAGCTTCGTACGC
FP420	3’GTO3 KO	GTGATGTGTGTGCGTGCTAATCGAAAGAAAAAAAA AAATTGCATAGGCCACTAGTGGATCTG
FP421	5’GTO3 KO CHK	GCTAAAGGAAACAACAACGAGAA
FP422	3’GTO3 KO CHK	TTATTCTATTATCGAGACTGTAGC
FP423	5’YDR042C KO	ACTAGGTCTCTAAGAGAAAAAATCTTTTTCTTTTCA CAACCAGCTGAAGCTTCGTACGC
FP424	3’YDR042C KO	AACTATATGATGAACAATTTTGTACTAATATTGCGG CCCGGCATAGGCCACTAGTGGATCTG
FP425	5’YDR042C KO CHK	TGATGATATCCTATAACAACAACA
FP426	3’YDR042C KO CHK	GTCCGAAATATCGCTGGACTTG
FP427	5’HMX1 KO	ACAGCATATATACACACACACACATAAAATAACCG CAAAACAGCTGAAGCTTCGTACGC
FP428	3’HMX1 KO	GTATATATTATGTTTGTATTTAGACTTTTTTTTTTTAT ACGGCATAGGCCACTAGTGGATCTG
FP429	5’HMX1 KO CHK	CACCAAGACCCGTTGCCATGT
FP430	3’HMX1 KO CHK	AACAGCAATTAACACTACAATGC
FP431	5’MTH1 KO	GAATTTTATTCGAACGCATAGAGTACACACACTCA AAGGACAGCTGAAGCTTCGTACGC
FP432	3’MTH1 KO	TCTCCAAAAAAACCATCGGGAAGGTTTCTTTTTAG TATCTGCATAGGCCACTAGTGGATCTG
FP433	5’MTH1 KO CHK	CCTCATCTTATAATTTTGTGGAAA
FP434	3’MTH1 KO CHK	GATCGGTTTTGGTGGTTAGAAG
FP435	5’YKR075C KO	CAAGTGTTCATACACACACAAATAGATACATATAC AGAAACAGCTGAAGCTTCGTACGC
FP436	3’YKR075C KO	AAATGTGTATGTGGAAATGCAGAAGAGAGCAAAC TCTCCTGCATAGGCCACTAGTGGATCTG
FP437	5’YKR075C KO CHK	CGACTCGATACTCTTTACAAAGA
FP438	3’YKR075C KO CHK	TCAGACCATTCCGTAATGTTAAG

FP439	5’NCA3 KO	TATAGTCGCACATACTTAACTCGTCTCTCTCTAAC ACATACAGCTGAAGCTTCGTACGC
FP440	3’NCA3 KO	TCAAAATACAAGACATTCTTTTACCGAAAAGAAGA ATGACGCATAGGCCACTAGTGGATCTG
FP441	5’NCA3 KO CHK	GAGTGTAAGGTGGTAGAATTATG
FP442	3’NCA3 KO CHK	TCTTGTTAGTTCTGTTGCAACTC
FP443	5’YJR115W KO	CCTGTCGAAGAGTAGCATAACAGCAGCGTAGTGA ACGTGCCAGCTGAAGCTTCGTACGC
FP444	3’YJR115W KO	AAATGTTCTTAAGAAAGGAAAAGGGGAAAATGCAT GCTAAGCATAGGCCACTAGTGGATCTG
FP445	5’YJR115W KO CHK	CGAAACCACACGGGTCTGCCA
FP446	3’YJR115W KO CHK	TATACTGTTATGTTGCGTTGAGT
FP447	5’CYC7 KO	AAGTAAACTTCAGTAAACTACATTACATCATAAACA AAACCAGCTGAAGCTTCGTACGC
FP448	3’CYC7 KO	GAATAATAAAAGTAATAAATATCTCCTCCGACGAC ATAGCGCATAGGCCACTAGTGGATCTG
FP449	5’CYC7 KO CHK	CACTCACCACCGTCATCGTTG
FP450	3’CYC7 KO CHK	TATCCTCCGTATCCTCTTCCGTCACT
FP451	5’YDR119W-A KO	CACAGATATTTACAGACTCTTTTAATTCTAAATAGG TAAACAGCTGAAGCTTCGTACGC
FP452	3’YDR119W-A KO	GTTACACTCATTTTTAGCAAATTTTTTTTTCTTATCA AACGCATAGGCCACTAGTGGATCTG
FP453	5’YDR119W-A KO CHK	GCTTAGATAAAGATGCAGGGAAC
FP454	3’YDR119W-A KO CHK	GCTAAAAATTGTGAGATATCAGGA
FP455	5’YJL133C-A KO	TTAAATATTACATTCATAAGACAGTAAATAAACGTA TTAACAGCTGAAGCTTCGTACGC
FP456	3’YJL133C-A KO	TTAATAAACCAGGAAAGAAAAGAGCATAATTAAGA TACGCGCATAGGCCACTAGTGGATCTG
FP457	5’YJL133C-A KO CHK	AGCACGTGATACAAACCTGTCA
FP458	3’YJL133C-A KO CHK	GCACAAAGAAGGTGCAAGCAAGT
FP463	5’AHP1 KO	ACCAGAACAACACAAGTACTACCAATAACCACAAC AAAACCAGCTGAAGCTTCGTACGC
FP464	3’AHP1 KO	TTTTTATATAAACATGGTTTTATTGTCTATTACATAG CATGCATAGGCCACTAGTGGATCTG
FP465	5’AHP1 KO CHK	CTGATTTGTAATTATACGGGGAG
FP466	3’AHP1 KO CHK	CCGCTGCTTTGTTGTTGTAAACT

FP467	5’SIR3 KO	TTAAGAAAGTTGTTTTGTTCTAACAATTGGATTAGC TAAACAGCTGAAGCTTCGTACGC
FP468	3’SIR3 KO	TAGGCATATCTATGGCGGAAGTGAAAATGAATGTT GGTGGGCATAGGCCACTAGTGGATCTG
FP469	5’SIR3 KO CHK	ACACAAAGAAATGGTGTAAATGAA
FP470	3’SIR3 KO CHK	TTCGTGTGCTTGTTTTGTTTCCT
FP471	5’SIR4 KO	GCTTCAACCCACAATACCAAAAAAGCGAAGAAAAC AGCCACAGCTGAAGCTTCGTACGC
FP472	5’SIR4 KO	GGTACACTTCGTTACTGGTCTTTTGTAGAATGATA AAAAGGCATAGGCCACTAGTGGATCTG
FP473	5’SIR4 KO CHK	GTATGTGAGTACATATATCCGCA
FP474	5’SIR4 KO CHK	TGAAACGTCGCAAAATTCAAGC
FP275	5’P_{GPD}-DDR2	CCATTCTTTGGTTAATTCTTTCTTCATTCTTTTTTTT TTCGAATTCGAGCTCGTTTAAAC
FP276	3’P_{GPD}-DDR2	CGAAGACAGAGATGGCAGAAATGAAAACTTGTGA TACTTTCATTCGAAACTAAGTTCTTGGTGTTT

Table 3: Yeast Strains

Strains	Genotype	Plasmids Integrated	Figure	Reference
SLL2600	*MATa* [*PSI*$^{+}$]^{Weak} *ade1-14 his3Δ200 trp1-289 ura3-52 leu2-3, 112*	-	1A, 1B,1E, 3A, 3B, 3C, 4A, 4B, 4C, 4D, 4E, S1B	(Derkatch et al, 1996)
SY945	*MATa/α* [*PSI*$^{+}$]^{Weak} *ade1-14/ade1-14 his3Δ200/his3Δ200 trp1-289/ trp1-289 ura3-52/ura3-52 leu2-3, 112/ leu2-3, 112*	-	3D, 3E, 3F	(Klaips et al, 2014)
SY2126	*MATa* [*PSI*$^{+}$]^{Weak} *ade1-14 his3Δ200 trp1-289 ura3-52 leu2-3, 112 HSP104GFP::kanMX6*	-	1C, 1D, S1A	(Klaips et al, 2014)
SY2760	*MATa* [*PSI*$^{+}$]^{Weak} *ade1-14 his3Δ200 trp1-289 ura3-52 leu2-3, 112 SIR2/sir2::hphMX4*	-	1A, 1B, 3B, 4A, 4B, 4C, 4D, 4E, S1B	This study
SY2761	*MATa* [*PSI*$^{+}$]^{Weak} *ade1-14 his3Δ200 trp1-289 ura3-52 leu2-3, 112 SIR2/sir2::hphMX4 HSP104GFP::kanMX6*	-	1C, 1D, S1A	This study
SY3038	*MATa* [*PSI*$^{+}$]^{Weak} *ade1-14 his3Δ200 trp1-289 ura3-52 leu2-3, 112 SIR2/sir2::hphMX4 HML/hml::HIS3*	SB1076	1A, 1B,1E, 3C, S1B	This study
SY3039	*MATa* [*PSI*$^{+}$]^{Weak} *ade1-14 his3Δ200 trp1-289 ura3-52 leu2-3, 112 SIR2/sir2::hphMX4 HML/hml::HIS3 HSP104GFP::kanMX6*	SB1076	1C, 1D, S1A	This study
SY3184	*MATa* [*PSI*$^{+}$]^{Weak} *ade1-14 his3Δ200 trp1-289 ura3-52 leu2-3, 112 ABP140GFP::kanMX6*	-	2	This study
SY3186	*MATa* [*PSI*$^{+}$]^{Weak} *ade1-14 his3Δ200 trp1-289 ura3-52 leu2-3, 112 SIR2/sir2::hphMX4 ABP140GFP::kanMX6*	-	2	This study
SY3188	*MATa* [*PSI*$^{+}$]^{Weak} *ade1-14 his3Δ200 trp1-289 ura3-52 leu2-3, 112 SIR2/sir2::hphMX4 HML/hml::HIS3 ABP140GFP::kanMX6*	SB1076	2	This study

SY3295	*MATa* [*PSI*$^{+}$]^{Weak} *ade1-14 his3Δ200 trp1-289 ura3-52 leu2-3, 112 AXL1/axl1::HIS3*	-	3B, 3C	This study
SY3540	*MATa* [*PSI*$^{+}$]^{Weak} *ade1-14 his3Δ200 trp1-289 ura3-52 leu2-3, 112 BUD3/bud3::HIS3*	-	3B, 3C	This study
SY3541	*MATa* [*PSI*$^{+}$]^{Weak} *ade1-14 his3Δ200 trp1-289 ura3-52 leu2-3, 112 BUD4/bud4::HIS3*	-	3B, 3C	This study
SY3557	*MATa* [*PSI*$^{+}$]^{Weak} *ade1-14 his3Δ200 trp1-289 ura3-52 leu2-3, 112 HML/hml::HIS3*	SB1076	1A	This study
SY3585	*MATa* [*PSI*$^{+}$]^{Weak} *ade1-14 his3Δ200 trp1-289 ura3-52::URA3::*$P_{MAT\alpha}$*MATα leu2-3, 112*	-	4A, 4B	This study
SY3586	*MATa* [*PSI*$^{+}$]^{Weak} *ade1-14 his3Δ200 trp1-289 ura3-52 leu2-3, 112 SIR2/sir2::hphMX4 YJL047C-A/yjl047c-a::HIS3*	-	4D,	This study
SY3587	*MATa* [*PSI*$^{+}$]^{Weak} *ade1-14 his3Δ200 trp1-289 ura3-52 leu2-3, 112 SIR2/sir2::hphMX4 YER053C-A/yer053c-a::HIS3*	-	4D	This study
SY3588	*MATa* [*PSI*$^{+}$]^{Weak} *ade1-14 his3Δ200 trp1-289 ura3-52 leu2-3, 112 SIR2/sir2::hphMX4 SFC1/sfc1::HIS3*	-	4D	This study
SY3589	*MATa* [*PSI*$^{+}$]^{Weak} *ade1-14 his3Δ200 trp1-289 ura3-52 leu2-3, 112 SIR2/sir2::hphMX4 FMP43/fmp43::HIS3*	-	4D	This study
SY3590	*MATa* [*PSI*$^{+}$]^{Weak} *ade1-14 his3Δ200 trp1-289 ura3-52 leu2-3, 112 SIR2/sir2::hphMX4 JID1/jid1::HIS3*	-	4D	This study
SY3591	*MATa* [*PSI*$^{+}$]^{Weak} *ade1-14 his3Δ200 trp1-289 ura3-52 leu2-3, 112 SIR2/sir2::hphMX4 GTO3/gto3::HIS3*	-	4D	This study
SY3592	*MATa* [*PSI*$^{+}$]^{Weak} *ade1-14 his3Δ200 trp1-289 ura3-52 leu2-3, 112 SIR2/sir2::hphMX4 YDR042C/ydr042c::HIS3*	-	4D	This study
SY3593	*MATa* [*PSI*$^{+}$]^{Weak} *ade1-14 his3Δ200 trp1-289 ura3-52 leu2-3, 112 SIR2/sir2::hphMX4 HMX1/hmx1::HIS3*	-	4D	This study
SY3594	*MATa* [*PSI*$^{+}$]^{Weak} *ade1-14 his3Δ200 trp1-289 ura3-52 leu2-3, 112 SIR2/sir2::hphMX4 MTH1/mth1::HIS3*	-	4D	This study
SY3595	*MATa* [*PSI*$^{+}$]^{Weak} *ade1-14 his3Δ200 trp1-289 ura3-52 leu2-3, 112 SIR2/sir2::hphMX4 YKR075C/ykr075c::HIS3*	-	4D	This study

SY3596	*MATa* [*PSI*$^{+}$]^{Weak} *ade1-14 his3Δ200 trp1-289 ura3-52 leu2-3, 112 SIR2/sir2::hphMX4 NCA3/nca3::HIS3*	-	4D	This study
SY3597	*MATa* [*PSI*$^{+}$]^{Weak} *ade1-14 his3Δ200 trp1-289 ura3-52 leu2-3, 112 SIR2/sir2::hphMX4 CYC7/cyc7::HIS3*	-	4D	This study
SY3598	*MATa* [*PSI*$^{+}$]^{Weak} *ade1-14 his3Δ200 trp1-289 ura3-52 leu2-3, 112 SIR2/sir2::hphMX4 YDR119W/ydr119w::HIS3*	-	4D	This study
SY3599	*MATa* [*PSI*$^{+}$]^{Weak} *ade1-14 his3Δ200 trp1-289 ura3-52 leu2-3, 112 SIR2/sir2::hphMX4 YJL133C-A/yjl133c-a::HIS3*	-	4D, 4E	This study
SY3600	*MATa* [*PSI*$^{+}$]^{Weak} *ade1-14 his3Δ200 trp1-289 ura3-52 leu2-3, 112 SIR2/sir2::hphMX4 AHP1/ahp1::HIS3*	-	4D	This study
SY3601	*MATa* [*PSI*$^{+}$]^{Weak} *ade1-14 his3Δ200 trp1-289 ura3-52 leu2-3, 112 SIR2/sir2::hphMX4* P_{DDR2}*-DDR2/*P_{GPD}*-DDR2::kanMX4*	-	4D	This study
SY3602	*MATa* [*PSI*$^{+}$]^{Weak} *ade1-14 his3Δ200 trp1-289 ura3-52 leu2-3, 112 SIR3/sir3::HIS3*	-	4C	This study
SY3603	*MATa* [*PSI*$^{+}$]^{Weak} *ade1-14 his3Δ200 trp1-289 ura3-52 leu2-3, 112 SIR4/sir4::HIS3*	-	4C	This study
SY3612	*MATa/α* [*PSI*$^{+}$]^{Weak} *ade1-14/ade1-14/ade1-14 his3Δ200/his3Δ200/his3Δ200 trp1-289/trp1-289/trp1-289 ura3-52/ura3-52/ura3-52 leu2-3, 112/leu2-3, 112/leu2-3, 112*	-	3D, 3E, 3F	This study
SY3613	*MATa/α* [*PSI*$^{+}$]^{Weak} *ade1-14/ade1-14/ade1-14/ade1-14 his3Δ200/his3Δ200/his3Δ200/his3Δ200 trp1-289/trp1-289/trp1-289/trp1-289 ura3-52/ura3-52/ura3-52/ura3-52 leu2-3, 112/leu2-3, 112/leu2-3, 112/leu2-3, 112*	-	3D, 3E, 3F	This study

References

Aguilaniu H, Gustafsson L, Rigoulet M, Nystrom T (2003) Asymmetric inheritance of oxidatively damaged proteins during cytokinesis. Science 299: 1751-3

Aparicio OM, Billington BL, Gottschling DE (1991) Modifiers of position effect are shared between telomeric and silent mating-type loci in S. cerevisiae. Cell 66: 1279-87

Bi E, Park HO (2012) Cell polarization and cytokinesis in budding yeast. Genetics 191: 347-87

Blander G, Guarente L (2004) The Sir2 family of protein deacetylases. Annual review of biochemistry 73: 417-35

Chernoff YO, Lindquist SL, Ono B, Inge-Vechtomov SG, Liebman SW (1995) Role of the chaperone protein Hsp104 in propagation of the yeast prion-like factor [psi+]. Science 268: 880-4

Derkatch IL, Chernoff YO, Kushnirov VV, Inge-Vechtomov SG, Liebman SW (1996) Genesis and variability of [PSI] prion factors in Saccharomyces cerevisiae. Genetics 144: 1375-86

Dukan S, Nystrom T (1998) Bacterial senescence: stasis results in increased and differential oxidation of cytoplasmic proteins leading to developmental induction of the heat shock regulon. Genes & development 12: 3431-41

Dutnall RN, Pillus L (2001) Deciphering NAD-dependent deacetylases. Cell 105: 161-4

Ellahi A, Thurtle DM, Rine J (2015) The Chromatin and Transcriptional Landscape of Native Saccharomyces cerevisiae Telomeres and Subtelomeric Domains. Genetics 200: 505-21

Erjavec N, Larsson L, Grantham J, Nystrom T (2007) Accelerated aging and failure to segregate damaged proteins in Sir2 mutants can be suppressed by overproducing the protein aggregation-remodeling factor Hsp104p. Genes & development 21: 2410-21

Gotz M, Huttner WB (2005) The cell biology of neurogenesis. Nature reviews Molecular cell biology 6: 777-88

Grune T, Jung T, Merker K, Davies KJ (2004) Decreased proteolysis caused by protein aggregates, inclusion bodies, plaques, lipofuscin, ceroid, and 'aggresomes' during oxidative stress, aging, and disease. The international journal of biochemistry & cell biology 36: 2519-30

Haber JE (2012) Mating-type genes and MAT switching in Saccharomyces cerevisiae. Genetics 191: 33-64

Hall MN, Johnson AD (1987) Homeo domain of the yeast repressor alpha 2 is a sequence-specific DNA-binding domain but is not sufficient for repression. Science 237: 1007-12

Henderson KA, Gottschling DE (2008) A mother's sacrifice: what is she keeping for herself? Current opinion in cell biology 20: 723-8

Homem CC, Knoblich JA (2012) Drosophila neuroblasts: a model for stem cell biology. Development 139: 4297-310

Imai S, Armstrong CM, Kaeberlein M, Guarente L (2000) Transcriptional silencing and longevity protein Sir2 is an NAD-dependent histone deacetylase. Nature 403: 795-800

Inaba M, Yamashita YM (2012) Asymmetric stem cell division: precision for robustness. Cell stem cell 11: 461-9

Kaeberlein M, McVey M, Guarente L (1999) The SIR2/3/4 complex and SIR2 alone promote longevity in Saccharomyces cerevisiae by two different mechanisms. Genes & development 13: 2570-80

Kennedy BK, Austriaco NR, Jr., Guarente L (1994) Daughter cells of Saccharomyces cerevisiae from old mothers display a reduced life span. The Journal of cell biology 127: 1985-93

Klaips CL, Hochstrasser ML, Langlois CR, Serio TR (2014) Spatial quality control bypasses cell-based limitations on proteostasis to promote prion curing. eLife 3

Klar AJ, Fogel S, Macleod K (1979) MAR1-a Regulator of the HMa and HMalpha Loci in SACCHAROMYCES CEREVISIAE. Genetics 93: 37-50

Kryndushkin DS, Alexandrov IM, Ter-Avanesyan MD, Kushnirov VV (2003) Yeast [PSI+] prion aggregates are formed by small Sup35 polymers fragmented by Hsp104. The Journal of biological chemistry 278: 49636-43

Liu B, Larsson L, Caballero A, Hao X, Oling D, Grantham J, Nystrom T (2010) The polarisome is required for segregation and retrograde transport of protein aggregates. Cell 140: 257-67

Moazed D, Kistler A, Axelrod A, Rine J, Johnson AD (1997) Silent information regulator protein complexes in Saccharomyces cerevisiae: a SIR2/SIR4 complex and evidence for a regulatory domain in SIR4 that inhibits its interaction with SIR3. Proceedings of the National Academy of Sciences of the United States of America 94: 2186-91

Morrison SJ, Kimble J (2006) Asymmetric and symmetric stem-cell divisions in development and cancer. Nature 441: 1068-74

Newnam GP, Birchmore JL, Chernoff YO (2011) Destabilization and recovery of a yeast prion after mild heat shock. J Mol Biol 408: 432-48

Pelletier L, Yamashita YM (2012) Centrosome asymmetry and inheritance during animal development. Current opinion in cell biology 24: 541-6

Pezza JA, Langseth SX, Raupp Yamamoto R, Doris SM, Ulin SP, Salomon AR, Serio TR (2009) The NatA acetyltransferase couples Sup35 prion complexes to the [PSI+] phenotype. Molecular biology of the cell 20: 1068-80

Reinders J, Zahedi RP, Pfanner N, Meisinger C, Sickmann A (2006) Toward the complete yeast mitochondrial proteome: multidimensional separation techniques for mitochondrial proteomics. Journal of proteome research 5: 1543-54

Reverter-Branchat G, Cabiscol E, Tamarit J, Ros J (2004) Oxidative damage to specific proteins in replicative and chronological-aged Saccharomyces cerevisiae: common

targets and prevention by calorie restriction. The Journal of biological chemistry 279: 31983-9

Rine J, Herskowitz I (1987) Four genes responsible for a position effect on expression from HML and HMR in Saccharomyces cerevisiae. Genetics 116: 9-22

Rine J, Strathern JN, Hicks JB, Herskowitz I (1979) A suppressor of mating-type locus mutations in Saccharomyces cerevisiae: evidence for and identification of cryptic mating-type loci. Genetics 93: 877-901

Rusche LN, Kirchmaier AL, Rine J (2003) The establishment, inheritance, and function of silenced chromatin in Saccharomyces cerevisiae. Annual review of biochemistry 72: 481-516

Schlissel G, Krzyzanowski MK, Caudron F, Barral Y, Rine J (2017) Aggregation of the Whi3 protein, not loss of heterochromatin, causes sterility in old yeast cells. Science 355: 1184-1187

Smeal T, Claus J, Kennedy B, Cole F, Guarente L (1996) Loss of transcriptional silencing causes sterility in old mother cells of S. cerevisiae. Cell 84: 633-42

Spokoini R, Moldavski O, Nahmias Y, England JL, Schuldiner M, Kaganovich D (2012) Confinement to organelle-associated inclusion structures mediates asymmetric inheritance of aggregated protein in budding yeast. Cell reports 2: 738-47

Stadtman ER (1992) Protein oxidation and aging. Science 257: 1220-4

Wright J, Schneider BL (2013) Cell size control is sirtuin(ly) exciting. Mol Syst Biol 9: 706

Yang HC, Pon LA (2002) Actin cable dynamics in budding yeast. Proceedings of the National Academy of Sciences of the United States of America 99: 751-6

Yang J, Dungrawala H, Hua H, Manukyan A, Abraham L, Lane W, Mead H, Wright J, Schneider BL (2011) Cell size and growth rate are major determinants of replicative lifespan. Cell cycle 10: 144-55

Zhou C, Slaughter BD, Unruh JR, Eldakak A, Rubinstein B, Li R (2011) Motility and segregation of Hsp104-associated protein aggregates in budding yeast. Cell 147: 1186-96

Zhou C, Slaughter BD, Unruh JR, Guo F, Yu Z, Mickey K, Narkar A, Ross RT, McClain M, Li R (2014) Organelle-based aggregation and retention of damaged proteins in asymmetrically dividing cells. Cell 159: 530-42

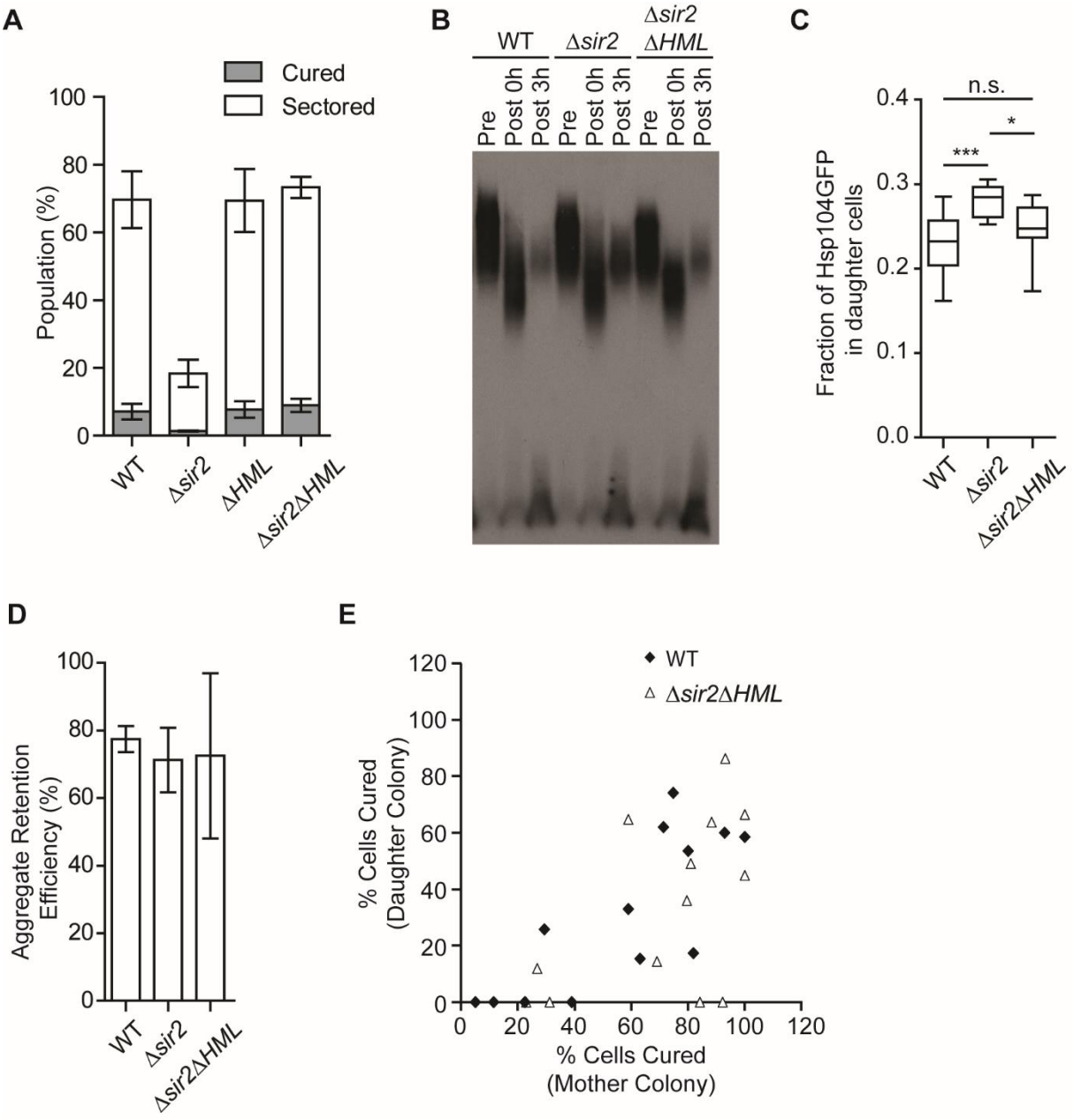

Fig.1. Reduction of heat-induced prion curing in *Δsir2* cells resulted from derepression of HM loci. (*A*) Quantification of [*PSI*$^{+}$]^{Weak} colony-color phenotypes in wild type (WT), *Δsir2*, *ΔHML* and *Δsir2ΔHML* cells following 30 min incubation at 40°C. Colonies were scored as completely [*psi*$^{-}$] (grey), or sectored (partially [*psi*$^{-}$], white). Data represent averages; error bars represent standard deviations; n=3. (*B*) Semi-native lysates of [*PSI*$^{+}$]^{Weak} WT, *Δsir2* and *Δsir2ΔHML* cultures were analyzed by semi-denaturing detergent agarose gel

electrophoresis (SDD-AGE) and immunoblotting for Sup35 before treatment (Pre), following a 30 min incubation at 40°C (Post 0h) and recovery at 30°C for 3 h following 40°C for 30 min (Post 3h). (*C*) [*PSI*$^{+}$]^{Weak} *HSP104GFP* WT, *Δsir2* and *Δsir2ΔHML* cells were imaged over time in a microfluidics chamber at 30°C after a 30 min incubation at 40°C. Fluorescence intensity in daughter and mother cells was quantified at the first cell division. Lines represent medians; boxes represent upper and lower quartiles; and whiskers represent maximum and minimum. (Unpaired t-test, n ≥ 10, ****P*= 0.0005, **P*= 0.014). (*D*) With the same treatment as described in (*C*), percentage of mother cells capable of retaining all Hsp104-GFP aggregates was quantified at the first cell division. Data represent averages; error bars represent standard deviations; n=3. (*E*) [*PSI*$^{+}$]^{Weak} WT and *Δsir2ΔHML* cells were incubated at 40°C for 30 min and plated on rich medium. Mother and daughter pairs were separated by micromanipulation and allowed to form colonies, which were then dispersed to YPD for analysis of curing by colony color phenotype. n ≥ 12.

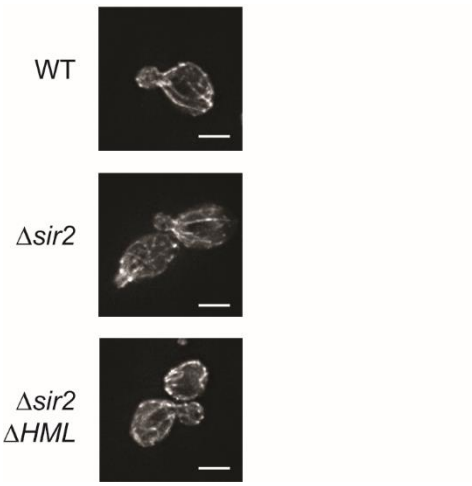

Fig.2. Actin cables were not affected by deletion of Sir2 and HML. The pattern of Abp140-GFP fluorescence in WT, *Δsir2* and *Δsir2ΔHML* cells was examined by microscopy. Scale bar = 3 μm.

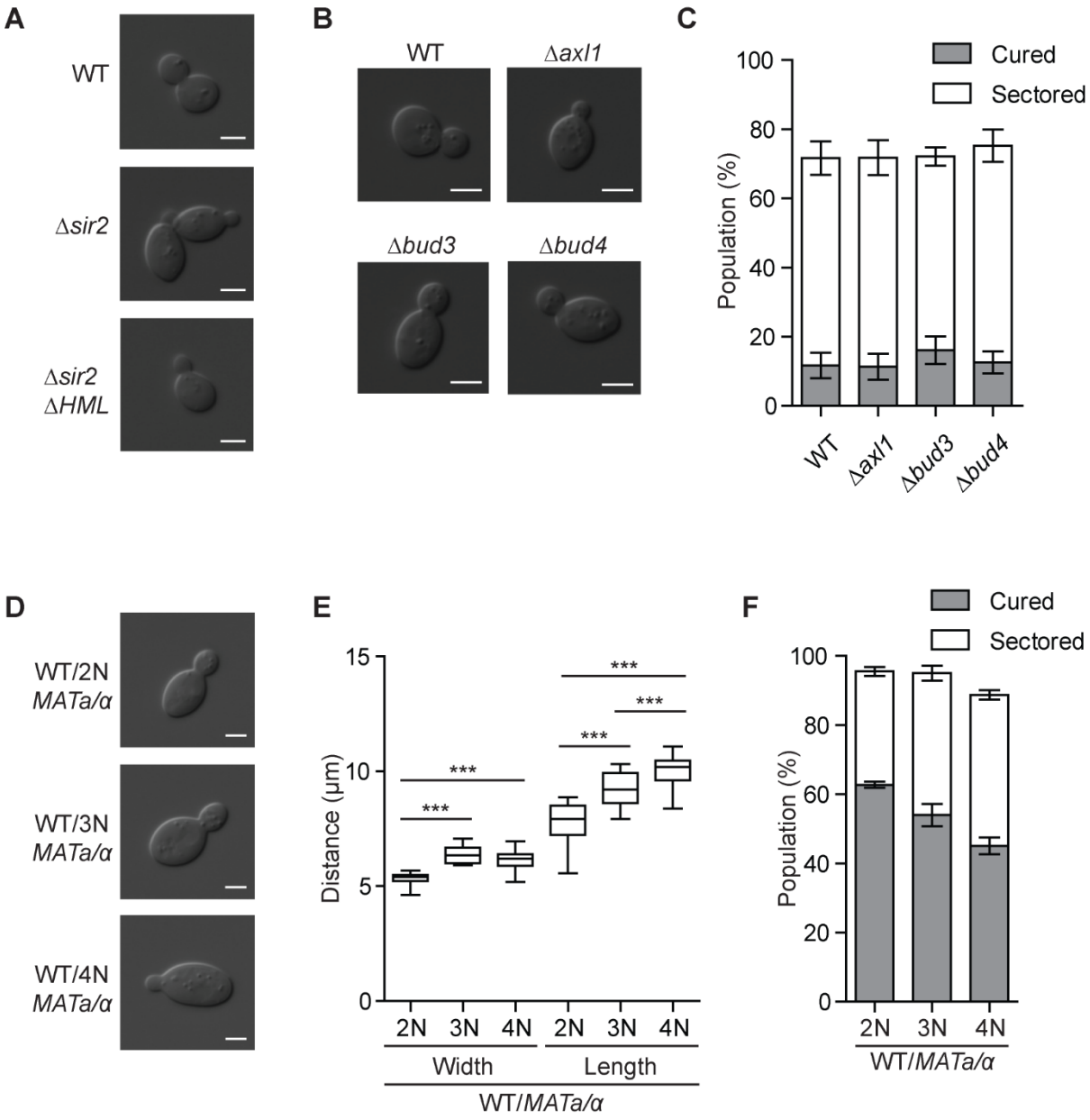

Fig.3. Cell size, but not budding pattern slightly affects heat-induced prion curing. (*A*) DIC images of WT, *Δsir2* and *Δsir2ΔHML* cells was examined by microscopy. Scale bar = 2 μm. (*B*) DIC images of WT, *Δaxl1*, *Δbud3* and *Δbud4* cells was examined by microscopy. Scale bar = 2 μm. (*C*) Quantification of [*PSI*$^{+}$]^{Weak} colony color phenotypes in WT, *Δaxl1*, *Δbud3* and *Δbud4* cells following 30 min incubation at 40°C. Colonies were scored as described in Figure 1A. Data represent averages; error bars represent standard

deviations; n=3. (*D*) DIC images of WT (2N), WT (3N) and WT (4N) cells was examined by microscopy. Scale bar = 2 μm. (*E*) Quantification of width and length of *MATa/α* [*PSI*$^{+}$]^{Weak} WT (2N), WT (3N) and WT (4N) cells. Lines represent medians; boxes represent upper and lower quartiles; and whiskers represent maximum and minimum. (Unpaired t-test, n ≥ 10, ****P*< 0.0001). (*F*) Quantification of *MATa/α* [*PSI*$^{+}$]^{Weak} colony color phenotypes in WT (2N), WT (3N) and WT (4N) cells following a 30 min incubation at 40°C. Colonies were scored as described in Figure 1A. Data represent averages; error bars represent standard deviations; n=3.

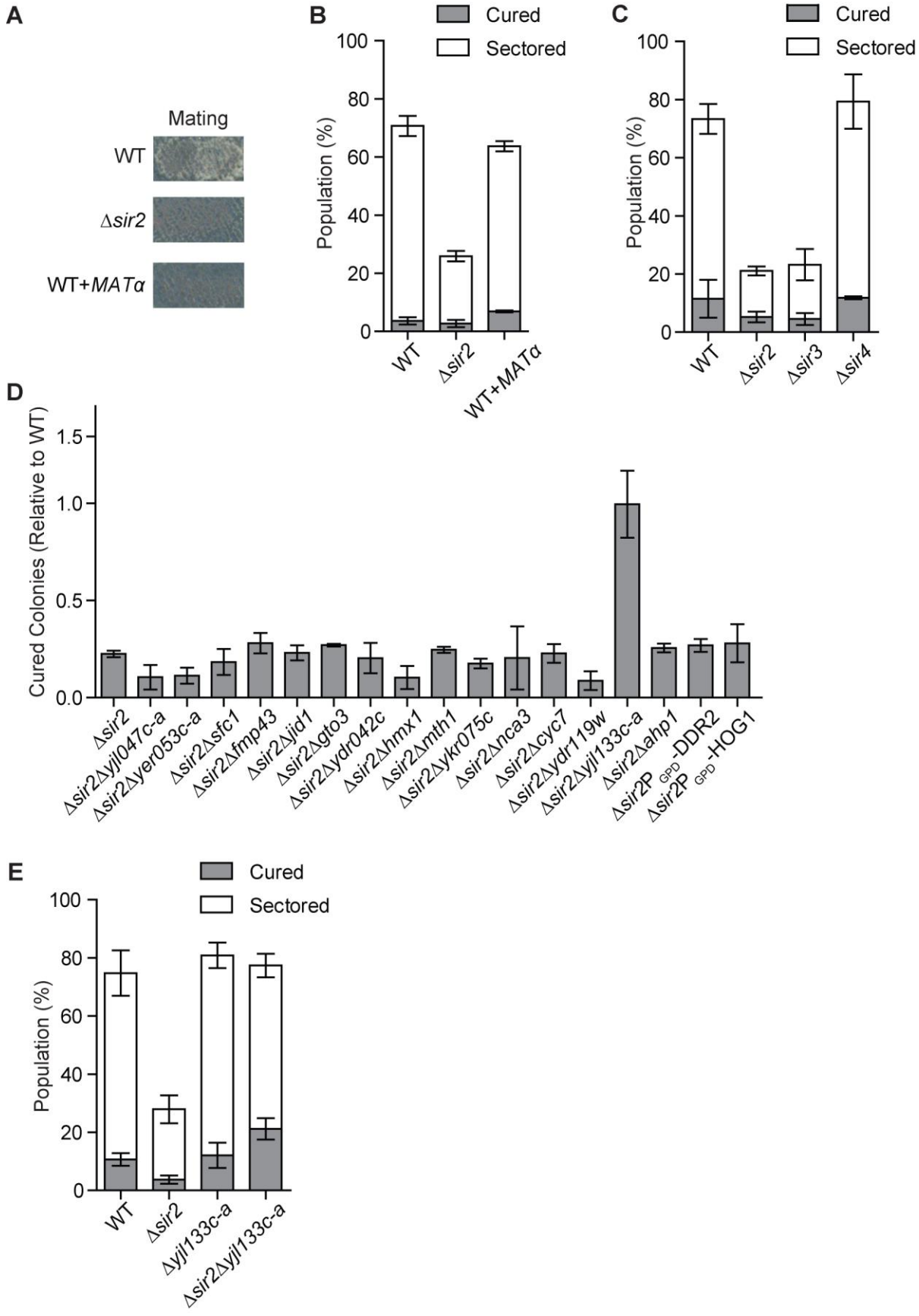
A
Mating
WT
Δsir2
WT+MATα
B
Cured
Sectored
Population (%)
WT
Δsir2
WT+MATα
C
Cured
Sectored
Population (%)
WT
Δsir2
Δsir3
Δsir4
D
Cured Colonies (Relative to WT)
Δsir2
Δsir2Δyjl047c-a
Δsir2Δyer053c-a
Δsir2Δsfc1
Δsir2Δfmp43
Δsir2Δjid1
Δsir2Δgto3
Δsir2Δydr042c
Δsir2Δhmx1
Δsir2Δmth1
Δsir2Δykr075c
Δsir2Δnca3
Δsir2Δcyc7
Δsir2Δydr119w
Δsir2Δyjl133c-a
Δsir2Δahp1
Δsir2P GPD -DDR2
Δsir2P GPD -HOG1
E
Cured
Sectored
Population (%)
WT
Δsir2
Δyjl133c-a
Δsir2Δyjl133c-a

Fig.4. Derepression of YJL133C-A by Sir2 is required for reduction of heat-induced prion curing. (*A*) The mating efficiency of WT, *Δsir2* and WT+*MATa/α* is reflected by the growth of colonies on media lacking amino acids. (*B*) Quantification of [*PSI*$^{+}$]^{Weak} colony color phenotypes in WT, *Δsir2* and WT+*MATa/α* (*MATa* WT strains with integrated expression of *MATα*) cells following a 30 min incubation at 40°C. Colonies were scored as described in Figure 1A. Data represent averages; error bars represent standard deviations; n=3. (*C*) Quantification of [*PSI*$^{+}$]^{Weak} colony color phenotypes in WT, *Δsir2*, *Δsir3* and *Δsir4* cells following a 30 min incubation at 40°C. Colonies were scored as described in Figure 1A. Data represent averages; error bars represent standard deviations; n=3. (*D*) [*PSI*$^{+}$]^{Weak} colony color phenotypes in *Δsir2* and *Δsir2Δmating-type gene* cells following a 30 min incubation at 40°C was quantified relative to that in WT cells. Fully cured and sectored colonies were combined in the 'cured' category. Data represent averages; error bars represent standard deviations; n=3. (*E*) Quantification of [*PSI*$^{+}$]^{Weak} colony color phenotypes in WT, *Δsir2*, *Δyjl133c-a* and *Δsir2Δyjl133c-a* cells following a 30 min incubation at 40°C. Colonies were scored as described in Figure 1A. Data represent averages; error bars represent standard deviations; n=3.

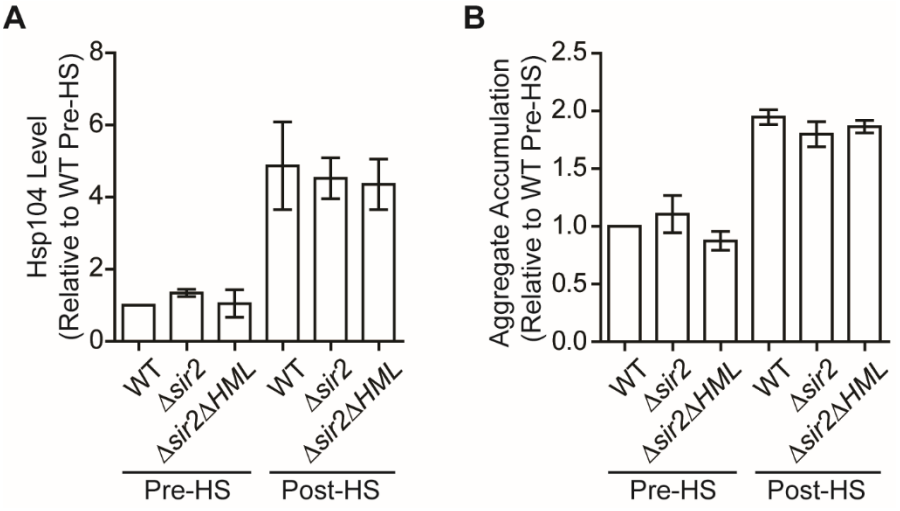

Fig.S1. Neither the chaperone level nor the heat-induced aggregate accumulation correlates with heat-induced prion curing. (*A*) The [*PSI*$^{+}$]^{Weak} WT, ***Δsir2*** and ***Δsir2ΔHML*** were incubated at 40°C for 30 min, and lysates were prepared and analyzed by SDS-PAGE and quantitative immunoblotting for Hsp104. Data represent means; error bars represent standard deviations; n ≥ 5. (*B*) Aggregates from lysates of a [*PSI*$^{+}$]^{Weak} strain WT, ***Δsir2*** and ***Δsir2ΔHML*** cells following treatment as described in (*A*) were prepared and analyzed by differential centrifugation and Bradford assay. Data represent means; error bars represent standard error; n = 3.

Chapter 4: Discussion

Prion cycle inhibition at any step leads to prion curing but with distinct effects on existing aggregates

Prions are thought to be incurable in mammals due to their efficient and autocatalytic pathways of misfolding. However, studies of prion dynamics in yeast indicate multiple possible routes of elimination of prion aggregates. For example, alterations in synthesis, conversion, fragmentation or transmission rate changes the balance between soluble and aggregated protein, leading to either complete resolubilization or retention of aggregated prion protein within cells, and thus prion loss.

Synthesis/conversion

Prion protein synthesis is clearly an important contributor to persistence of prion phenotypes. In mammals, PrP expression is required for prion disease establishment and progression (Bueler et al, 1993; Büeler et al, 1994; Prusiner, 1993). In our studies, the steady-state size and number of yeast Sup35 aggregates reflects a balance between conversion and fragmentation. When Sup35 synthesis is blocked upon cycloheximide treatment, aggregates increase in number and decrease in size as there is no new source of Sup35 and, without this counterbalance, fragmentation contributes more significantly to the outcome of the prion cycle.

In addition to blocking of synthesis, there are also dominant-negative mutants that are conversion-defective. Yeast Sup35(Q24R) has been reported to inhibit conversion of soluble Sup35 into pre-existing aggregates. This defect was revealed in mating experiments: after [*psi*$^{-}$] haploids expressing either wild type or Sup35(Q24R) with a fluorescent reporter of translation termination efficiency (GST-UGA-DsRed-NLS) were mated to wild type [*PSI*$^{+}$] cells, the fluorescence intensity in zygotes with Q24R expression

was significantly lower than wild type zygotes (DiSalvo et al, 2011). With Q24R expression, aggregates decrease in size and also in number. Both of these effects can be explained by a defect in conversion, which increases the soluble and functional pool of Sup35 and amplifies the effects of fragmentation by removing fiber regrowth (DiSalvo et al, 2011). The dominant-negative hamster PrP Q172R mutant appears to be functionally analogous to Sup35 Q24R, converting to the prion form ineffectively and inhibiting conformational self-replication (Bossers et al, 1997; Geoghegan et al, 2009).

Together, these studies suggest that synthesis and conversion are a counterbalance to naturally occurring processes that promote amyloid disassembly *in vivo*.

Fragmentation

Changes of fragmentation rate either increase or decrease, leading to prion curing but with distinct effects on existing aggregates. For fragmentation inhibition, aggregate size becomes larger because conversion continues and reaches a threshold that limits its transmission to daughter cells (Derdowski et al, 2010). As a result, daughter cells are cured of the prion state.

However, the fragmentation rate can also be elevated, either by increased Hsp104 expression or by asymmetric localization, to create an imbalance with conversion in the opposite direction. In this scenario, prion amyloid can be dissolved, and thus [*PSI*$^{+}$] state changed to [*psi*$^{-}$] state ((DiSalvo et al, 2011; Klaips et al, 2014), as demonstrated by our studies in Chapter 2. In contrast to the curing occurring upon Hsp104 inhibition in daughter cells, curing by enhanced fragmentation can occur in either mother or daughter cells depending on the conditions, and revealing distinct niches to evoke clearance.

Inhibition of Hsp104, either by treatment with GdnHCl or introduction of dominant-negative Hsp104 mutants, leads to accumulation of large, non-transmissible aggregates (Kryndushkin et al, 2003; Satpute-Krishnan et al, 2007; Wegrzyn et al, 2001). Interestingly, this mechanism of prion curing is effective against all prion variants but varies in its efficiency. For example, [*PSI*$^{+}$]^{Strong} cells that have smaller and more numerous aggregates must be treated longer with GdnHCl than [*PSI*$^{+}$]^{Weak} cells, which have larger and fewer aggregates, before non-prion cells appear in the population. But in both cases, the cured cells are daughters which complete cytokinesis before aggregates are transferred to them.

Increasing fragmentation efficiency, such as during heat shock and following the introduction of the Sup35(G58D) mutant, cures the [*PSI*$^{+}$] prion through the dissolution of Sup35 aggregates within cells. In the case of heat shock, both the elevation of Hsp104 expression and the asymmetric retention of proteins in mothers were required for curing in this compartment (Klaips et al, 2014). In the case of G58D expression, incorporation of the mutant destabilizes Sup35 aggregates and makes them easier to fragment and be cleared. Interestingly, in contrast to heat shock, dominant-negative mutants cure daughter cells rather than mother cells, presumably because the small number of aggregates transmitted to daughter cells are more readily cleared due to their reduced stability. Thus, fragmentation-induced prion clearance can occur by increasing the accumulation of chaperones relative to aggregates or by decreasing aggregates relative to chaperones.

Transmission

Alterations in prion transmission can affect prion propagation and even cure prions. First, blocking transmission cures prions as no aggregates would be inherited by daughter

cells upon cells division, similar to what we discussed above when fragmentation was inhibited. Another example was that [*PSI*$^{+}$]^{Weak} strains accumulate larger aggregates compared to [*PSI*$^{+}$]^{Strong} strains (Bagriantsev et al, 2006; Kryndushkin et al, 2003; Uptain et al, 2001; Zhou et al, 1999). Consistent with the size-based transmission model, fewer aggregates are transmitted into daughter cells (Derdowski et al, 2010), which correlates with the decrease mitotic stability for [*PSI*$^{+}$]^{Weak} strains (Derkatch et al, 1996). Thus, changes in prion transmission can effectively influence prion inheritance.

Prion Variant Evolution/Mutation/ Adaptation and Challenges for Therapies

Although prions adapt, transmute, and evolve, our studies on G58D suggests that a common therapy inhibiting prion persistence could be used to cure prion disease.

Selection vs. Induction of new conformations

Changes in the biological characteristics of prions either upon crossing the species barrier or in experiments with subcloned cell lines indicate that prions undergo mutation, evolution and adaptation (Li et al, 2010; Mahal et al, 2007; Prusiner, 1993). However, the exact molecular mechanism underlying this effect remains unknown.

The evolutionary conformational selection mechanism was raised to explain the evolution and adaptation of prion strains. In this theory, a single prion protein can spontaneously populate multiple, structurally distinct self-templating conformations, which provides the natural variation upon which selection can act (Ghaemmaghami et al, 2013; Haldiman et al, 2013). Specifically, natural selection can enrich or deplete different prion strains from populations depending on their conformational fitness in the prevailing

environment. This evolutionary conformational selection mechanism of PrP^{Sc} may explain the drug-induced evolution of mammalian prions (Oelschlegel & Weissmann, 2013). In these experiments, drug-resistant prion populations propagated more rapidly in the presence of the drug, but not in the absence of the drug, indicating the selection strains with conformational fitness in the environment (Oelschlegel & Weissmann, 2013).

Specific vs. General Inhibition

There are no effective anti-prion inhibitors or therapies so far. The evolutionary conformational selection and switching between different prion strains significantly complicate the development of anti-prion therapies. The problem is whether anti-prion therapies can antagonize the entire repertoire of structurally distinct misfolded prion forms. Our studies on the dominant-negative G58D mutants implies that a common therapy could be used to antagonize different prion diseases with different dosages to inhibit prions with different conformations.

Two broad anti-prion strategies were used to design and develop effective therapies: either specific interaction with a prion protein or general modulation of cellular pathways to eliminate prions. For the first, several small inhibitors have been discovered to interfere with (Crowe et al, 2009; Ehrnhoefer et al, 2008; Ehrnhoefer et al, 2006; Feng et al, 2008; Gestwicki et al, 2004; Hammarstrom et al, 2003; Masuda et al, 2006) and sometimes even reverse amyloidogenesis (Blanchard et al, 2004; Chirita et al, 2004; Li et al, 2004; Roberts et al, 2009; Wang et al, 2008). These small-molecule-antagonists can reduce the intrinsic toxicity of amyloid conformers in cell culture settings (Blanchard et al, 2004; Ehrnhoefer et al, 2008; Gestwicki et al, 2004). For the second, inhibitors might be developed to operate more generally by modulating proteostasis to enhance

cellular pathways that eliminate prions. These inhibitors do not interact with amyloid directly; instead, they manipulate molecular chaperones in the heat shock response (Balch et al, 2008; Powers et al, 2009). The promise of this approach is supported by several studies. First, genetic deletion of Hsf1, the master regulator of heat-shock gene expression (Mahat et al, 2016; Sorger & Pelham, 1987), confers a more rapid progression of prion disease in mice infected with the RML prion strain (Steele et al, 2008). Second, prion-infected cells appear to have a defective heat shock response (Tatzelt et al, 1995), which can be restored by inhibiting Hsp90 with geldanamycin (Winklhofer et al, 2001). Last, heat shock dissolves prion aggregates in yeast system (Klaips et al, 2014). However, approved drugs have yet to be proven effective in resolving amyloid or prion conformers.

Examples of combinations that are effective

Since there are no effective drugs for the specific or general strategies for treating prion disease, a combination of several less effective drugs might be another way to clear prions completely. For example, both desipramine and quinacrine are anti-prion drugs with slightly different anti-prion effects (Doh-ura et al, 2004; Klingenstein et al, 2006; Murakami-Kubo et al, 2004). Previous studies have shown that when ScN2a cells were treated with a combination of quinacrine and desipramine at dosages at which either the drug alone did not exhibit anti-prion effect, prions were completely cleared (Klingenstein et al, 2006). Similarly, combination of both dominant-negative prion mutant G58D with heat shock cures [*PSI*$^{+}$]^{Strong} (Klaips et al, 2014), which usually is not very efficiently cured under heat shock. Furthermore, a Sup35(Q24R, G58D) double mutant or a Sup35(Q172R, Q214I, Q219K) triple dominant-negative mutant leads to a better prion

inhibition effect that is capable of interfering with different prion variants (DiSalvo et al, 2011; Zulianello et al, 2000). Taken together, combination therapy might potentiate the anti-prion effect and be the most promising avenue to antagonize prion disease.

Protein concentration/transmission

Protein aggregates, including both prion aggregates and oxidatively damaged protein aggregates, are suggested to be asymmetrically transmitted in a diffuse manner. Disruption of the asymmetric inheritance not only affects prion-associated phenotypes, but also oxidatively damaged protein-associated disease progression.

Protein aggregate transmission

The asymmetric inheritance of damaged proteins has been studied in yeast and in mammalian systems (Denoth Lippuner et al, 2014; Knoblich, 2010). In the mammalian system, the majority of studies have focused on induced protein aggregates to correlate with cellular events occurring in different degenerative diseases. The mammalian aggresome, where aggregated, misfolded proteins localize, is transported on microtubules to the microtubule organizing center and caged in the intermediate filament vimentin (Johnston et al, 1998). But still, the mechanism governing the asymmetric segregation of aggregates remains unknown. To answer this question, extensive studies have also been done in the yeast system as we discussed above.

Based on our studies, reduction of heat-induced prion curing in *Δsir2* cells resulted from derepression of YJL133C-A, a protein that localizes to the mitochondria (Reinders et al, 2006). Our studies suggest that asymmetric damaged protein inheritance might be

mediated by organelle-based confinement, which favors the passive diffuse instead of the active transport model. However, the machinery mediating aggregate transport is still under debate. The active transport model is mainly supported by the experimental results demonstrating that disruption of the actin network leads to defects in asymmetric inheritance of aggregates and that some aggregates in the bud moved across the bud neck into the mother compartment (Liu et al, 2010). However, our experimental results of actin cable morphology showed no difference between wild type and *Δsir2* cells although asymmetric inheritance of damaged protein was disrupted. Moreover, cell polarity and well-oriented actin cables only exist in a limited time window prior to entry into mitosis, significantly before cell division (Moseley & Goode, 2006). Consistent with this idea, later studies shed light on the cellular basis of the confined diffusion of protein aggregates and demonstrated its importance in the asymmetric inheritance of misfolded proteins (Spokoini et al, 2012; Zhou et al, 2011; Zhou et al, 2014). However, clear and direct evidence is lacking to exclude either of the possibilities.

Although actin does not appear to play a role in aggregate segregation through the polarized, actin cable-based transport system, actin does seem to influence aggregate mobility in the cytoplasm. Further studies of this mechanism might also help us better understand the aggregate transport and also its interaction with other cellular components.

Impact on prion cycle

Prion transmission was reported to be sized-based. Smaller aggregates seem to partition more efficiently than larger aggregates (Derdowski et al, 2010), which suggests a passive transport model. Since prion aggregates are in a dynamic state of assembly

and disassembly, changes in fragmentation efficiency will affect aggregate size, prion transmission, and phenotypic effects (Derdowski et al, 2010). For example, in our studies, G58D incorporation leads to less [*PSI*$^{+}$]^{Sc4} and [*PSI*$^{+}$]^{Sc37} propagon formation in the mother cells. Within daughter cells after cell division, the aggregates are more susceptible to dissolution due to the limiting number of aggregates transmitted added to the destabilization by G58D incorporation. Like heat-induced aggregates, propagons also appear to distribute differentially between mother and daughter cells, with daughters inheriting approximately only one-third of those aggregates, which is proportional to the relative volumes of the mother and daughter compartments during cell division (Cox *et al*, 2003). This differential asymmetric transmission of aggregates from one cell to another gives rise to phenotypic heterogeneity within a population (Derdowski et al, 2010; DiSalvo et al, 2011; Klaips et al, 2014).

The asymmetric transmission of aggregates also creates age-dependent variations. The limited number of aggregates inherited by a daughter progressively amplifies and reaches a steady state as that cell grows and ages: early daughters inherit fewer aggregates than later daughters (Derdowski et al, 2010). This provides a mechanistic explanation for previously observed cell-to-cell variability in propagons (Byrne et al, 2009; Cox et al, 2003) and reveal age-dependent [*PSI*$^{+}$] phenotypes at the single-cell level.

This differential transmission of aggregates from one cell to another and the resulting asymmetry likely skews substrate-to-chaperone ratios, thus creating an imbalance between assembly and disassembly. For example, this heterogeneity created by asymmetric inheritance of prion aggregates promotes G58D dominant-negative

inhibition in daughter cells upon cell division. In our studies, daughter cells inherit significantly less aggregates, due to the G58D-induced reduction in propagon numbers, and become more susceptible to Hsp104-mediated fragmentation due to the G58D-induced reduction in aggregate kinetic stability: thus, prion curing occurs. Another example of the importance of substrate-to-chaperone ratios on prion stability is the curing occurring in mother cells following thermal stress. Since young mother cells have a greater ability to retain damaged proteins (Aguilaniu et al, 2003) and thereby Hsp104, we predict that young mother cells are cured more efficiently than old mother cells. Through these examples, the importance of maintaining the substrate-to-chaperone balance in prion stability and curing emerges, and this understanding may also shed light on neurodegenerative disease and aging progression, and potentially may provide some clues for designing inhibitors to combat these events.

Implications in disease progression

The symmetric or asymmetric inheritance of proteins has been shown to regulate many cellular activities and development. For example, asymmetric division plays an important role for stem cells to generate both self-renewing and differentiating daughter cells (Knoblich, 2008): Numb, for example, segregates asymmetrically during mitosis in muscle stem cells (Shinin et al, 2006) and T lymphocytes (Shinin et al, 2006). However, it is currently unknown whether the sirtuin protein family (homolog of yeast Sir2 protein) plays a role in asymmetric inheritance in stem cells.

Defects leading to the disruption of asymmetric cell division can cause the establishment and progression of several diseases. In fact, many of the key regulators of asymmetric cell division act as tumor suppressors (Bello et al, 2006; Betschinger et al,

2006; Castellanos et al, 2008; Caussinus & Gonzalez, 2005; Gonzalez, 2007; Lee et al, 2006). Moreover, defects in asymmetric cell division can turn neural stem cells into tumor-initiating cells in Drosophila (Li et al, 2014).

Not limited to tumor progression, the imbalance of chaperone and substrate ratios, or even overloading of the proteostasis network resulting from disruption of asymmetric inheritance, can lead to aggregation of proteins that normally do not have that propensity. In this way, a decline in the levels and/or activities of factors in the proteostasis network might contribute to age-associated neurodegenerative disease. For example, the ability to activate Hsf1 during stress decreases with aging (Shamovsky & Gershon, 2004), and chaperones and other proteostasis factors might be sequestered into inclusions once aggregation occurs, further limiting their protection (Yu et al, 2014). Taken together, maintaining the balance of chaperone and substrate ratio, or the proteostasis network, plays a crucial role for protection from neurodegeneration.

Impact of aging

As cells age, oxidatively damaged proteins begin to accumulate, forming toxic protein aggregates. These protein aggregates are preferentially retained in the mother cell, which promotes mother cell aging and production of a daughter cell with a reset of the aging clock (Aguilaniu et al, 2003; Erjavec et al, 2007; Liu et al, 2010). This asymmetric inheritance can be established by two mechanisms: one retains damaged protein aggregates in the mother cell and the other clears aggregates from the daughter cell. Both of them are important for cellular health and normal lifespan (Hill et al, 2014; Song et al, 2014). For example, increasing the expression level of the type I metacaspase, Mca1p, promotes clearance of aggregates in daughter cells and extends yeast lifespan

(Hill et al, 2014). In addition, an extensive body of work, largely from Leonard Guarente and his colleagues, has demonstrated that asymmetric damaged-protein inheritance mediated by Sir2 correlates with yeast replicative life span, measured by the number of daughter cells that one mother cell can produce: *SIR2* deletion strains are short lived, whereas strains that overexpress *SIR2* are long lived (Kaeberlein et al, 1999). Increasing the dosage of Sir2 extends the replicative life span of yeast and the chronological life span of *Caenorhabditis elegans* (Tissenbaum & Guarente, 2001) and *Drosophila melanogaster* (Rogina & Helfand, 2004). All of these studies imply a correlation between the accumulation of protein aggregates and aging. However, it is not clear whether protein aggregates are the (only) aging determinants.

Future directions

Yeast as a model

As previously mentioned, dominant-negative prion inhibition extends to mammalian diseases, and the mechanisms underlying prion protection in this system may suggest promising strategies for therapeutic interventions. For instance, individuals with some PrP polymorphisms are genetically less susceptible to prion disease (Belt et al, 1995; Bossers et al, 2000; Dickinson & Outram, 1988; Dickinson et al, 1968; Goldmann et al, 1998; Hizume et al, 2009; Laplanche et al, 1994; Maciulis et al, 1992; Shibuya et al, 1998b), and certain polymorphisms can also function as dominant inhibitors of prion propagation in vivo (Atarashi et al, 2006; Crozet et al, 2004; Furuya et al, 2006; Hizume et al, 2009; Kaneko et al, 1997; Ott et al, 2008; Perrier et al, 2002; Toupet et al, 2008; Zulianello et al, 2000). Interestingly, our studies on the yeast dominant-negative mutant

Sup35(G58D) may illuminate mechanisms of prion protection that operate in the mammalian system; indeed, the PrP sequence variant, Q219 dominantly inhibits wild type PrP^{Sc} propagation in a process that shares similarities with G58D inhibition of [*PSI*$^{+}$] in yeast (Hizume et al, 2009; Kaneko et al, 1997; Perrier et al, 2002).

The expression of the dominant-negative PrP mutant Q219K has been linked to defects in propagation of the prion state (Hizume et al, 2009; Kaneko et al, 1997; Perrier et al, 2002). Excitingly, this mutant appears to hold potential for protecting against, or even reversing, prion disease post-infection, suggesting that it can inhibit or resolve prion complexes that have already established themselves in vivo (Crozet et al, 2004; Furuya et al, 2006; Toupet et al, 2008). Furthermore, understanding the mechanism of prion inhibition by this mutant may suggest other methods that could be effective therapies for prion or other protein misfolding diseases.

PrP(Q219K) has several traits which parallel those of Sup35(G58D): both convert to the prion conformer efficiently, destabilize aggregates, and are incompatible only with prion variants of reduced thermodynamic stability (Atarashi et al, 2006; Geoghegan et al, 2009; Hizume et al, 2009; Lee et al, 2007; Safar et al, 1998). Instead of acting to decrease prion conversion, Q219K might target a distinct event in the prion propagation pathway, such as aggregate disassembly. These observations suggest that a similar competition between aggregate assembly and disassembly pathways may occur in the mammalian prion system, with the kinetics of these pathways modulating the metastability and phenotypic outcome of mammalian prion disease.

Dominant-negative mutations

Our data suggests that dominant-negative inhibition of Sup35(G58D) was promoted by Hsp104-mediated fragmentation, either by more efficient binding to or processing by Hsp104. Previous studies showed that Hsp104 had a similar binding efficiency to both wild type and G58D aggregates (Verges et al, 2011), which ruled out the possibility of more efficient binding to Hsp104. Moreover, both our studies and previous studies indirectly support the idea of a more efficient Hsp104-mediated processing activity. First, promotion of Hsp104-mediated fragmentation corresponded to destabilization of G58D aggregates in our studies. Second, overexpression of Hsp104 ΔNTD, a truncation mutant defective in substrate processing but not binding, is unable to cure WT [*PSI*$^{+}$] but effectively cures G58D [*PSI*$^{+}$], suggesting the latter is more easily resolved (Sweeny et al, 2015). However, the mechanism promoting more efficient Hsp104 processing is unknown.

G58 of Sup35, which lies in the central part of the amyloid core, might face the central pore of the Hsp104 hexamer and may thus affect the processing efficiency by Hsp104. We hypothesize that mutation from G to D leads to more efficient pulling of prion aggregates through the Hsp104 central pore, thus increasing the processing efficiency. This hypothesis is supported by our experimental results showing destabilization of prion aggregates by G58D and by the Hsp104(ΔNTD) mutant as it has been reported to selectively cut tail-to-tail interaction of aggregates (Sweeny et al, 2015).

Our studies highlight that protein disaggregases could be manipulated or engineered to combat misfolding diseases as they can safely refold self-templating amyloid and toxic soluble oligomers back into soluble, functional proteins (Shorter, 2008; Shorter, 2016). Studies to define, engineer, and apply protein disaggregases, including

Hsp104 in yeast, G3 in bacteria, Hsp110, Hsp70, and Hsp40 in humans, HtrA1 in humans and NMNAT2 and Hsp90 in humans to reverse deleterious protein misfolding in neurodegenerative disease have been advanced recently (Reviewed in (Shorter, 2017)). A potentiated Hsp104 variant has been engineered that can antagonize the aggregation and toxicity of prioinoids associated with neurodegenerative disease such as TDP-43, FUS, TAF15, and a-syn; more excitingly, the working efficacy of this Hsp104 variant is greatly improved as it can rescue neurodegeneration at the concentrations where original Hsp104 is ineffective (Jackrel et al, 2014; Jackrel & Shorter, 2014; Jackrel & Shorter, 2015; Jackrel et al, 2015; Ovsepian et al, 2016; Torrente & Shorter, 2013). Further studies need to focus on determining whether Hsp104 or enhanced variants can also be of benefit in mammalian cells, patient-derived neurons, and additional animal models of neurodegeneration.

Prion transmission

Prion transmission was reported to be sized-based (Derdowski et al, 2010), which indicates a passive transport. However, overexpression of Art5 or Lsb3, which are actin-binding proteins, reverse G58D-mediated prion loss (Verges et al, 2011), suggesting that actin cytoskeleton somehow influences prion persistence, probably through promoting prion transmission. However, it is unknown how the actin cytoskeleton influences prion aggregates's transmission.

The actin cytoskeleton network might act as a diffusion barrier for aggregate transport, which was supported by the fact the asymmetric aggregate inheritance was disrupted by the disintegration of actin cytoskeleton networking (Erjavec et al, 2007).

However, it is unknown whether actin cytoskeleton also act as a diffusion barrier for prion aggregate transmission.

In addition to a possible diffusion barrier in the cytoplasm, a diffusion barrier might also exist at the bud neck where the transmission of large Sup35 aggregates are restricted by an unknown mechanism. One possibility is that the septin rings work as diffusion barriers at the bud neck. Further studies are needed to clarify the mechanism of the involvement of actin cytoskeleton in asymmetric inheritance of prion transmission.

A similar debate about active or passive transport also exists for damaged protein transport as we discussed earlier. Based on our studies, reduction of heat-induced prion curing in *Δsir2* cells resulted from derepression of YJL133C-A, a protein localized at the mitochondria (Reinders et al, 2006). This observation suggests that YJL133C-A might play an important role in the stress response, either through damaged protein or chaperone asymmetry.

A previous study showed that stress conditions can induce hyperpolarization of mitochondrial membrane, which is required for the induction of chaperone expression (Rikhvanov et al, 2005), indicating that it is possible for YJL133C-A to regulate chaperone levels, including Hsp104, following thermal stress. However, this is unlikely to explain our observed inhibition of aggregate dissolution by deletion of Sir2 because Hsp104 induction after heat shock did not appear to be changed in the absence of Sir2. Another possibility is that mitochondrial membrane potential contributes to chaperone or proteasome efficiency, or affects aggregate dissolution indirectly through other essential mitochondria-mediated processes.

YJL133C-A, which localizes at mitochondria, might also be directly involved in asymmetric retention of damaged protein. Previous studies have shown that aggregates are tethered to well-anchored maternal mitochondria, whereas mitochondria acquired by buds are largely free of aggregates during cytokinesis. Disruption of aggregate-mitochondria association results in increased mobility and leakage of mother-accumulated aggregates into the bud (Zhou et al, 2014). YJL133C-A might affect aggregate-mitochondria association. Previous studies have also shown that mitochondria-aggregate interactions contribute to neurodegenerative disease. For example, mutant SOD1 binds to mitochondria and thus disrupts normal mitochondrial distribution and size homeostasis, which is the early pathogenic features of SOD1 mutant-mediated ALS (Vande Velde et al, 2011). Future studies focusing on YJL133C-A might also shed light on the mechanism of the pathogenic progression of neurodegeneration.

Interestingly, aggregate transmission directly and indirectly influences cellular phenotypes and development, including [*PSI*$^{+}$] persistence in our studies and neurodegeneration and aging in other studies. These phenotypes depend on cell-to-cell heterogeneity and the balance of chaperone and substrate within individual cells, which are all closely correlated with aggregate transmission. However, the machineries to mediate this process remain largely unknown. Our results highlight that actin cytoskeleton might be involved but may not directly mediate aggregate transport. Meanwhile, our studies point out that further studies need to focus on the important but unknown role of mitochondria in aggregate transport.

Table 1: Mammalian Prion Diseases

Disease	Host	Mechanism
infective Creutzfeldt-Jakob disease (iCJD)	Human	Infection
variant Creutzfeldt-Jakob disease (iCJD)	Human	Infection
familial Creutzfeldt-Jakob disease (fCJD)	Human	Genetic: octarepeat insertion, D178N-129V, V180I, T183A, T188K, T188R-129V, E196K, E200K, V203I, R208H, V210I, E211Q, M232R
sporadic Creutzfeldt-Jakob disease (sCJD)	Human	unknown
Gerstmann-Straüssler-Sheinker disease (GSS)	Human	Genetic: octarepreat insertion, P102L-129M, P105-129M, A117-129V, G131V-129M, Y145-129M, H197R- 129V, F198S-129V, D202N-129V, Q212P, Q217R-129M, M232T
Fatal Familial Insomnia (FFI)	Human	Genetic: D178-129M
Kuru	Human	Infection
sporadic fatal insomnia (sFI)	Human	unknown
Scrapie	Sheep and goat	Infection
Bovine Spongiform Encephalopathy (BSE)	Cattle	Infection
Transmissible Mink Encephalopathy (TME)	Mink	Infection
Chronic Wasting Disease (CWD)	Mule, deer and elk	Infection

Feline Spongiform Encephalopathy (FSE)	Cat	Infection
Exotic ungulate encephalopathy	greater kudu, nyala, oryx	Infection

Adapted from (Benetti & Legname, 2009)

Table 2: Fungal Prions

Determinant	Protein	Cellular Function	Phenotype
[*PSI*$^{+}$]	Sup35	Translation termination factor (eRF3)	Nonsense suppression and resistance to toxic compounds
[*PIN*$^{+}$]/[*RNQ*$^{+}$]	Rnq1	Unknown	De novo prion formation
[*URE3*]	Ure2	Transcriptional co-repressor	Poor nitrogen source use Nonsense
[*SWI*$^{+}$]	Swi1	Subunit of the SWI–SNF chromatin remodelling complex	Repression of transcription
[*OCT*$^{+}$]	Cyc8	Transcriptional co-repressor	Derepression of transcription
[*MOT3*$^{+}$]	Mot3	Transcriptional co-repressor	Derepression of transcription
[*Het-s*]	HET-s	Unknown	Vegetative incompatibility and cell death
[*ISP*$^{+}$]	Sfp1	Transcriptional activator	Translational accuracy

Adapted from (Tuite & Serio, 2010)

Table 3: Potential Prionoids in Health and Disease

Phenotype/Function	Protein	Molecular Transmissibility	Infectivity
Alzheimer's disease	Aβ (luminal)	Yes	In APP-overexpressing mice
Tauopathies	Tau (cytosolic)	Possibly	Not shown
Parkinson's disease	α-synuclein (cytosolic)	Host-to-graft	Not shown
AA amyloidosis	SAA (luminal)	Yes	Probable
Huntington's disease	PolyQ (nuclear)	Yes	Not shown

Adapted from (Aguzzi & Rajendran, 2009)

Full Dissertation References

Afanasieva EG, Kushnirov VV, Ter-Avanesyan MD (2011) Interspecies transmission of prions. *Biochemistry (Mosc)* **76:** 1375-1384

Aguilaniu H, Gustafsson L, Rigoulet M, Nystrom T (2003) Asymmetric inheritance of oxidatively damaged proteins during cytokinesis. *Science* **299:** 1751-1753

Aguzzi A (2009) Cell biology: Beyond the prion principle. *Nature* **459:** 924-925

Aguzzi A, Baumann F, Bremer J (2008) The Prion ' s Elusive Reason for Being. *Annu Rev Neurosci***:** 439-477

Aguzzi A, Lakkaraju AK (2016) Cell Biology of Prions and Prionoids: A Status Report. *Trends in cell biology* **26:** 40-51

Aguzzi A, Rajendran L (2009) The transcellular spread of cytosolic amyloids, prions, and prionoids. *Neuron* **64:** 783-790

Allen KD, Wegrzyn RD, Chernova TA, Muller S, Newnam GP, Winslett PA, Wittich KB, Wilkinson KD, Chernoff YO (2005) Hsp70 chaperones as modulators of prion life cycle: novel effects of Ssa and Ssb on the Saccharomyces cerevisiae prion [PSI+]. *Genetics* **169:** 1227-1242

Alper T, Cramp Wa, Haig Da, Clarke MC (1967) Does the agent of scrapie replicate without nucleic acid? *Nature* **214:** 764-766

Alper T, Haig DA, Clarke MC (1966) The exceptionally small size of the scrapie agent. *Biochemical and biophysical research communications* **22:** 278-284

Andreoletti O, Morel N, Lacroux C, Rouillon V, Barc C, Tabouret G, Sarradin P, Berthon P, Bernardet P, Mathey J, Lugan S, Costes P, Corbiere F, Espinosa JC, Torres JM, Grassi J, Schelcher F, Lantier F (2006) Bovine spongiform encephalopathy agent in spleen from an ARR/ARR orally exposed sheep. *The Journal of general virology* **87:** 1043-1046

Aparicio OM, Billington BL, Gottschling DE (1991) Modifiers of position effect are shared between telomeric and silent mating-type loci in S. cerevisiae. *Cell* **66:** 1279-1287

Appleby BS, Lyketsos CG (2011) Rapidly progressive dementias and the treatment of human prion diseases. *Expert opinion on pharmacotherapy* **12:** 1-12

Atarashi R, Sim VL, Nishida N, Caughey B, Katamine S (2006) Prion strain-dependent differences in conversion of mutant prion proteins in cell culture. *J Virol* **80:** 7854-7862

Ayers JI, Schutt CR, Shikiya RA, Aguzzi A, Kincaid AE, Bartz JC (2011) The strain-encoded relationship between PrP replication, stability and processing in neurons is predictive of the incubation period of disease. *PLoS pathogens* **7:** e1001317

Bagriantsev SN, Kushnirov VV, Liebman SW (2006) Analysis of amyloid aggregates using agarose gel electrophoresis. *Methods in enzymology* **412:** 33-48

Bailleul PA, Newnam GP, Steenbergen JN, Chernoff YO (1999) Genetic study of interactions between the cytoskeletal assembly protein sla1 and prion-forming domain of the release factor Sup35 (eRF3) in Saccharomyces cerevisiae. *Genetics* **153:** 81-94

Balch WE, Morimoto RI, Dillin A, Kelly JW (2008) Adapting proteostasis for disease intervention. *Science* **319:** 916-919

Baskakov I, Disterer P, Breydo L, Shaw M, Gill A, James W, Tahiri-Alaoui A (2005) The presence of valine at residue 129 in human prion protein accelerates amyloid formation. *FEBS letters* **579:** 2589-2596

Basler K, Oesch B, Scott M, Westaway D, Walchli M, Groth DF, McKinley MP, Prusiner SB, Weissmann C (1986) Scrapie and cellular PrP isoforms are encoded by the same chromosomal gene. *Cell* **46:** 417-428

Baumann F, Tolnay M, Brabeck C, Pahnke J, Kloz U, Niemann HH, Heikenwalder M, Rülicke T, Bürkle A, Aguzzi A (2007) Lethal recessive myelin toxicity of prion protein lacking its central domain. *The EMBO Journal* **26:** 538-547

Beekes M, McBride PA, Baldauf E (1998) Cerebral targeting indicates vagal spread of infection in hamsters fed with scrapie. *The Journal of general virology* **79 (Pt 3):** 601-607

Bellinger-Kawahara C, Cleaver JE, Diener TO, Prusiner SB (1987) Purified scrapie prions resist inactivation by UV irradiation. *Journal of virology* **61:** 159-166

Bello B, Reichert H, Hirth F (2006) The brain tumor gene negatively regulates neural progenitor cell proliferation in the larval central brain of Drosophila. *Development* **133:** 2639-2648

Belt PB, Muileman IH, Schreuder BE, Bos-de Ruijter J, Gielkens AL, Smits MA (1995) Identification of five allelic variants of the sheep PrP gene and their association with natural scrapie. *The Journal of general virology* **76 (Pt 3):** 509-517

Benestad SL, Arsac JN, Goldmann W, Noremark M (2008) Atypical/Nor98 scrapie: properties of the agent, genetics, and epidemiology. *Veterinary research* **39:** 19

Benetti F, Legname G (2009) De novo mammalian prion synthesis. *Prion* **3:** 213-219

Berry DB, Lu D, Geva M, Watts JC, Bhardwaj S, Oehler A, Renslo AR, DeArmond SJ, Prusiner SB, Giles K (2013) Drug resistance confounding prion therapeutics. *Proceedings of the National Academy of Sciences of the United States of America* **110:** E4160-4169

Bessen RA, Marsh RF (1992) Biochemical and physical properties of the prion protein from two strains of the transmissible mink encephalopathy agent. *J Virol* **66:** 2096-2101

Bessen RA, Marsh RF (1994) Distinct PrP properties suggest the molecular basis of strain variation in transmissible mink encephalopathy. *J Virol* **68:** 7859-7868

Betschinger J, Mechtler K, Knoblich JA (2006) Asymmetric segregation of the tumor suppressor brat regulates self-renewal in Drosophila neural stem cells. *Cell* **124:** 1241-1253

Bi E, Park HO (2012) Cell polarization and cytokinesis in budding yeast. *Genetics* **191:** 347-387

Blanchard BJ, Chen A, Rozeboom LM, Stafford KA, Weigele P, Ingram VM (2004) Efficient reversal of Alzheimer's disease fibril formation and elimination of neurotoxicity

by a small molecule. *Proceedings of the National Academy of Sciences of the United States of America* **101:** 14326-14332

Blander G, Guarente L (2004) The Sir2 family of protein deacetylases. *Annual review of biochemistry* **73:** 417-435

Bolton DC, McKinley MP, Prusiner SB (1982) Identification of a protein that purifies with the scrapie prion. *Science* **218:** 1309-1311

Borchelt DR, Scott M, Taraboulos A, Stahl N, Prusiner SB (1990) Scrapie and cellular prion proteins differ in their kinetics of synthesis and topology in cultured cells. *The Journal of cell biology* **110:** 743-752

Bossers A, Belt P, Raymond GJ, Caughey B, de Vries R, Smits MA (1997) Scrapie susceptibility-linked polymorphisms modulate the in vitro conversion of sheep prion protein to protease-resistant forms. *Proceedings of the National Academy of Sciences of the United States of America* **94:** 4931-4936

Bossers A, de Vries R, Smits MA (2000) Susceptibility of sheep for scrapie as assessed by in vitro conversion of nine naturally occurring variants of PrP. *J Virol* **74:** 1407-1414

Brachmann A, Baxa U, Wickner RB (2005) Prion generation in vitro: amyloid of Ure2p is infectious. *The EMBO Journal* **24:** 3082-3092

Brown K, Mastrianni JA (2010) The prion diseases. *Journal of geriatric psychiatry and neurology* **23:** 277-298

Bruce ME (2003) TSE strain variation. *British medical bulletin* **66:** 99-108

Bruce ME, Dickinson AG (1987) Biological evidence that scrapie agent has an independent genome. *The Journal of general virology* **68 (Pt 1):** 79-89

Bruce ME, McBride PA, Farquhar CF (1989) Precise targeting of the pathology of the sialoglycoprotein, PrP, and vacuolar degeneration in mouse scrapie. *Neuroscience letters* **102:** 1-6

Bruce ME, McConnell I, Fraser H, Dickinson AG (1991) The disease characteristics of different strains of scrapie in Sinc congenic mouse lines: implications for the nature of the agent and host control of pathogenesis. *The Journal of general virology* **72 (Pt 3):** 595-603

Bueler H, Aguzzi A, Sailer A, Greiner RA, Autenried P, Aguet M, Weissmann C (1993) Mice devoid of PrP are resistant to scrapie. *Cell* **73:** 1339-1347

Büeler H, Raeber a, Sailer a, Fischer M, Aguzzi a, Weissmann C (1994) High prion and PrPSc levels but delayed onset of disease in scrapie-inoculated mice heterozygous for a disrupted PrP gene. *Molecular medicine (Cambridge, Mass)* **1:** 19-30

Bufalino MR, van der Kooy D (2014) The aggregation and inheritance of damaged proteins determines cell fate during mitosis. *Cell cycle* **13:** 1201-1207

Buschmann A, Luhken G, Schultz J, Erhardt G, Groschup MH (2004) Neuronal accumulation of abnormal prion protein in sheep carrying a scrapie-resistant genotype (PrPARR/ARR). *The Journal of general virology* **85:** 2727-2733

Byrne LJ, Cole DJ, Cox BS, Ridout MS, Morgan BJ, Tuite MF (2009) The number and transmission of [PSI] prion seeds (Propagons) in the yeast Saccharomyces cerevisiae. *PloS one* **4:** e4670

Byrne LJ, Cox BS, Cole DJ, Ridout MS, Morgan BJ, Tuite MF (2007) Cell division is essential for elimination of the yeast [PSI+] prion by guanidine hydrochloride. *Proceedings of the National Academy of Sciences of the United States of America* **104:** 11688-11693

Carp RI, Callahan SM, Sersen EA, Moretz RC (1984) Preclinical changes in weight of scrapie-infected mice as a function of scrapie agent-mouse strain combination. *Intervirology* **21:** 61-69

Castellanos E, Dominguez P, Gonzalez C (2008) Centrosome dysfunction in Drosophila neural stem cells causes tumors that are not due to genome instability. *Current biology : CB* **18:** 1209-1214

Castilla J, Gonzalez-Romero D, Saa P, Morales R, De Castro J, Soto C (2008) Crossing the species barrier by PrP(Sc) replication in vitro generates unique infectious prions. *Cell* **134:** 757-768

Castilla J, Saa P, Hetz C, Soto C (2005) In vitro generation of infectious scrapie prions. *Cell* **121:** 195-206

Caughey B, Raymond GJ (1991) The scrapie-associated form of PrP is made from a cell surface precursor that is both protease- and phospholipase-sensitive. *The Journal of biological chemistry* **266:** 18217-18223

Caughey B, Raymond GJ, Kocisko DA, Lansbury PT, Jr. (1997) Scrapie infectivity correlates with converting activity, protease resistance, and aggregation of scrapie-associated prion protein in guanidine denaturation studies. *J Virol* **71:** 4107-4110

Caussinus E, Gonzalez C (2005) Induction of tumor growth by altered stem-cell asymmetric division in Drosophila melanogaster. *Nature genetics* **37:** 1125-1129

Chandler RL (1961) Encephalopathy in mice produced by inoculation with scrapie brain material. *Lancet* **1:** 1378-1379

Chen B, Bruce KL, Newnam GP, Gyoneva S, Romanyuk AV, Chernoff YO (2010) Genetic and epigenetic control of the efficiency and fidelity of cross-species prion transmission. *Molecular microbiology* **76:** 1483-1499

Chen B, Newnam GP, Chernoff YO (2007) Prion species barrier between the closely related yeast proteins is detected despite coaggregation. *Proceedings of the National Academy of Sciences of the United States of America* **104:** 2791-2796

Chernoff YO, Derkach IL, Inge-Vechtomov SG (1993) Multicopy SUP35 gene induces de-novo appearance of psi-like factors in the yeast Saccharomyces cerevisiae. *Current genetics* **24:** 268-270

Chernoff YO, Inge-Vechtomov SG, Derkach IL, Ptyushkina MV, Tarunina OV, Dagkesamanskaya AR, Ter-Avanesyan MD (1992) Dosage-dependent translational suppression in yeast Saccharomyces cerevisiae. *Yeast* **8:** 489-499

Chernoff YO, Lindquist SL, Ono B, Inge-Vechtomov SG, Liebman SW (1995) Role of the chaperone protein Hsp104 in propagation of the yeast prion-like factor [psi+]. *Science* **268:** 880-884

Chien P, Weissman JS (2001) Conformational diversity in a yeast prion dictates its seeding specificity. *Nature* **410:** 223-227

Chirita C, Necula M, Kuret J (2004) Ligand-dependent inhibition and reversal of tau filament formation. *Biochemistry* **43:** 2879-2887

Clouscard C, Beaudry P, Elsen JM, Milan D, Dussaucy M, Bounneau C, Schelcher F, Chatelain J, Launay JM, Laplanche JL (1995) Different allelic effects of the codons 136 and 171 of the prion protein gene in sheep with natural scrapie. *The Journal of general virology* **76 (Pt 8):** 2097-2101

Coustou V, Deleu C, Saupe S, Begueret J (1997) The protein product of the het-s heterokaryon incompatibility gene of the fungus Podospora anserina behaves as a prion analog. *Proceedings of the National Academy of Sciences of the United States of America* **94:** 9773-9778

Cox B, Ness F, Tuite M (2003) Analysis of the generation and segregation of propagons: entities that propagate the [PSI+] prion in yeast. *Genetics* **165:** 23-33

Cox BS (1965) Ψ, A cytoplasmic suppressor of super-suppressor in yeast. *Heredity* **20:** 505-521

Crowe A, Huang W, Ballatore C, Johnson RL, Hogan AM, Huang R, Wichterman J, McCoy J, Huryn D, Auld DS, Smith AB, 3rd, Inglese J, Trojanowski JQ, Austin CP, Brunden KR, Lee VM (2009) Identification of aminothienopyridazine inhibitors of tau assembly by quantitative high-throughput screening. *Biochemistry* **48:** 7732-7745

Crozet C, Lin YL, Mettling C, Mourton-Gilles C, Corbeau P, Lehmann S, Perrier V (2004) Inhibition of PrPSc formation by lentiviral gene transfer of PrP containing dominant negative mutations. *Journal of cell science* **117:** 5591-5597

Dawson M, Hoinville LJ, Hosie BD, Hunter N (1998) Guidance on the use of PrP genotyping as an aid to the control of clinical scrapie. Scrapie Information Group. *The Veterinary record* **142:** 623-625

Denoth Lippuner A, Julou T, Barral Y (2014) Budding yeast as a model organism to study the effects of age. *FEMS Microbiol Rev* **38:** 300-325

DePace AH, Santoso A, Hillner P, Weissman JS (1998) A critical role for amino-terminal glutamine/asparagine repeats in the formation and propagation of a yeast prion. *Cell* **93:** 1241-1252

Derdowski A, Sindi SS, Klaips CL, DiSalvo S, Serio TR (2010) A size threshold limits prion transmission and establishes phenotypic diversity. *Science* **330:** 680-683

Derkatch IL, Bradley ME, Hong JY, Liebman SW (2001) Prions Affect the Appearance of Other Prions : The Story of [PIN+]. *Cell* **106:** 171-182

Derkatch IL, Bradley ME, Masse SV, Zadorsky SP, Polozkov GV, Inge-Vechtomov SG, Liebman SW (2000) Dependence and independence of [PSI(+)] and [PIN(+)]: a two-prion system in yeast? *EMBO J* **19:** 1942-1952

Derkatch IL, Bradley ME, Zhou P, Chernoff YO, Liebman SW (1997) Genetic and environmental factors affecting the de novo appearance of the [PSI+] prion in Saccharomyces cerevisiae. *Genetics* **147:** 507-519

Derkatch IL, Bradley ME, Zhou P, Liebman SW (1999) The PNM2 mutation in the prion protein domain of SUP35 has distinct effects on different variants of the [PSI+] prion in yeast. *Current genetics* **35:** 59-67

Derkatch IL, Chernoff YO, Kushnirov VV, Inge-Vechtomov SG, Liebman SW (1996) Genesis and variability of [PSI] prion factors in Saccharomyces cerevisiae. *Genetics* **144:** 1375-1386

Detwiler LA, Baylis M (2003) The epidemiology of scrapie. *Rev Sci Tech* **22:** 121-143

Dickinson AG, Fraser H (1969) Genetical control of the concentration of ME7 scrapie agent in mouse spleen. *Journal of comparative pathology* **79:** 363-366

Dickinson AG, Meikle VM (1969) A comparison of some biological characteristics of the mouse-passaged scrapie agents, 22A and ME7. *Genetical research* **13:** 213-225

Dickinson AG, Outram GW (1988) Genetic aspects of unconventional virus infections: the basis of the virino hypothesis. *Ciba Foundation symposium* **135:** 63-83

Dickinson AG, Stamp JT, Renwick CC, Rennie JC (1968) Some factors controlling the incidence of scrapie in Cheviot sheep injected with a Cheviot-passaged scrapie agent. *Journal of comparative pathology* **78:** 313-321

Dickinson AG, Taylor DM (1978) Resistance of scrapie agent to decontamination. *The New England journal of medicine* **299:** 1413-1414

DiSalvo S, Derdowski A, Pezza JA, Serio TR (2011) Dominant prion mutants induce curing through pathways that promote chaperone-mediated disaggregation. *Nature structural & molecular biology* **18:** 486-492

Doel SM, McCready SJ, Nierras CR, Cox BS (1994) The dominant PNM2- mutation which eliminates the psi factor of Saccharomyces cerevisiae is the result of a missense mutation in the SUP35 gene. *Genetics* **137:** 659-670

Doh-ura K, Ishikawa K, Murakami-Kubo I, Sasaki K, Mohri S, Race R, Iwaki T (2004) Treatment of transmissible spongiform encephalopathy by intraventricular drug infusion in animal models. *J Virol* **78:** 4999-5006

Dong J, Castro CE, Boyce MC, Lang MJ, Lindquist S (2010) Optical trapping with high forces reveals unexpected behaviors of prion fibrils. *Nature structural & molecular biology* **17:** 1422-1430

Dukan S, Nystrom T (1998) Bacterial senescence: stasis results in increased and differential oxidation of cytoplasmic proteins leading to developmental induction of the heat shock regulon. *Genes & development* **12:** 3431-3441

Dutnall RN, Pillus L (2001) Deciphering NAD-dependent deacetylases. *Cell* **105:** 161-164

Eaglestone SS, Ruddock LW, Cox BS, Tuite MF (2000) Guanidine hydrochloride blocks a critical step in the propagation of the prion-like determinant [PSI(+)] of Saccharomyces cerevisiae. *Proceedings of the National Academy of Sciences of the United States of America* **97:** 240-244

Ehrnhoefer DE, Bieschke J, Boeddrich A, Herbst M, Masino L, Lurz R, Engemann S, Pastore A, Wanker EE (2008) EGCG redirects amyloidogenic polypeptides into unstructured, off-pathway oligomers. *Nature structural & molecular biology* **15:** 558-566

Ehrnhoefer DE, Duennwald M, Markovic P, Wacker JL, Engemann S, Roark M, Legleiter J, Marsh JL, Thompson LM, Lindquist S, Muchowski PJ, Wanker EE (2006) Green tea (-)-epigallocatechin-gallate modulates early events in huntingtin misfolding and reduces toxicity in Huntington's disease models. *Human molecular genetics* **15:** 2743-2751

Eiden M, Soto EO, Mettenleiter TC, Groschup MH (2011) Effects of polymorphisms in ovine and caprine prion protein alleles on cell-free conversion. *Veterinary research* **42:** 30

Eisenberg DS, Sawaya MR (2017) Structural Studies of Amyloid Proteins at the Molecular Level. *Annual review of biochemistry* **86:** 69-95

Ellahi A, Thurtle DM, Rine J (2015) The Chromatin and Transcriptional Landscape of Native Saccharomyces cerevisiae Telomeres and Subtelomeric Domains. *Genetics* **200:** 505-521

Erjavec N, Larsson L, Grantham J, Nystrom T (2007) Accelerated aging and failure to segregate damaged proteins in Sir2 mutants can be suppressed by overproducing the protein aggregation-remodeling factor Hsp104p. *Genes & development* **21:** 2410-2421

Escusa-Toret S, Vonk WI, Frydman J (2013) Spatial sequestration of misfolded proteins by a dynamic chaperone pathway enhances cellular fitness during stress. *Nature cell biology* **15:** 1231-1243

Feng BY, Toyama BH, Wille H, Colby DW, Collins SR, May BC, Prusiner SB, Weissman J, Shoichet BK (2008) Small-molecule aggregates inhibit amyloid polymerization. *Nat Chem Biol* **4:** 197-199

Ferreira PC, Ness F, Edwards SR, Cox BS, Tuite MF (2001) The elimination of the yeast [PSI+] prion by guanidine hydrochloride is the result of Hsp104 inactivation. *Molecular microbiology* **40:** 1357-1369

Foster JD, Parnham D, Chong A, Goldmann W, Hunter N (2001) Clinical signs, histopathology and genetics of experimental transmission of BSE and natural scrapie to sheep and goats. *The Veterinary record* **148:** 165-171

Fraser H (1976) The pathology of a natural and experimental scrapie. *Frontiers of biology* **44:** 267-305

Fritze CE, Verschueren K, Strich R, Easton Esposito R (1997) Direct evidence for SIR2 modulation of chromatin structure in yeast rDNA. *EMBO J* **16:** 6495-6509

Furuya K, Kawahara N, Yamakawa Y, Kishida H, Hachiya NS, Nishijima M, Kirino T, Kaneko K (2006) Intracerebroventricular delivery of dominant negative prion protein in a

mouse model of iatrogenic Creutzfeldt-Jakob disease after dura graft transplantation. *Neuroscience letters* **402:** 222-226

Gabizon R, McKinley MP, Groth DF, Kenaga L, Prusiner SB (1988) Properties of scrapie prion protein liposomes. *The Journal of biological chemistry* **263:** 4950-4955

Gabizon R, McKinley MP, Prusiner SB (1987) Purified prion proteins and scrapie infectivity copartition into liposomes. *Proceedings of the National Academy of Sciences of the United States of America* **84:** 4017-4021

Gao X, Carroni M, Nussbaum-Krammer C, Mogk A, Nillegoda NB, Szlachcic A, Guilbride DL, Saibil HR, Mayer MP, Bukau B (2015) Human Hsp70 Disaggregase Reverses Parkinson's-Linked alpha-Synuclein Amyloid Fibrils. *Mol Cell* **59:** 781-793

Gavier-Widen D, Noremark M, Benestad S, Simmons M, Renstrom L, Bratberg B, Elvander M, af Segerstad CH (2004) Recognition of the Nor98 variant of scrapie in the Swedish sheep population. *Journal of veterinary diagnostic investigation : official publication of the American Association of Veterinary Laboratory Diagnosticians, Inc* **16:** 562-567

Geoghegan JC, Miller MB, Kwak AH, Harris BT, Supattapone S (2009) Trans-dominant inhibition of prion propagation in vitro is not mediated by an accessory cofactor. *PLoS pathogens* **5:** e1000535

Geschwind MD (2015) Prion Diseases. *Continuum (Minneap Minn)* **21:** 1612-1638

Gestwicki JE, Crabtree GR, Graef IA (2004) Harnessing chaperones to generate small-molecule inhibitors of amyloid beta aggregation. *Science* **306:** 865-869

Ghaemmaghami S (2016) Biology and Genetics of PrP Prion Strains. *Cold Spring Harbor perspectives in medicine*

Ghaemmaghami S, Ahn M, Lessard P, Giles K, Legname G, DeArmond SJ, Prusiner SB (2009) Continuous quinacrine treatment results in the formation of drug-resistant prions. *PLoS pathogens* **5:** e1000673

Ghaemmaghami S, Colby DW, Nguyen HO, Hayashi S, Oehler A, DeArmond SJ, Prusiner SB (2013) Convergent replication of mouse synthetic prion strains. *The American journal of pathology* **182:** 866-874

Glover JR, Kowal AS, Schirmer EC, Patino MM, Liu JJ, Lindquist S (1997) Self-seeded fibers formed by Sup35, the protein determinant of [PSI+], a heritable prion-like factor of S. cerevisiae. *Cell* **89:** 811-819

Goldfarb LG, Brown P, Cervenakova L, Gajdusek DC (1994) Genetic analysis of Creutzfeldt-Jakob disease and related disorders. *Philosophical transactions of the Royal Society of London Series B, Biological sciences* **343:** 379-384

Goldmann W, Chong A, Foster J, Hope J, Hunter N (1998) The shortest known prion protein gene allele occurs in goats, has only three octapeptide repeats and is non-pathogenic. *The Journal of general virology* **79 (Pt 12):** 3173-3176

Goldmann W, Hunter N, Smith G, Foster J, Hope J (1994) PrP genotype and agent effects in scrapie: change in allelic interaction with different isolates of agent in sheep, a natural host of scrapie. *The Journal of general virology* **75 (Pt 5):** 989-995

Gonzalez C (2007) Spindle orientation, asymmetric division and tumour suppression in Drosophila stem cells. *Nat Rev Genet* **8:** 462-472

Gottlieb S, Esposito RE (1989) A new role for a yeast transcriptional silencer gene, SIR2, in regulation of recombination in ribosomal DNA. *Cell* **56:** 771-776

Gotz M, Huttner WB (2005) The cell biology of neurogenesis. *Nature reviews Molecular cell biology* **6:** 777-788

Green KM, Castilla J, Seward TS, Napier DL, Jewell JE, Soto C, Telling GC (2008) Accelerated high fidelity prion amplification within and across prion species barriers. *PLoS pathogens* **4:** e1000139

Griffith JS (1967) Self-replication and scrapie. *Nature* **215:** 1043-1044

Grune T, Jung T, Merker K, Davies KJ (2004) Decreased proteolysis caused by protein aggregates, inclusion bodies, plaques, lipofuscin, ceroid, and 'aggresomes' during oxidative stress, aging, and disease. *The international journal of biochemistry & cell biology* **36:** 2519-2530

Haber JE (2012) Mating-type genes and MAT switching in Saccharomyces cerevisiae. *Genetics* **191:** 33-64

Haldiman T, Kim C, Cohen Y, Chen W, Blevins J, Qing L, Cohen ML, Langeveld J, Telling GC, Kong Q, Safar JG (2013) Co-existence of distinct prion types enables conformational evolution of human PrPSc by competitive selection. *The Journal of biological chemistry* **288:** 29846-29861

Hall D, Edskes H (2004) Silent prions lying in wait: a two-hit model of prion/amyloid formation and infection. *J Mol Biol* **336:** 775-786

Hall MN, Johnson AD (1987) Homeo domain of the yeast repressor alpha 2 is a sequence-specific DNA-binding domain but is not sufficient for repression. *Science* **237:** 1007-1012

Hammarstrom P, Wiseman RL, Powers ET, Kelly JW (2003) Prevention of transthyretin amyloid disease by changing protein misfolding energetics. *Science* **299:** 713-716

Harman JL, Silva CJ (2009) Bovine spongiform encephalopathy. *Journal of the American Veterinary Medical Association* **234:** 59-72

Harrison PM, Khachane A, Kumar M (2010) Genomic assessment of the evolution of the prion protein gene family in vertebrates. *Genomics* **95:** 268-277

Henderson KA, Gottschling DE (2008) A mother's sacrifice: what is she keeping for herself? *Current opinion in cell biology* **20:** 723-728

Higurashi T, Hines JK, Sahi C, Aron R, Craig EA (2008) Specificity of the J-protein Sis1 in the propagation of 3 yeast prions. *Proceedings of the National Academy of Sciences of the United States of America* **105:** 16596-16601

Hill AF, Desbruslais M, Joiner S, Sidle KC, Gowland I, Collinge J, Doey LJ, Lantos P (1997) The same prion strain causes vCJD and BSE. *Nature* **389:** 448-450, 526

Hill SM, Hao X, Liu B, Nystrom T (2014) Life-span extension by a metacaspase in the yeast Saccharomyces cerevisiae. *Science* **344:** 1389-1392

Hizume M, Kobayashi A, Teruya K, Ohashi H, Ironside JW, Mohri S, Kitamoto T (2009) Human prion protein (PrP) 219K is converted to PrPSc but shows heterozygous inhibition in variant Creutzfeldt-Jakob disease infection. *The Journal of biological chemistry* **284:** 3603-3609

Holmes WM, Mannakee BK, Gutenkunst RN, Serio TR (2014) Loss of amino-terminal acetylation suppresses a prion phenotype by modulating global protein folding. *Nature communications* **5:** 4383

Homem CC, Knoblich JA (2012) Drosophila neuroblasts: a model for stem cell biology. *Development* **139:** 4297-4310

Hope J, Wood SC, Birkett CR, Chong A, Bruce ME, Cairns D, Goldmann W, Hunter N, Bostock CJ (1999) Molecular analysis of ovine prion protein identifies similarities between BSE and an experimental isolate of natural scrapie, CH1641. *The Journal of general virology* **80 (Pt 1):** 1-4

Houston F, Goldmann W, Chong A, Jeffrey M, Gonzalez L, Foster J, Parnham D, Hunter N (2003) Prion diseases: BSE in sheep bred for resistance to infection. *Nature* **423:** 498

Ikeda T, Horiuchi M, Ishiguro N, Muramatsu Y, Kai-Uwe GD, Shinagawa M (1995) Amino acid polymorphisms of PrP with reference to onset of scrapie in Suffolk and Corriedale sheep in Japan. *The Journal of general virology* **76 (Pt 10):** 2577-2581

Imai S, Armstrong CM, Kaeberlein M, Guarente L (2000) Transcriptional silencing and longevity protein Sir2 is an NAD-dependent histone deacetylase. *Nature* **403:** 795-800

Inaba M, Yamashita YM (2012) Asymmetric stem cell division: precision for robustness. *Cell stem cell* **11:** 461-469

Ironside JW (1996) Prion diseases: update on Creutzfeldt-Jakob disease. *Neuropathology and applied neurobiology* **22:** 446

Jackrel ME, DeSantis ME, Martinez BA, Castellano LM, Stewart RM, Caldwell KA, Caldwell GA, Shorter J (2014) Potentiated Hsp104 variants antagonize diverse proteotoxic misfolding events. *Cell* **156:** 170-182

Jackrel ME, Shorter J (2014) Potentiated Hsp104 variants suppress toxicity of diverse neurodegenerative disease-linked proteins. *Dis Model Mech* **7:** 1175-1184

Jackrel ME, Shorter J (2015) Engineering enhanced protein disaggregases for neurodegenerative disease. *Prion* **9:** 90-109

Jackrel ME, Yee K, Tariq A, Chen AI, Shorter J (2015) Disparate Mutations Confer Therapeutic Gain of Hsp104 Function. *ACS Chem Biol* **10:** 2672-2679

Jacobs JG, Bossers A, Rezaei H, van Keulen LJ, McCutcheon S, Sklaviadis T, Lantier I, Berthon P, Lantier F, van Zijderveld FG, Langeveld JP (2011) Proteinase K-resistant

material in ARR/VRQ sheep brain affected with classical scrapie is composed mainly of VRQ prion protein. *J Virol* **85:** 12537-12546

Jeong BH, Lee KH, Kim NH, Jin JK, Kim JI, Carp RI, Kim YS (2005) Association of sporadic Creutzfeldt-Jakob disease with homozygous genotypes at PRNP codons 129 and 219 in the Korean population. *Neurogenetics* **6:** 229-232

Johnston JA, Ward CL, Kopito RR (1998) Aggresomes: a cellular response to misfolded proteins. *The Journal of cell biology* **143:** 1883-1898

Jung G, Masison DC (2001) Guanidine hydrochloride inhibits Hsp104 activity in vivo: a possible explanation for its effect in curing yeast prions. *Current microbiology* **43:** 7-10

Kaeberlein M, McVey M, Guarente L (1999) The SIR2/3/4 complex and SIR2 alone promote longevity in Saccharomyces cerevisiae by two different mechanisms. *Genes & development* **13:** 2570-2580

Kaneko K, Zulianello L, Scott M, Cooper CM, Wallace AC, James TL, Cohen FE, Prusiner SB (1997) Evidence for protein X binding to a discontinuous epitope on the cellular prion protein during scrapie prion propagation. *Proceedings of the National Academy of Sciences of the United States of America* **94:** 10069-10074

Kawai-Noma S, Ayano S, Pack CG, Kinjo M, Yoshida M, Yasuda K, Taguchi H (2006) Dynamics of yeast prion aggregates in single living cells. *Genes to cells : devoted to molecular & cellular mechanisms* **11:** 1085-1096

Kawai-Noma S, Pack CG, Tsuji T, Kinjo M, Taguchi H (2009) Single mother-daughter pair analysis to clarify the diffusion properties of yeast prion Sup35 in guanidine-HCl-treated [PSI] cells. *Genes to cells : devoted to molecular & cellular mechanisms* **14:** 1045-1054

Kennedy BK, Austriaco NR, Jr., Guarente L (1994) Daughter cells of Saccharomyces cerevisiae from old mothers display a reduced life span. *The Journal of cell biology* **127:** 1985-1993

Kim JI, Cali I, Surewicz K, Kong Q, Raymond GJ, Atarashi R, Race B, Qing L, Gambetti P, Caughey B, Surewicz WK (2010) Mammalian prions generated from bacterially expressed prion protein in the absence of any mammalian cofactors. *The Journal of biological chemistry* **285:** 14083-14087

Kimberlin RH, Walker C (1977) Characteristics of a short incubation model of scrapie in the golden hamster. *The Journal of general virology* **34:** 295-304

Kimberlin RH, Walker CA (1978) Pathogenesis of mouse scrapie: effect of route of inoculation on infectivity titres and dose-response curves. *Journal of comparative pathology* **88:** 39-47

Kimberlin RH, Walker CA (1986) Pathogenesis of scrapie (strain 263K) in hamsters infected intracerebrally, intraperitoneally or intraocularly. *The Journal of general virology* **67 (Pt 2):** 255-263

Kimberlin RH, Walker CA, Fraser H (1989) The genomic identity of different strains of mouse scrapie is expressed in hamsters and preserved on reisolation in mice. *The Journal of general virology* **70 (Pt 8):** 2017-2025

Kimberlin RH, Walker CA, Millson GC (1975) Interspecies transmission of scrapie-like diseases. *Lancet* **2:** 1309-1310

King C-Y, Diaz-Avalos R (2004a) Protein-only transmission of three yeast prion strains. *Nature* **428:** 319-323

King CY (2001) Supporting the structural basis of prion strains: induction and identification of [PSI] variants. *Journal of molecular biology* **307:** 1247-1260

King CY, Diaz-Avalos R (2004b) Protein-only transmission of three yeast prion strains. *Nature* **428:** 319-323

King CY, Tittmann P, Gross H, Gebert R, Aebi M, Wuthrich K (1997) Prion-inducing domain 2-114 of yeast Sup35 protein transforms in vitro into amyloid-like filaments. *Proceedings of the National Academy of Sciences of the United States of America* **94:** 6618-6622

Kirby L, Birkett CR, Rudyk H, Gilbert IH, Hope J (2003) In vitro cell-free conversion of bacterial recombinant PrP to PrPres as a model for conversion. *The Journal of general virology* **84:** 1013-1020

Kishida H, Sakasegawa Y, Watanabe K, Yamakawa Y, Nishijima M, Kuroiwa Y, Hachiya NS, Kaneko K (2004) Non-glycosylphosphatidylinositol (GPI)-anchored recombinant prion protein with dominant-negative mutation inhibits PrPSc replication in vitro. *Amyloid* **11:** 14-20

Klaips CL, Hochstrasser ML, Langlois CR, Serio TR (2014) Spatial quality control bypasses cell-based limitations on proteostasis to promote prion curing. *eLife* **3**

Klar AJ, Fogel S, Macleod K (1979) MAR1-a Regulator of the HMa and HMalpha Loci in SACCHAROMYCES CEREVISIAE. *Genetics* **93:** 37-50

Klingenstein R, Lober S, Kujala P, Godsave S, Leliveld SR, Gmeiner P, Peters PJ, Korth C (2006) Tricyclic antidepressants, quinacrine and a novel, synthetic chimera thereof clear prions by destabilizing detergent-resistant membrane compartments. *Journal of neurochemistry* **98:** 748-759

Knoblich JA (2008) Mechanisms of asymmetric stem cell division. *Cell* **132:** 583-597

Knoblich JA (2010) Asymmetric cell division: recent developments and their implications for tumour biology. *Nature reviews Molecular cell biology* **11:** 849-860

Knowles TP, Vendruscolo M, Dobson CM (2014) The amyloid state and its association with protein misfolding diseases. *Nature reviews Molecular cell biology* **15:** 384-396

Kobayashi A, Teruya K, Matsuura Y, Shirai T, Nakamura Y, Yamada M, Mizusawa H, Mohri S, Kitamoto T (2015) The influence of PRNP polymorphisms on human prion disease susceptibility: an update. *Acta neuropathologica* **130:** 159-170

Kochneva-Pervukhova NV, Paushkin SV, Kushnirov VV, Cox BS, Tuite MF, Ter-Avanesyan MD (1998) Mechanism of inhibition of Psi+ prion determinant propagation by a mutation of the N-terminus of the yeast Sup35 protein. *EMBO J* **17:** 5805-5810

Kocisko DA, Come JH, Priola SA, Chesebro B, Raymond GJ, Lansbury PT, Caughey B (1994) Cell-free formation of protease-resistant prion protein. *Nature* **370:** 471-474

Kryndushkin DS, Alexandrov IM, Ter-Avanesyan MD, Kushnirov VV (2003) Yeast [PSI+] prion aggregates are formed by small Sup35 polymers fragmented by Hsp104. *The Journal of biological chemistry* **278:** 49636-49643

Lacroute F (1971) Non-Mendelian mutation allowing ureidosuccinic acid uptake in yeast. *Journal of Bacteriology* **106:** 519-522

Landreh M, Sawaya MR, Hipp MS, Eisenberg DS, Wuthrich K, Hartl FU (2016) The formation, function and regulation of amyloids: insights from structural biology. *J Intern Med* **280:** 164-176

Langeveld JP, Jacobs JG, Hunter N, van Keulen LJ, Lantier F, van Zijderveld FG, Bossers A (2015) Prion Type-Dependent Deposition of PRNP Allelic Products in Heterozygous Sheep. *J Virol* **90:** 805-812

Langlois CR, Pei F, Sindi SS, Serio TR (2016) Distinct Prion Domain Sequences Ensure Efficient Amyloid Propagation by Promoting Chaperone Binding or Processing In Vivo. *PLoS genetics* **12:** e1006417

Laplanche JL, Chatelain J, Westaway D, Thomas S, Dussaucy M, Brugere-Picoux J, Launay JM (1993) PrP polymorphisms associated with natural scrapie discovered by denaturing gradient gel electrophoresis. *Genomics* **15:** 30-37

Laplanche JL, Delasnerie-Laupretre N, Brandel JP, Chatelain J, Beaudry P, Alperovitch A, Launay JM (1994) Molecular genetics of prion diseases in France. French Research Group on Epidemiology of Human Spongiform Encephalopathies. *Neurology* **44:** 2347-2351

Lee CI, Yang Q, Perrier V, Baskakov IV (2007) The dominant-negative effect of the Q218K variant of the prion protein does not require protein X. *Protein science : a publication of the Protein Society* **16:** 2166-2173

Lee CY, Andersen RO, Cabernard C, Manning L, Tran KD, Lanskey MJ, Bashirullah A, Doe CQ (2006) Drosophila Aurora-A kinase inhibits neuroblast self-renewal by regulating aPKC/Numb cortical polarity and spindle orientation. *Genes & development* **20:** 3464-3474

Legname G, Nguyen HO, Peretz D, Cohen FE, DeArmond SJ, Prusiner SB (2006) Continuum of prion protein structures enciphers a multitude of prion isolate-specified phenotypes. *Proceedings of the National Academy of Sciences of the United States of America* **103:** 19105-19110

Lewis PA, Tattum MH, Jones S, Bhelt D, Batchelor M, Clarke AR, Collinge J, Jackson GS (2006) Codon 129 polymorphism of the human prion protein influences the kinetics of amyloid formation. *The Journal of general virology* **87:** 2443-2449

Li J, Browning S, Mahal SP, Oelschlegel AM, Weissmann C (2010) Darwinian evolution of prions in cell culture. *Science* **327:** 869-872

Li J, Zhu M, Rajamani S, Uversky VN, Fink AL (2004) Rifampicin inhibits alpha-synuclein fibrillation and disaggregates fibrils. *Chemistry & biology* **11:** 1513-1521

Li S, Wang H, Groth C (2014) Drosophila neuroblasts as a new model for the study of stem cell self-renewal and tumour formation. *Bioscience reports* **34**

Liebman SW, Derkatch IL (1965) The Yeast [PSI+] Prion: Making Sense of Nonsense. *The Journal of biological chemistry* **274:** 1181-1184

Liu B, Larsson L, Caballero A, Hao X, Oling D, Grantham J, Nystrom T (2010) The polarisome is required for segregation and retrograde transport of protein aggregates. *Cell* **140:** 257-267

Luhken G, Buschmann A, Groschup MH, Erhardt G (2004) Prion protein allele A136 H154Q171 is associated with high susceptibility to scrapie in purebred and crossbred German Merinoland sheep. *Archives of virology* **149:** 1571-1580

Lukic A, Beck J, Joiner S, Fearnley J, Sturman S, Brandner S, Wadsworth JD, Collinge J, Mead S (2010) Heterozygosity at polymorphic codon 219 in variant creutzfeldt-jakob disease. *Archives of neurology* **67:** 1021-1023

Maciulis A, Hunter N, Wang S, Goldmann W, Hope J, Foote WC (1992) Polymorphisms of a scrapie-associated fibril protein (PrP) gene and their association with susceptibility to experimentally induced scrapie in Cheviot sheep in the United States. *American journal of veterinary research* **53:** 1957-1960

Maddelein ML, Dos Reis S, Duvezin-Caubet S, Coulary-Salin B, Saupe SJ (2002) Amyloid aggregates of the HET-s prion protein are infectious. *Proceedings of the National Academy of Sciences of the United States of America* **99:** 7402-7407

Madec JY, Simon S, Lezmi S, Bencsik A, Grassi J, Baron T (2004) Abnormal prion protein in genetically resistant sheep from a scrapie-infected flock. *The Journal of general virology* **85:** 3483-3486

Mahal SP, Baker CA, Demczyk CA, Smith EW, Julius C, Weissmann C (2007) Prion strain discrimination in cell culture: the cell panel assay. *Proceedings of the National Academy of Sciences of the United States of America* **104:** 20908-20913

Mahal SP, Browning S, Li J, Suponitsky-Kroyter I, Weissmann C (2010) Transfer of a prion strain to different hosts leads to emergence of strain variants. *Proceedings of the National Academy of Sciences of the United States of America* **107:** 22653-22658

Mahat DB, Salamanca HH, Duarte FM, Danko CG, Lis JT (2016) Mammalian Heat Shock Response and Mechanisms Underlying Its Genome-wide Transcriptional Regulation. *Mol Cell* **62:** 63-78

Mallucci G, Dickinson A, Linehan J, Brandner S, Collinge J, Mallucci G, Dickinson A, Linehan J (2003) Depleting Neuronal PrP in Prion Infection Prevents Disease and Reverses Spongiosis Published by : American Association for the Advancement of Science Stable URL : http://www.jstor.org/stable/3835558 Your use of the JSTOR archive indicates your acceptance. *Science* **302:** 871-874

Mallucci GR, White MD, Farmer M, Dickinson A, Khatun H, Powell AD, Brandner S, Jefferys JGR, Collinge J (2007) Targeting Cellular Prion Protein Reverses Early Cognitive Deficits and Neurophysiological Dysfunction in Prion-Infected Mice. *Neuron* **53:** 325-335

Malone TG, Marsh RF, Hanson RP, Semancik JS (1978) Membrane-free scrapie activity. *J Virol* **25:** 933-935

Manning M, Colon W (2004) Structural basis of protein kinetic stability: resistance to sodium dodecyl sulfate suggests a central role for rigidity and a bias toward beta-sheet structure. *Biochemistry* **43:** 11248-11254

Marchante R, Rowe M, Zenthon J, Howard MJ, Tuite MF (2013) Structural definition is important for the propagation of the yeast [PSI+] prion. *Mol Cell* **50:** 675-685

Masel J, Jansen VA (2000) Designing drugs to stop the formation of prion aggregates and other amyloids. *Biophysical chemistry* **88:** 47-59

Masel J, Jansen VA, Nowak MA (1999) Quantifying the kinetic parameters of prion replication. *Biophysical chemistry* **77:** 139-152

Mastrianni JA (2010) The genetics of prion diseases. *Genetics in medicine : official journal of the American College of Medical Genetics* **12:** 187-195

Masuda M, Suzuki N, Taniguchi S, Oikawa T, Nonaka T, Iwatsubo T, Hisanaga S, Goedert M, Hasegawa M (2006) Small molecule inhibitors of alpha-synuclein filament assembly. *Biochemistry* **45:** 6085-6094

McLean CA (2008) Review. The neuropathology of kuru and variant Creutzfeldt-Jakob disease. *Philosophical transactions of the Royal Society of London Series B, Biological sciences* **363:** 3685-3687

McLean CA, Ironside JW, Alpers MP, Brown PW, Cervenakova L, Anderson RM, Masters CL (1998) Comparative neuropathology of Kuru with the new variant of Creutzfeldt-Jakob disease: evidence for strain of agent predominating over genotype of host. *Brain pathology* **8:** 429-437

Moazed D, Kistler A, Axelrod A, Rine J, Johnson AD (1997) Silent information regulator protein complexes in Saccharomyces cerevisiae: a SIR2/SIR4 complex and evidence for a regulatory domain in SIR4 that inhibits its interaction with SIR3. *Proceedings of the National Academy of Sciences of the United States of America* **94:** 2186-2191

Moore DL, Jessberger S (2017) Creating Age Asymmetry: Consequences of Inheriting Damaged Goods in Mammalian Cells. *Trends in cell biology* **27:** 82-92

Morales R, Abid K, Soto C (2007) The prion strain phenomenon : Molecular basis and unprecedented features. *Biochimica et biophysica acta* **1772:** 681-691

Moriyama H, Edskes HK, Wickner RB (2000) [URE3] prion propagation in Saccharomyces cerevisiae: requirement for chaperone Hsp104 and curing by overexpressed chaperone Ydj1p. *Molecular and cellular biology* **20:** 8916-8922

Morrison SJ, Kimble J (2006) Asymmetric and symmetric stem-cell divisions in development and cancer. *Nature* **441:** 1068-1074

Moseley JB, Goode BL (2006) The yeast actin cytoskeleton: from cellular function to biochemical mechanism. *Microbiology and molecular biology reviews : MMBR* **70:** 605-645

Murakami-Kubo I, Doh-Ura K, Ishikawa K, Kawatake S, Sasaki K, Kira J, Ohta S, Iwaki T (2004) Quinoline derivatives are therapeutic candidates for transmissible spongiform encephalopathies. *J Virol* **78:** 1281-1288

Ness F, Ferreira P, Cox BS, Tuite MF (2002) Guanidine hydrochloride inhibits the generation of prion "seeds" but not prion protein aggregation in yeast. *Molecular and cellular biology* **22:** 5593-5605

Newnam GP, Birchmore JL, Chernoff YO (2011) Destabilization and recovery of a yeast prion after mild heat shock. *J Mol Biol* **408:** 432-448

Nillegoda NB, Kirstein J, Szlachcic A, Berynskyy M, Stank A, Stengel F, Arnsburg K, Gao X, Scior A, Aebersold R, Guilbride DL, Wade RC, Morimoto RI, Mayer MP, Bukau B (2015) Crucial HSP70 co-chaperone complex unlocks metazoan protein disaggregation. *Nature* **524:** 247-251

Noguchi-Shinohara M, Hamaguchi T, Kitamoto T, Sato T, Nakamura Y, Mizusawa H, Yamada M (2007) Clinical features and diagnosis of dura mater graft associated Creutzfeldt Jakob disease. *Neurology* **69:** 360-367

Nozaki I, Hamaguchi T, Sanjo N, Noguchi-Shinohara M, Sakai K, Nakamura Y, Sato T, Kitamoto T, Mizusawa H, Moriwaka F, Shiga Y, Kuroiwa Y, Nishizawa M, Kuzuhara S, Inuzuka T, Takeda M, Kuroda S, Abe K, Murai H, Murayama S, Tateishi J, Takumi I, Shirabe S, Harada M, Sadakane A, Yamada M (2010) Prospective 10-year surveillance of human prion diseases in Japan. *Brain : a journal of neurology* **133:** 3043-3057

Oelschlegel AM, Weissmann C (2013) Acquisition of drug resistance and dependence by prions. *PLoS pathogens* **9:** e1003158

Ogrodnik M, Salmonowicz H, Brown R, Turkowska J, Sredniawa W, Pattabiraman S, Amen T, Abraham AC, Eichler N, Lyakhovetsky R, Kaganovich D (2014) Dynamic JUNQ inclusion bodies are asymmetrically inherited in mammalian cell lines through the asymmetric partitioning of vimentin. *Proceedings of the National Academy of Sciences of the United States of America* **111:** 8049-8054

Onnasch H, Gunn HM, Bradshaw BJ, Benestad SL, Bassett HF (2004) Two Irish cases of scrapie resembling Nor98. *The Veterinary record* **155:** 636-637

Orge L, Galo A, Machado C, Lima C, Ochoa C, Silva J, Ramos M, Simas JP (2004) Identification of putative atypical scrapie in sheep in Portugal. *The Journal of general virology* **85:** 3487-3491

Orge L, Oliveira A, Machado C, Lima C, Ochoa C, Silva J, Carvalho R, Tavares P, Almeida P, Ramos M, Pinto MJ, Simas JP (2010) Putative emergence of classical scrapie in a background of enzootic atypical scrapie. *The Journal of general virology* **91:** 1646-1650

Osherovich LZ, Cox BS, Tuite MF, Weissman JS (2004) Dissection and design of yeast prions. *PLoS Biol* **2:** E86

Osherovich LZ, Weissman JS (2001) Multiple Gln/Asn-rich prion domains confer susceptibility to induction of the yeast [PSI(+)] prion. *Cell* **106:** 183-194

Ott D, Taraborrelli C, Aguzzi A (2008) Novel dominant-negative prion protein mutants identified from a randomized library. *Protein engineering, design & selection : PEDS* **21:** 623-629

Outram GW (1976) The pathogenesis of scrapie in mice. *Frontiers of biology* **44:** 325-357

Ovsepian SV, O'Leary VB, Ntziachristos V, Dolly JO (2016) Circumventing Brain Barriers: Nanovehicles for Retroaxonal Therapeutic Delivery. *Trends in molecular medicine* **22:** 983-993

Palmer MS, Dryden AJ, Hughes JT, Collinge J (1991) Homozygous prion protein genotype predisposes to sporadic Creutzfeldt-Jakob disease. *Nature* **352:** 340-342

Paludi D, Thellung S, Chiovitti K, Corsaro A, Villa V, Russo C, Ianieri A, Bertsch U, Kretzschmar HA, Aceto A, Florio T (2007) Different structural stability and toxicity of PrP(ARR) and PrP(ARQ) sheep prion protein variants. *Journal of neurochemistry* **103:** 2291-2300

Parchi P, Chen SG, Brown P, Zou W, Capellari S, Budka H, Hainfellner J, Reyes PF, Golden GT, Hauw JJ, Gajdusek DC, Gambetti P (1998) Different patterns of truncated prion protein fragments correlate with distinct phenotypes in P102L Gerstmann-Straussler-Scheinker disease. *Proceedings of the National Academy of Sciences of the United States of America* **95:** 8322-8327

Parham SN, Resende CG, Tuite MF (2001) Oligopeptide repeats in the yeast protein Sup35p stabilize intermolecular prion interactions. *EMBO J* **20:** 2111-2119

Park PU, Defossez PA, Guarente L (1999) Effects of mutations in DNA repair genes on formation of ribosomal DNA circles and life span in Saccharomyces cerevisiae. *Molecular and cellular biology* **19:** 3848-3856

Patel BK, Liebman SW (2007) "Prion-proof" for [PIN+]: Infection with In Vitro-made Amyloid Aggregates of Rnq1p-(132-405) Induces [PIN+]. *Journal of Molecular Biology* **365:** 773-782

Patino MM, Liu JJ, Glover JR, Lindquist S (1996) Support for the prion hypothesis for inheritance of a phenotypic trait in yeast. *Science* **273:** 622-626

Pattison IH, Jones KM (1968) Modification of a strain of mouse-adapted scrapie by passage through rats. *Research in veterinary science* **9:** 408-410

Pattison IH, Millson GC (1961) Scrapie produced experimentally in goats with special reference to the clinical syndrome. *Journal of comparative pathology* **71:** 101-109

Paushkin SV, Kushnirov VV, Smirnov VN, Ter-Avanesyan MD (1996) Propagation of the yeast prion-like [psi+] determinant is mediated by oligomerization of the SUP35-encoded polypeptide chain release factor. *EMBO J* **15:** 3127-3134

Pelletier L, Yamashita YM (2012) Centrosome asymmetry and inheritance during animal development. *Current opinion in cell biology* **24:** 541-546

Perrier V, Kaneko K, Safar J, Vergara J, Tremblay P, DeArmond SJ, Cohen FE, Prusiner SB, Wallace AC (2002) Dominant-negative inhibition of prion replication in transgenic mice. *Proceedings of the National Academy of Sciences of the United States of America* **99:** 13079-13084

Pezza JA, Langseth SX, Raupp Yamamoto R, Doris SM, Ulin SP, Salomon AR, Serio TR (2009) The NatA acetyltransferase couples Sup35 prion complexes to the [PSI+] phenotype. *Molecular biology of the cell* **20:** 1068-1080

Powers ET, Morimoto RI, Dillin A, Kelly JW, Balch WE (2009) Biological and chemical approaches to diseases of proteostasis deficiency. *Annual review of biochemistry* **78:** 959-991

Priola SA, Chesebro B (1995) A single hamster PrP amino acid blocks conversion to protease-resistant PrP in scrapie-infected mouse neuroblastoma cells. *J Virol* **69:** 7754-7758

Prusiner SB (1982a) Novel proteinaceous infectious particles cause scrapie. *Science* **216:** 136-144

Prusiner SB (1982b) Novel Proteinaceous Infectious Particles Cause Scrapie Author (s): Stanley B . Prusiner Source : Science , New Series , Vol . 216 , No . 4542 (Apr . 9 , 1982), pp . 136-144 Published by : American Association for the Advancement of Science Stable URL. *Science* **216:** 136-144

Prusiner SB (1993) Transgenetic investigations of prion diseases of humans and animals. *Philosophical transactions of the Royal Society of London Series B, Biological sciences* **339:** 239-254

Prusiner SB (1994) Biology and genetics of prion diseases. *Annual review of microbiology* **48:** 655-686

Prusiner SB (1998) Prions. *Proceedings of the National Academy of Sciences of the United States of America* **95:** 13363-13383

Prusiner SB, Groth D, Serban A, Koehler R, Foster D, Torchia M, Burton D, Yang SL, DeArmond SJ (1993) Ablation of the prion protein (PrP) gene in mice prevents scrapie and facilitates production of anti-PrP antibodies. *Proceedings of the National Academy of Sciences of the United States of America* **90:** 10608-10612

Prusiner SB, Scott M, Foster D, Pan KM, Groth D, Mirenda C, Torchia M, Yang SL, Serban D, Carlson GA, et al. (1990) Transgenetic studies implicate interactions between homologous PrP isoforms in scrapie prion replication. *Cell* **63:** 673-686

Reinders J, Zahedi RP, Pfanner N, Meisinger C, Sickmann A (2006) Toward the complete yeast mitochondrial proteome: multidimensional separation techniques for mitochondrial proteomics. *Journal of proteome research* **5:** 1543-1554

Reverter-Branchat G, Cabiscol E, Tamarit J, Ros J (2004) Oxidative damage to specific proteins in replicative and chronological-aged Saccharomyces cerevisiae: common targets and prevention by calorie restriction. *The Journal of biological chemistry* **279:** 31983-31989

Rikhvanov EG, Varakina NN, Rusaleva TM, Rachenko EI, Knorre DA, Voinikov VK (2005) Do mitochondria regulate the heat-shock response in Saccharomyces cerevisiae? *Current genetics* **48:** 44-59

Rine J, Herskowitz I (1987) Four genes responsible for a position effect on expression from HML and HMR in Saccharomyces cerevisiae. *Genetics* **116:** 9-22

Rine J, Strathern JN, Hicks JB, Herskowitz I (1979) A suppressor of mating-type locus mutations in Saccharomyces cerevisiae: evidence for and identification of cryptic mating-type loci. *Genetics* **93:** 877-901

Roberts BE, Duennwald ML, Wang H, Chung C, Lopreiato NP, Sweeny EA, Knight MN, Shorter J (2009) A synergistic small-molecule combination directly eradicates diverse prion strain structures. *Nat Chem Biol* **5:** 936-946

Rogina B, Helfand SL (2004) Sir2 mediates longevity in the fly through a pathway related to calorie restriction. *Proceedings of the National Academy of Sciences of the United States of America* **101:** 15998-16003

Ronzon F, Bencsik A, Lezmi S, Vulin J, Kodjo A, Baron T (2006) BSE inoculation to prion diseases-resistant sheep reveals tricky silent carriers. *Biochemical and biophysical research communications* **350:** 872-877

Rujano MA, Bosveld F, Salomons FA, Dijk F, van Waarde MA, van der Want JJ, de Vos RA, Brunt ER, Sibon OC, Kampinga HH (2006) Polarised asymmetric inheritance of accumulated protein damage in higher eukaryotes. *PLoS Biol* **4:** e417

Rusche LN, Kirchmaier AL, Rine J (2003) The establishment, inheritance, and function of silenced chromatin in Saccharomyces cerevisiae. *Annual review of biochemistry* **72:** 481-516

Saborio GP, Permanne B, Soto C (2001) Sensitive detection of pathological prion protein by cyclic amplification of protein misfolding. *Nature* **411:** 810-813

Safar J, Wille H, Itri V, Groth D, Serban H, Torchia M, Cohen FE, Prusiner SB (1998) Eight prion strains have PrP(Sc) molecules with different conformations. *Nature medicine* **4:** 1157-1165

Sanchez Y, Lindquist SL (1990) HSP104 required for induced thermotolerance. *Science* **248:** 1112-1115

Sanchez Y, Taulien J, Borkovich KA, Lindquist S (1992) Hsp104 is required for tolerance to many forms of stress. *EMBO J* **11:** 2357-2364

Sandberg MK, Al-Doujaily H, Sharps B, Clarke AR, Collinge J (2011) Prion propagation and toxicity in vivo occur in two distinct mechanistic phases. *Nature* **470:** 540-542

Satpute-Krishnan P, Langseth SX, Serio TR (2007) Hsp104-dependent remodeling of prion complexes mediates protein-only inheritance. *PLoS Biol* **5:** e24

Satpute-Krishnan P, Serio TR (2005) Prion protein remodelling confers an immediate phenotypic switch. *Nature* **437:** 262-265

Schlissel G, Krzyzanowski MK, Caudron F, Barral Y, Rine J (2017) Aggregation of the Whi3 protein, not loss of heterochromatin, causes sterility in old yeast cells. *Science* **355:** 1184-1187

Scott M, Foster D, Mirenda C, Serban D, Coufal F, Walchli M, Torchia M, Groth D, Carlson G, DeArmond SJ, Westaway D, Prusiner SB (1989) Transgenic mice expressing hamster prion protein produce species-specific scrapie infectivity and amyloid plaques. *Cell* **59:** 847-857

Serio TR, Cashikar AG, Kowal AS, Sawicki GJ, Moslehi JJ, Serpell L, Arnsdorf MF, Lindquist SL (2000) Nucleated conformational conversion and the replication of conformational information by a prion determinant. *Science* **289:** 1317-1321

Serio TR, Lindquist SL (1999) [PSI +]: An Epigenetic Modulator of Translation Termination Efficiency. *Annual Review of Cell and Developmental Biology* **15:** 661-703

Shamovsky I, Gershon D (2004) Novel regulatory factors of HSF-1 activation: facts and perspectives regarding their involvement in the age-associated attenuation of the heat shock response. *Mechanisms of ageing and development* **125:** 767-775

Shibuya S, Higuchi J, Shin RW, Tateishi J, Kitamoto T (1998a) Codon 219 Lys allele of PRNP is not found in sporadic Creutzfeldt-Jakob disease. *Annals of neurology* **43:** 826-828

Shibuya S, Higuchi J, Shin RW, Tateishi J, Kitamoto T (1998b) Protective prion protein polymorphisms against sporadic Creutzfeldt-Jakob disease. *Lancet* **351:** 419

Shinin V, Gayraud-Morel B, Gomes D, Tajbakhsh S (2006) Asymmetric division and cosegregation of template DNA strands in adult muscle satellite cells. *Nature cell biology* **8:** 677-687

Shmerling D, Hegyi I, Fischer M, Blättler T, Brandner S, Götz J, Rülicke T, Flechsig E, Cozzio A, Von Mering C, Hangartner C, Aguzzi A, Weissmann C (1998) Expression of amino-terminally truncated PrP in the mouse leading to ataxia and specific cerebellar lesions. *Cell* **93:** 203-214

Shorter J (2008) Hsp104: a weapon to combat diverse neurodegenerative disorders. *Neurosignals* **16:** 63-74

Shorter J (2010) Emergence and natural selection of drug-resistant prions. *Molecular bioSystems* **6:** 1115-1130

Shorter J (2016) Engineering therapeutic protein disaggregases. *Molecular biology of the cell* **27:** 1556-1560

Shorter J (2017) Designer protein disaggregases to counter neurodegenerative disease. *Curr Opin Genet Dev* **44:** 1-8

Sievers SA, Karanicolas J, Chang HW, Zhao A, Jiang L, Zirafi O, Stevens JT, Munch J, Baker D, Eisenberg D (2011) Structure-based design of non-natural amino-acid inhibitors of amyloid fibril formation. *Nature* **475:** 96-100

Smeal T, Claus J, Kennedy B, Cole F, Guarente L (1996) Loss of transcriptional silencing causes sterility in old mother cells of S. cerevisiae. *Cell* **84:** 633-642

Smith JS, Brachmann CB, Pillus L, Boeke JD (1998) Distribution of a limited Sir2 protein pool regulates the strength of yeast rDNA silencing and is modulated by Sir4p. *Genetics* **149:** 1205-1219

Somerville RA, Birkett CR, Farquhar CF, Hunter N, Goldmann W, Dornan J, Grover D, Hennion RM, Percy C, Foster J, Jeffrey M (1997) Immunodetection of PrPSc in spleens of some scrapie-infected sheep but not BSE-infected cows. *The Journal of general virology* **78 (Pt 9):** 2389-2396

Sondheimer N, Lindquist S (2000) Rnq1: an epigenetic modifier of protein function in yeast. *Molecular cell* **5:** 163-172

Song J, Yang Q, Yang J, Larsson L, Hao X, Zhu X, Malmgren-Hill S, Cvijovic M, Fernandez-Rodriguez J, Grantham J, Gustafsson CM, Liu B, Nystrom T (2014) Essential genetic interactors of SIR2 required for spatial sequestration and asymmetrical inheritance of protein aggregates. *PLoS genetics* **10:** e1004539

Sorger PK, Pelham HR (1987) Purification and characterization of a heat-shock element binding protein from yeast. *EMBO J* **6:** 3035-3041

Soto C, Saborio GP, Anderes L (2002) Cyclic amplification of protein misfolding: application to prion-related disorders and beyond. *Trends in neurosciences* **25:** 390-394

Spokoini R, Moldavski O, Nahmias Y, England JL, Schuldiner M, Kaganovich D (2012) Confinement to organelle-associated inclusion structures mediates asymmetric inheritance of aggregated protein in budding yeast. *Cell reports* **2:** 738-747

Stadtman ER (1992) Protein oxidation and aging. *Science* **257:** 1220-1224

Steele AD, Hutter G, Jackson WS, Heppner FL, Borkowski AW, King OD, Raymond GJ, Aguzzi A, Lindquist S (2008) Heat shock factor 1 regulates lifespan as distinct from disease onset in prion disease. *Proceedings of the National Academy of Sciences of the United States of America* **105:** 13626-13631

Sweeny EA, Jackrel ME, Go MS, Sochor MA, Razzo BM, DeSantis ME, Gupta K, Shorter J (2015) The Hsp104 N-terminal domain enables disaggregase plasticity and potentiation. *Mol Cell* **57:** 836-849

Tahiri-Alaoui A, Gill AC, Disterer P, James W (2004) Methionine 129 variant of human prion protein oligomerizes more rapidly than the valine 129 variant: implications for disease susceptibility to Creutzfeldt-Jakob disease. *The Journal of biological chemistry* **279:** 31390-31397

Tanaka M, Chien P, Naber N, Cooke R, Weissman JS (2004) Conformational variations in an infectious protein determine prion strain differences. *Nature* **428:** 323-328

Tanaka M, Chien P, Yonekura K, Weissman JS (2005) Mechanism of cross-species prion transmission: an infectious conformation compatible with two highly divergent yeast prion proteins. *Cell* **121:** 49-62

Tanaka M, Collins SR, Toyama BH, Weissman JS (2006) The physical basis of how prion conformations determine strain phenotypes. *Nature* **442:** 585-589

Tatzelt J, Zuo J, Voellmy R, Scott M, Hartl U, Prusiner SB, Welch WJ (1995) Scrapie prions selectively modify the stress response in neuroblastoma cells. *Proceedings of the National Academy of Sciences of the United States of America* **92:** 2944-2948

Taylor KL, Cheng N, Williams RW, Steven AC, Wickner RB (1999) Prion domain initiation of amyloid formation in vitro from native Ure2p. *Science* **283:** 1339-1343

Telling GC, Scott M, Hsiao KK, Foster D, Yang SL, Torchia M, Sidle KC, Collinge J, DeArmond SJ, Prusiner SB (1994) Transmission of Creutzfeldt-Jakob disease from humans to transgenic mice expressing chimeric human-mouse prion protein. *Proceedings of the National Academy of Sciences of the United States of America* **91:** 9936-9940

Telling GC, Scott M, Mastrianni J, Gabizon R, Torchia M, Cohen FE, DeArmond SJ, Prusiner SB (1995) Prion propagation in mice expressing human and chimeric PrP transgenes implicates the interaction of cellular PrP with another protein. *Cell* **83:** 79-90

Ter-Avanesyan MD, Dagkesamanskaya AR, Kushnirov VV, Smirnov VN (1994) The SUP35 omnipotent suppressor gene is involved in the maintenance of the non-Mendelian determinant [psi+] in the yeast Saccharomyces cerevisiae. *Genetics* **137:** 671-676

Tessier PM, Lindquist S (2007) Prion recognition elements govern nucleation, strain specificity and species barriers. *Nature* **447:** 556-561

Tipton KA, Verges KJ, Weissman JS (2008) In vivo monitoring of the prion replication cycle reveals a critical role for Sis1 in delivering substrates to Hsp104. *Mol Cell* **32:** 584-591

Tissenbaum HA, Guarente L (2001) Increased dosage of a sir-2 gene extends lifespan in Caenorhabditis elegans. *Nature* **410:** 227-230

Torrente MP, Shorter J (2013) The metazoan protein disaggregase and amyloid depolymerase system: Hsp110, Hsp70, Hsp40, and small heat shock proteins. *Prion* **7:** 457-463

Toupet K, Compan V, Crozet C, Mourton-Gilles C, Mestre-Frances N, Ibos F, Corbeau P, Verdier JM, Perrier V (2008) Effective gene therapy in a mouse model of prion diseases. *PloS one* **3:** e2773

Toyama BH, Kelly MJ, Gross JD, Weissman JS (2007) The structural basis of yeast prion strain variants. *Nature* **449:** 233-237

Tranulis MA (2002) Influence of the prion protein gene, Prnp, on scrapie susceptibility in sheep. *APMIS* **110:** 33-43

Tremblay P, Meiner Z, Galou M, Heinrich C, Petromilli C, Lisse T, Cayetano J, Torchia M, Mobley W, Bujard H, DeArmond SJ, Prusiner SB (1998) Doxycycline control of prion protein transgene expression modulates prion disease in mice. *Proceedings of the National Academy of Sciences of the United States of America* **95:** 12580-12585

Trevitt CR, Collinge J (2006) A systematic review of prion therapeutics in experimental models. *Brain : a journal of neurology* **129:** 2241-2265

Tuite MF, Serio TR (2010) The prion hypothesis: from biological anomaly to basic regulatory mechanism. *Nature reviews Molecular cell biology* **11:** 823-833

Uptain SM, Sawicki GJ, Caughey B, Lindquist S (2001) Strains of [PSI(+)] are distinguished by their efficiencies of prion-mediated conformational conversion. *EMBO J* **20:** 6236-6245

Vande Velde C, McDonald KK, Boukhedimi Y, McAlonis-Downes M, Lobsiger CS, Bel Hadj S, Zandona A, Julien JP, Shah SB, Cleveland DW (2011) Misfolded SOD1 associated with motor neuron mitochondria alters mitochondrial shape and distribution prior to clinical onset. *PloS one* **6:** e22031

Verges KJ, Smith MH, Toyama BH, Weissman JS (2011) Strain conformation, primary structure and the propagation of the yeast prion [PSI+]. *Nature structural & molecular biology* **18:** 493-499

Vishveshwara N, Liebman SW (2009) Heterologous cross-seeding mimics cross-species prion conversion in a yeast model. *BMC biology* **7:** 26

Wang F, Wang X, Ma J (2011) Conversion of bacterially expressed recombinant prion protein. *Methods* **53:** 208-213

Wang F, Wang X, Yuan CG, Ma J (2010) Generating a prion with bacterially expressed recombinant prion protein. *Science* **327:** 1132-1135

Wang H, Duennwald ML, Roberts BE, Rozeboom LM, Zhang YL, Steele AD, Krishnan R, Su LJ, Griffin D, Mukhopadhyay S, Hennessy EJ, Weigele P, Blanchard BJ, King J, Deniz AA, Buchwald SL, Ingram VM, Lindquist S, Shorter J (2008) Direct and selective elimination of specific prions and amyloids by 4,5-dianilinophthalimide and analogs. *Proceedings of the National Academy of Sciences of the United States of America* **105:** 7159-7164

Wegrzyn RD, Bapat K, Newnam GP, Zink AD, Chernoff YO (2001) Mechanism of prion loss after Hsp104 inactivation in yeast. *Molecular and cellular biology* **21:** 4656-4669

Westaway D, Zuliani V, Cooper CM, Da Costa M, Neuman S, Jenny AL, Detwiler L, Prusiner SB (1994) Homozygosity for prion protein alleles encoding glutamine-171 renders sheep susceptible to natural scrapie. *Genes & development* **8:** 959-969

Westergard L, Christensen HM, Harris DA (2007) The cellular prion protein (PrPC): Its physiological function and role in disease. *Biochimica et Biophysica Acta (BBA) - Molecular Basis of Disease* **1772:** 629-644

White MD, Farmer M, Mirabile I, Brandner S, Collinge J, Mallucci GR (2008) Single treatment with RNAi against prion protein rescues early neuronal dysfunction and prolongs survival in mice with prion disease. *Proceedings of the National Academy of Sciences of the United States of America* **105:** 10238-10243

Wickner RB (1994) [URE3] as an altered URE2 protein: evidence for a prion analog in Saccharomyces cerevisiae. *Science (New York, NY)* **264:** 566-569

Wickner RB, Edskes HK, Shewmaker F, Nakayashiki T (2007) Prions of fungi: inherited structures and biological roles. *Nature Reviews Microbiology* **5:** 611-618

Will RG, Ironside JW, Zeidler M, Cousens SN, Estibeiro K (1996) A new variant of Creutzfeldt-Jakob disease in the UK. *The Lancet* **347:** 921-925

Winklhofer KF, Reintjes A, Hoener MC, Voellmy R, Tatzelt J (2001) Geldanamycin restores a defective heat shock response in vivo. *The Journal of biological chemistry* **276:** 45160-45167

Wright J, Schneider BL (2013) Cell size control is sirtuin(ly) exciting. *Mol Syst Biol* **9:** 706

Yamada M, Noguchi-Shinohara M, Hamaguchi T, Nozaki I, Kitamoto T, Sato T, Nakamura Y, Mizusawa H (2009) Dura mater graft-associated Creutzfeldt-Jakob disease in Japan:

clinicopathological and molecular characterization of the two distinct subtypes. *Neuropathology : official journal of the Japanese Society of Neuropathology* **29:** 609-618

Yang HC, Pon LA (2002) Actin cable dynamics in budding yeast. *Proceedings of the National Academy of Sciences of the United States of America* **99:** 751-756

Yang J, Dungrawala H, Hua H, Manukyan A, Abraham L, Lane W, Mead H, Wright J, Schneider BL (2011) Cell size and growth rate are major determinants of replicative lifespan. *Cell cycle* **10:** 144-155

Yu A, Shibata Y, Shah B, Calamini B, Lo DC, Morimoto RI (2014) Protein aggregation can inhibit clathrin-mediated endocytosis by chaperone competition. *Proceedings of the National Academy of Sciences of the United States of America* **111:** E1481-1490

Yuan AH, Hochschild A (2017) A bacterial global regulator forms a prion. *Science* **355:** 198-201

Zampieri M, Legname G, Altafini C (2009) Investigating the conformational stability of prion strains through a kinetic replication model. *PLoS computational biology* **5:** e1000420

Zhou C, Slaughter BD, Unruh JR, Eldakak A, Rubinstein B, Li R (2011) Motility and segregation of Hsp104-associated protein aggregates in budding yeast. *Cell* **147:** 1186-1196

Zhou C, Slaughter BD, Unruh JR, Guo F, Yu Z, Mickey K, Narkar A, Ross RT, McClain M, Li R (2014) Organelle-based aggregation and retention of damaged proteins in asymmetrically dividing cells. *Cell* **159:** 530-542

Zhou P, Derkatch IL, Uptain SM, Patino MM, Lindquist S, Liebman SW (1999) The yeast non-Mendelian factor [ETA+] is a variant of [PSI+], a prion-like form of release factor eRF3. *EMBO J* **18:** 1182-1191

Zulianello L, Kaneko K, Scott M, Erpel S, Han D, Cohen FE, Prusiner SB (2000) Dominant-negative inhibition of prion formation diminished by deletion mutagenesis of the prion protein. *J Virol* **74:** 4351-4360